Analytical And Experimental Study Of The Effects Of Oil On The Heat Transfer Coefficient Of Condensing Refrigerant Vapor At The External Surface Of Plain Horizontal Tubes

Adnan A. Al-Kalamchi

A Thesis

in

The Faculty

of

Engineering

and

Computer Science

Presented in Partial Fulfilment of the Requirements
for the degree of Doctor of Philosophy at
Concordia University
Montréal, Québec, Canada

July 1984


وما تشاؤن الا ان يشاء الله رب العالمين
قرآن کریم

ABSTRACT

Analytical And Experimental Study Of The Effects Of Oil On The Heat Transfer Coefficient Of Condensing Refrigerant Vapor At The External Surface Of Plain Horizontal Tubes

Adnan A. Al-Kalamchi, Ph.D.
Concordia University, 1984

Migration of lubricating oil from the compressor crankcase into the other components of a vapor compression refrigeration system, such as a condenser, is a common occurrence. The objective of this study is to investigate, experimentally and analytically, the effects of oil on vapor condensation at the external surface of a smooth, single and a vertical bank of 4 horizontal tubes.

Two commonly used refrigerants in reciprocating compressors, R-12 and R-22, along with alkylbenzene-based refrigeration oil, were investigated. Both refrigerants are completely miscible in the oil. Mixtures with 2, 4, 6 and 8 per cent oil-refrigerant mass ratios were condensed at 32.2, 40.6 and 48.9 °C (90, 105 and 120 °F) condensing temperatures

for R-12 and at 32.2 and 40.8° C (90 and 105° F) for R-22.

A test apparatus, to actually simulate the oil carry over into the condenser was designed and presented along with a special experimental technique for executing the tests at constant oil-to-refrigerant mass ratios.

The study revealed that the presence of oil in any proportion mixed with the vapor, affects the condensing heat transfer coefficient. The higher the oil concentration the lower is the coefficient. The presence of oil effects R-12 condensation more than R-22.

Analytical equations for predicting the pure vapor and oil-vapor condensing coefficients on single and multi-tube condensers, were derived, and empirical equations for the same cases were deduced.

The condensation of pure refrigerant showed that Nusselt's theories based on 32.2° C (90° F) saturation temperature for both single and multi-tube condensation, predict values lower than the experimental data by an average of 3 and 15 per cent respectively. Finally, there was a presentation of recommendations and suggestions for future work.

ACKNOWLEDGMENTS

The author wishes to express his sincere gratitude to his supervisor, Dr. Joseph Wang, for his help, valuable guidance and useful suggestions.

The author wishes to thank his co-supervisor, Dr. Paul Fazio for his thoughtful suggestions, guidance and his continuous encouragement throughout the course of this work.

The author wishes to place on record his profound thanks and gratitude to Dr. Rafaat Hussein for his encouragement and valuable advice during the period of study.

Special thanks are due to Mr. Joseph Hrib for his cooperation in building the experimental apparatus, also thanks are due to the technical staff at the Center of Building Studies, Mr. Hans Obermeir, Mr. Joseph Zilka and Mr. Tony Sum for their continuous readiness to help.

Last, but not least, the author would like to thank his wife, Nawal and his children Rana, Omar and Ahmed for their encouragement and long waiting.

To . .

My wife and children

for their love, patience and

sacrifices

TABLE OF CONTENTS

LIST OF PLATES

LIST OF FIGURES

LIST OF TABLES

NOMENCLATURE

A	=	as defined by equation (5.23 a).
A_L	=	receiver cross sectional area, m^2
A_s	=	condenser tube surface area, m^2
B	=	as defined by equation (5.23 b).
C	=	mathematical constant.
C_p	=	specific heat at constant pressure, kJ/kg °C.
D	=	outside diameter of condensing tube, m.
E	=	as defined by equation (5.25 a).
F	=	as defined by equation (5.29).
Fr	=	Froude number, $v^2 / g L$.
g	=	acceleration of gravity, m/s^2
H	=	dimensionless parameter, $C_p (T_v - T_s) / Pr\ h_{fg}$
h	=	mean heat transfer coefficient, W/m^2 °C
hx	=	local heat transfer coefficient, W/m^2 °C
h_{fg}	=	latent heat of condensation, kJ/kg.
K	=	as defined by equation (5.17 a).
k	=	thermal conductivity, W/m °C.
L	=	length, m.
M	=	mass flow rate, kg/s.
N	=	number of tubes in a vertical bank.
Noh	=	Ohesorage number, $\mu / (\rho g \nu \sigma)^{0.5}$

P = as defined by equation (5.19 d).

Pr = Prandtl number, $\mu C_p / k$

Q = heat flow rate, W

Re = Reynold number, $\rho v D / \mu$

R = dimensionless parameter, $\rho \mu / \rho_v \mu_v$

r = radius of the condensing tube, m.

T = temperature, °C.

T_{wi} = condensing tube inlet water temperature, °C.

T_{wo} = condensing tube outlet water temperature, °C.

U_∞ = vapor velocity, m/s

v = point velocity of condensate film in (y) direction.

V = volume flow rate, m^3 /s

w = weight fraction.

x = co-ordinate measuring radial distance outward from the tube surface.

X_0 = dimensionless parameter, $0.9(1 + 1/RH)^{0.33}$

y = co-ordinate measuring distance along circumference from upper stagnation point.

Z = oil to refrigerant mass ratio.

H_2O = water

Greek;

ΔT = film temperature drop, °C.

δ = thickness of condensate film, m.

μ = dynamic viscosity, kg./m.s.

ρ = density, kg./m^3.

θ = angle, measured from top of tube.

Ψ = as defined by equation (5.34).

σ = surface tension, N/m.

ν = kinematic viscosity, m^2/s.

Subscript;

h = high

L = low

m = oil-vapor mixture.

N = Nusselt

o = oil.

r = refrigerant.

s = condensing surface.

t = total.

v = vapor.

w = water.

1 = first vapor of two vapor mixture

2 = second vapor of two vapor mixture

CHAPTER 1

INTRODUCTION

The condenser is a heat exchanger in which the sensible and latent heat of the condensing vapor are transferred to the cooling medium. A refrigerating system condenser, Figure (1), removes both the heat absorbed by the refrigerant in the evaporator and the heat equivalent of the energy input to achieve compression of the refrigerant. The refrigerant is thereby converted back into the liquid phase at the condensing pressure and is available for re-expansion into the evaporator. The condenser has a major impact on the system efficiency and energy consumption.

Different types of condensers are available in use today, and the one which is studied here is the shell and tube, water cooled type. In this type of condenser the cooling water passes through the tubes while the vapor passes in the shell-side and condensation occurs on the outside surface of the tube, Figure (2).

Condensation is a process in which a change of phase takes place. A sudden change from the gaseous to the liquid phase occurs and then brings about a change in the density, viscosity, specific heat and thermal conductivity of the fluid, causing heat energy to be released.

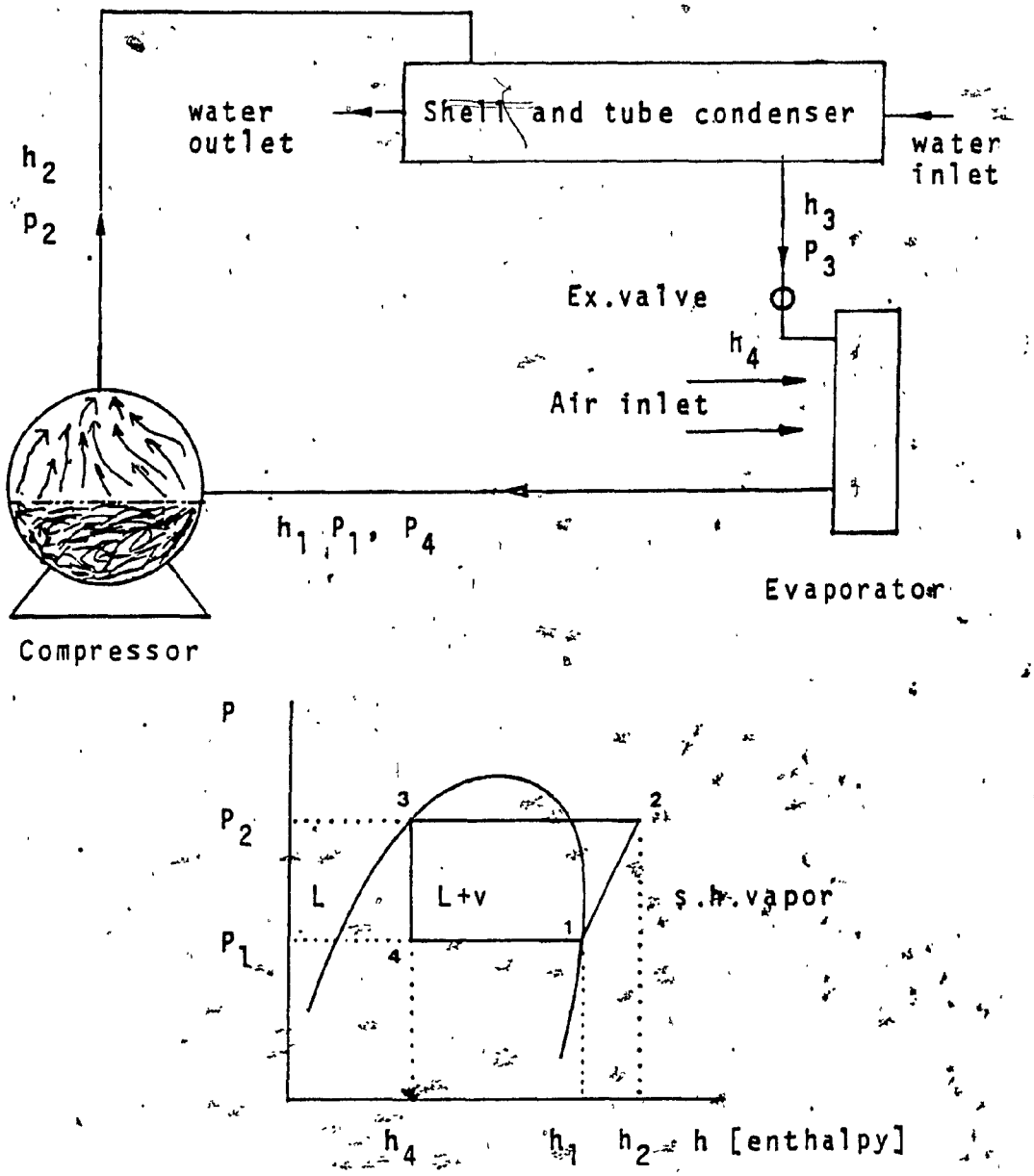

Figure no. 1: Refrigeration cycle

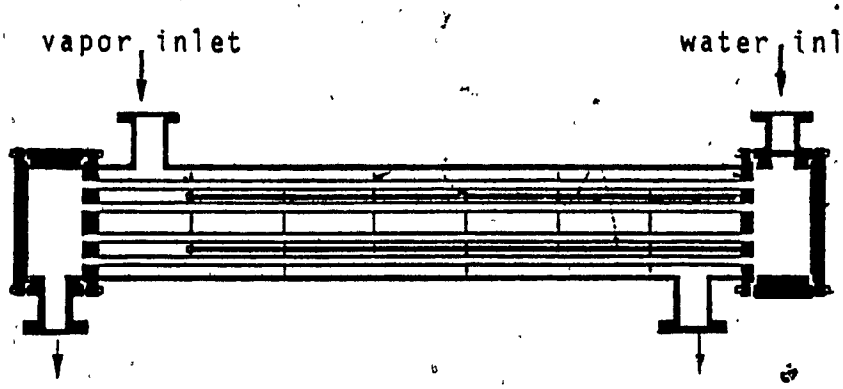

Fixed-head tubular exchanger

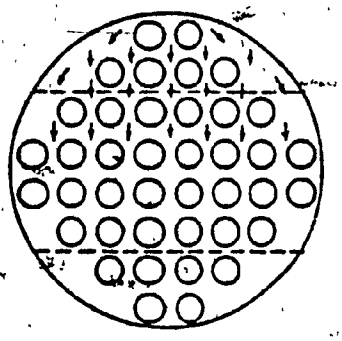

Flow across a bundle

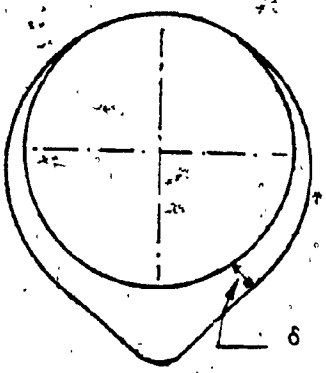

single condensing tube

Figure 2: Shell and tube condenser

Two modes of condensation can occur on a surface when the surface cools the surrounding vapor below the dew point: these are termed dropwise and filmwise condensation. The former consists of the formation of drops on the cold surface. These grow by coalescence and further condensation until they are removed from the surface under the influence of gravity and vapor friction.

In filmwise condensation, a thin layer of condensate covers the cooling surface, increases in thickness due to further condensation at the liquid vapor interface and flows away from the condensation surface under the influence of gravity and vapor flow, but due to gravity alone when stationary vapor is considered.

In either type of condensation mode, heat is carried from the vapor to the cooling surface by convection, conduction and mass transfer accompanied by condensation. In the filmwise mode, with the absence of non-condensible gases, the film formed on the cooling surface provides the major resistance to heat transfer from the vapor to the surface (1).

This study is a direct result of a nuisance problem which has long affected the air-conditioning and refrigeration industry and that is the migration of lubricating oil from the crankcase of the refrigeration

compressor in halogenated refrigerants, which is known to have a profound effect on system characteristics related to energy transfer from and to the circulating refrigerants. Under normal circumstances, oil presents a problem only with reciprocating or rotary compressors since the lubricating oil for these machines is in direct contact with the refrigerant gas. The rate of oil discharge is influenced by the type of compressor, the level of oil in the crankcase, and any refrigerant in liquid form reaching the suction of the compressor (2).

In Ref.(3) It is stated that "many of the halogenated refrigerants in use today are infinitely soluble in mineral oils at any temperature likely to be encountered. R-11 and R-12 are examples of such refrigerants. The only limit to the amount of these refrigerants that the oil can dissolve is that established by the refrigerant pressure at a given temperature. Other halogenated refrigerants such as R-22 and R-114 may show limited solubilites with the oil at the evaporator temperature and unlimited solubilities in the higher temperature region of a refrigerant system".

When oil and refrigerant get together, two modes of refrigerant-oil solution exist, depending on the mutual solubility of the oil and the refrigerant. Ref.(3) states "completely miscible refrigerants and oil are mutually soluble in all proportions and at any temperature under

consideration. A mixture of this type always forms a single liquid phase under equilibrium conditions no matter how much refrigerant or oil is present. Partially miscible refrigerant-oil systems are mutually soluble only to a limited extent. Above a certain temperature known as the critical solution temperature (CST), such an oil-refrigerant mixture is completely miscible and its behaviour is identical to the totally miscible oil and refrigerant. Below this temperature, however, the liquid may separate into two phases. Each phase may contain a substantial amount of the leaner component in the mutual solution, but these two solutions are themselves immiscible".

The presence of oil with the vapor at the condensing surface, therefore, results in a flowing condensate film of different thermal and physical properties than that which results when only pure vapors are condensed, and this is known to have an influence on the heat transfer performance of the condenser, although little information is available on the subject at present. It is however essential to quantitatively and qualitatively investigate the effects of the refrigerant-oil mixture on condensation heat transfer based on experimental and analytical studies as the condenser plays a major role in the refrigerant system. This is the objective of this study.

Refrigerants R-12 and R-22, along with the

alkylbenzene-based oil (150 SSU at 37.7 °C) were chosen for this study as they are commonly used in air-conditioning and refrigeration industries. Liquid R-12 and R-22 are completely miscible with the alkylbenzene-based oil in all proportions and at any operating temperature (above -.73 °C). The mixture will form a single liquid phase under equilibrium conditions. The properties of the mixture are different from those of the pure refrigerant and are dependent on the oil percentage (3). Consequently, with the presence of oil in the refrigerant vapor during condensation, the condensate layer on the tube wall surface can no longer be treated as a pure refrigerant condensate, but rather as a refrigerant-oil solution. Thus, the condensing coefficient is expected to be different from that of pure refrigerant condensation.

As an initial step, single tube tests were performed without oil in the refrigerant vapor to compare with the results from other investigators in the past. These were followed by tests with predetermined amounts of oil up to 8 per cent in weight.

The condensing heat transfer of a multi-tube bundle is quite different from that of a single tube. Therefore, condensation on four tubes, stacked in a vertical row, was investigated with the same oil contents as in the single tube tests.

On all test runs, the heat balances from both condensing refrigerant and cooling water were checked to ensure that both sides functioned properly. The condensing coefficients were then calculated from the direct method.

A test apparatus, to actually simulate the oil carry over into the condenser was designed and presented along with a special experimental technique for excuting the tests at constant oil-to-refrigerant mass ratios.

Several figures of condensing coefficients as function of oil percentage and film temperature drop were presented.

Analytical and empirical equations defining the condensing coefficient, for both single and multi-tube cases, with and without oil, were deduced and presented.

Finally, there was a presentation of conclusions, recommendations and suggestions for future work.

CHAPTER 2

LITERATURE SURVEY

Information concerning the heat transfer coefficient during filmwise condensation of steam and halogenated refrigerants condensing on the outside surface of plain horizontal tubes is presented in this survey. Low velocity vapors, high velocity vapors and the effects of oil on the film condensation are covered.

2.1- Condensation of oil free vapors:

The process of condensing vapors on tubes and cylinders has been treated experimentally and theoretically by many investigators and great progress has been made with analytical approaches. The phenomenon of film condensation was, first, mathematically analysed by Nusselt (4). He presented a theoretical relation for calculating the heat transfer coefficient of condensing vapor on the outside surface of a horizontal tube. The theory states that the condensate on the cooling surface flows down under the influence of gravity but is retarded by the viscous forces of the liquid. By combining the law of laminar flow of a fluid and the heat of conduction through it, Nusselt arrived at the following relation for the mean heat transfer coefficient on a single horizontal tube:

$$h = 0.725 \left[\frac{g\, h'_{fg}\, k^3\, \rho^2}{\mu\, \Delta T\, D} \right]^{0.25} \qquad \text{-------(2.1)}$$

According to Nusselt's theory, 59.4% of the total condensate rate takes place on the upper half of the tube and 40.6% on the lower half (5).

For a bank of horizontal tubes in one row, Nusselt arrived the following expression

$$h = 0.725 \left[\frac{g\, h'_{fg}\, k^3\, \rho^2}{\mu\, \Delta T\, D} \right]^{0.25} \left[\frac{1}{N} \right]^{0.25} \qquad \text{---(2.2)}$$

in which condensate loading per tube in a row is equal to the total condensation rate divided by the number of tubes in the row. The analysis does not include the turbulence and rippling of the condensate layer when descending from tube to other below.

Nusselt's equation had been verified experimentally and theoretically by many investigators. C.G.Kirkbride (6) attempted to predict the coefficient of heat transfer of two mixed vapors condensing on a horizontal tube. He assumed

that Nusselt's equation (2.1) could be used to compute the heat transfer coefficient for each component as if it was condensing alone. The average coefficient was then computed from the equation

$$h = \frac{h_1 Q_1 + h_2 Q_2}{Q_1 + Q_2} \qquad \text{----------(2.3)}$$

which is a weighted average of the coefficients of the two components as computed from equation (2.1). The coefficients are weighted according to the amount of heat received per unit time from both condensing vapors. An average deviation of 10 per cent between the experimental results and the predicted values was observed.

Edwin M. Baker and A. Mueller (7) concluded that the temperature variation around the perimeter of a horizontal tube on which vapor is condensing, is important and cannot be neglected in the calculation or determination of heat transfer. The authors described a method for measuring such temperature variation and they were the first among the investigators to do that.

An extension of the work conducted in (7) was performed by E.M. Baker and U.Tsao (8). The coefficient of heat transfer from vapor to the horizontal tube was determined

for the condensation of mixed vapors of water and a nonmiscible organic liquid. An empirical equation was derived which was reported to correlate the data presented in (7) as well as the data obtained by the authors. The equation is

$$h = \frac{366 \sqrt[4]{\frac{1}{D}} \left[1 - \frac{0.0284}{D} \right]}{1 - 0.0085 \text{ vol.\% } H_2O} + \frac{1.67}{D} \qquad \text{-------(2.4)}$$

Equation (2.4), which is in English units, was compared with the experimental results presented in (6). The limitations of equation (2.3) are reported to be overcome by equation (2.4). The results of the study show that the temperature drop has no effect upon the heat transfer coefficient, and that the heat transfer coefficient decreases with the decrease of tube diameter, and this contradicts Nusselt's theory (4). The reported explanation of this has not been confirmed by other investigators.

Nusselt's theory for the condensation heat transfer on multi-tubular condensers was experimentally checked for the first time by F.L. Young and W.J. Wohlenberg (9). Freon-12 was condensed on a vertical bank consisting of five horizontal tubes. The heat transfer coefficient for the top tube was found lower than what was predicted by Nusselt's

theory, but for the lower tubes, the theory seems to underestimate it. The relatively higher heat transfer coefficient for the lower tubes was attributed to the turbulence and mixing of the condensate layer which were not accounted for in Nusselt's theory. According to the experimental results, Nusselt's equation (2.1) was modified for the successive tubes in the bank. In evaluating the theoretical heat transfer coefficient, the physical properties of the fluid were taken at an average between the wall and the vapor temperatures, but no tables of properties were presented.

R.E.White (10) constructed an apparatus for the direct determination of the condensing film coefficient of heat transfer on 15.8 mm (5/8 inch) OD tubes. By direct measurements of the condensing surface temperature, he found that the experimental results fall 13 per cent below Nusselt's theory at all condensing temperatures. This seems to agree with the results obtained in (9). According to the data obtained, Nusselt's equation (2.1) was modified as follows

$$h = 0.63 \left[\frac{h_{fg}\ g\ k^3\ \rho^2}{D\ \mu\ \Delta T} \right]^{0.25} \qquad \text{------(2.5)}$$

Equation (2.5) is very close to the modified Nusselt

equation for the top tube of a tube bank reported in (9). It is mentioned that the physical and thermal properties used to obtain the theoretical heat transfer coefficient, were unpublished and no tables were presented.

Allan P.Colburn (11) presented Nusselt's equation for predicting the heat transfer coefficient of high velocity vapors condensing on a horizontal tube. Nusselt assumed that the entire condensate layer is in viscous flow similar to that of stagnant vapor. The thickness of the condensate layer was determined by the combined effects of gravity and vapor friction at the liquid-vapor interface. The heat transfer correlation as quoted in (11) is:

$$h^3 = \frac{k^3 g \rho^2}{3 \mu \Gamma} + \frac{k^2 \rho F_v h}{2 \mu \Gamma} \qquad \text{----------(2.6)}$$

where Γ = condensate rate per unit periphery, kg/m.s.

F_v = vapor shear force, kg/m^2 .

The condensation film heat transfer coefficients for individual horizontal tubes in a vertical bank of tubes were investigated experimentally by B.E. Short and H.E. Brown (12) with variable cooling flow rates. Freon-11 and steam were condensed on two different condensers each consisting

of twenty horizontal tubes mounted in a vertical bank. It was found that the overall thermal resistance for individual tubes decreases linearly with the increase of water flow rate inside the tubes. The reduction of the water side film resistance was found to increase the condensation rate on the tube and hence to result in a higher condensing side thermal resistance. A comparison between the experimental data and the results obtained from Nusselt's theory showed that the experimental heat transfer coefficient for the top tubes was higher than that predicted by the theory, but was lower for the middle tubes. The lowest tubes show a higher heat transfer coefficient than that predicted by Nusselt's theory, and that was attributed to turbulence of the condensate film. The results obtained for the lowest tubes were found to agree with the results obtained in (9).

The discrepancy between the experimental data of many investigators and Nusselt's theory was attributed by R.E.Peck and W.A.Reddie (13) to the assumptions made by Nusselt concerning the film temperature drop and acceleration forces. The former was assumed constant and the later negligible. After performing experiments, the authors concluded that the variation of temperature drop around the tube cannot account for the deviation from Nusselt's theory, but by including the acceleration effects, the authors arrived at a certain correlation with constants that had to be evaluated by empirical investigation based on

the experimental data taken by the authors and other investigators. The semi-empirical relation obtained is:

$$h = h_N \left[0.0206 \left(\frac{h_{fg}\, \mu}{\Delta T\, k} \right)^{0.5} + 0.79 \right] \qquad \text{-----(2.7)}$$

where h_N is Nusselt's theoretical heat transfer coefficient. It is reported that equation (2.7) gives more accurate values of the condensate film heat transfer coefficient for the case of saturated vapor condensing on a horizontal tube than that given by Nusselt's equation.

W.M.Rohsenow (14) attempted to obtain an analytical expression for the condensing heat transfer coefficient taking into account the effect of cross flow within the film and a nonlinear temperature distribution. The actual film temperature distribution was reported to be

$$\frac{T - T_s}{T_v - T_s} = \frac{\frac{x}{\delta} + \frac{C_p\, \Delta T}{h_{fg}'} \left[-\frac{1}{8} \left(\frac{x}{\delta} \right)^4 + \frac{1}{40} \left(\frac{x}{\delta} \right)^5 \right]}{1 - \frac{C_p\, \Delta T}{10\, h_{fg}'}} \qquad \text{-----(2.8)}$$

The condensing heat transfer coefficient found was

$$h = 0.943 \left[\frac{k^3\, g\, h_{fg}\, \rho\, (\rho - \rho_v) \left(1 + 0.68 \frac{C_p\, \Delta T}{h_{fg}} \right)}{\mu\, \Delta T\, L} \right]^{0.25} \qquad \text{-----(2.9)}$$

where $h'_{fg} = h_{fg} + 3/8\ C_p\ (T_v - T_s)$

It is reported that the results obtained with equation (2.9) are closer to the experimental results than the ones obtained with assumed linear distribution, equation (2.1).

Donald Q. Kern (15) modified Nusselt's average condensing coefficient for a tube in an N-tube vertical bank from $N^{-0.25}$ to $N^{-1/6}$ times the single tube coefficient. This modification accounts for the turbulence which occurs due to ripples and intermittent dripping of the condensate layer when descending from a higher tube to a lower one in the tube bank. The modified Nusselt's equation is

$$h = 0.725 \left[\frac{g\ h_{fg}\ k^3\ \rho^2}{\mu\ \Delta T\ D} \right]^{0.25} \left[\frac{1}{N} \right]^{\frac{1}{6}} \qquad \text{---(2.10)}$$

The problem of laminar film condensation on a horizontal cylinder was investigated by E.M. Sparrow and J.L. Gregg (16) by using the mathematical techniques of boundary layer theory. They were the first among the investigators who applied this technique to the condensation. The three partial differential equations of

mass, momentum and energy transfer were reduced to ordinary differential equations which then were solved numerically. Inertia forces and energy convection which were neglected in (4), were fully accounted for. The study revealed that for small film thickness, the heat transfer results are very close to Nusselt's theory and the effect of energy convection would be to increase the heat transfer, while the role of the inertia forces would be to decrease the heat transfer. So these two effects are in conflict. It is reported that with increasing film thickness for the high Prandtl number fluids, where the inertia forces are completely overriden by the viscous forces, the effects of energy convection win, thus increasing the heat transfer. But for the low Prandtl number fluids where the thermal conduction overrides the energy convection, the effects of the inertia forces win, resulting in a decrease of heat transfer.

M.M. Chen (17) performed an analytical study of laminar film condensation on single and multiple horizontal tubes, utilizing the boundary layer equation technique. For the case of a single tube inertia forces were accounted for. The theoretical results obtained were compared with those of (16) and good agreement was noticed. Also it was seen that the inertia forces have a larger effect on the heat transfer of round tubes than flat plates whose analysis was carried out by the same investigator.

For the case of condensation on a vertical bank of horizontal tubes, the analysis included the effects of condensation between the tubes and momentum gain. It is reported that the first tube in a vertical bank can be considered as a single tube and the heat transfer results obtained for the case of a single horizontal tube can be used without modification. But for the lower tubes the momentum gain and the condensation between the tubes resulted in higher results than Nusselt's theory. Higher heat transfer rates than the theory predicted were attributed to splashing, intermittent dripping and local dripping.

Condensation on the external surface of a cylinder in a transverse flow was analytically studied by I.G. Shekirladze and V.I. Gomlari (18). Separation of the boundary layer due to high vapor velocity was considered, and the boundary layer was assumed to be laminar up to the separation point. Analytical expressions for the case of flow without separation, with and without body forces, were determined. The heat transfer coefficient in condensation on a horizontal cylinder in a downward flow of vapor without separation and with body forces was found to be

$$h = 0.64 \left[\frac{U_\infty \rho k^2}{\mu D} \right]^{0.5} \left[1 + \left(1 + \frac{1.69\ D\ g\ r\ \mu}{U_\infty^2\ \Delta T\ k} \right)^{0.5} \right] \qquad \text{---(2.11)}$$

Equation (2.11) was compared with experimental data of three experimental sets of results, in which the maximum velocity of the incoming vapor was less than 3 m/s, (which was assumed to be small) and the flow around the tube was without separation.

A similar expression was determined for a flow with minimum separation angle θ = 82 degrees where the coefficient of equation (2.11) decreased by 35 per cent. Under real conditions, separation may begin at any point from θ = 82 to 180 degrees. Therefore, equation (2.11) with the largest and smallest coefficients (i.e. 0.64 and 0.42) will yield the upper and lower limits of the range of the mean heat transfer coefficient with a separated boundary layer. The theories were compared with experimental results of condensing vapors flowing at velocities higher than 3 m/s. It was found that the experimental points fall between the highest and lowest value of the theoretical results, where the flow was accompanied by a boundary layer separation. It was concluded that the theories deduced were satifactory, and the boundary layer separation leads to a sharp decrease of the heat transfer rate over a portion of the cylinder surface behind the separation point.

G.L.Henderson and J.M.Marchello (19) proposed a

correlation to deal with a region near the bottom of a condensing horizontal tube where Nusselt's theory (2.1) fails due to thickening of the film and droplet break-off. Surface tension forces were accounted for. The authors correlated the experimental data of various observers and Nusselt's theory with the Ohnesorage number to derive an equation which provides a means of accounting for the process occurring at the bottom of the pipe. The general correlation of the heat transfer coefficient deduced is:

$$h \left[\frac{\mu^2}{g \rho^2 k^2} \right]^{\frac{1}{3}} = 0.069 \, Noh^{-0.373} \, Re^{-0.333} \qquad \text{-------(2.12)}$$

Equation (2.12) contains Nusselt's analysis and the correction for the effects of surface tension.

An analytical solution, based on Nusselt's assumptions, has been obtained for laminar condensation of a flowing vapor on a horizontal cylinder by Denny and Mills (20). The variable fluid properties were accounted for and evaluated at a reference temperature. Verification was obtained by comparison with an exact numerical solution based on a finite difference analogue to the conservation equations in boundary layer form. Vapor drag due to vapor velocity was accounted for through an asymptotic solution of the vapor

boundary layer under strong suction. The local theoretical heat transfer coefficient obtained was compared with the numerical solution as a function of the angle (θ) around the tube. The discrepancy was found to be less than 2 per cent for (θ) less than 140°, but for 140° < (θ) < 180° the discrepancy increased. It is reported that the increased discrepancy as (θ) approaches 180 degrees could be due to either inadequencies in the $\sin\theta$ averaging or violation of Nusselt's assumptions of negligible inertial effects which are grossly violated as (θ) approaches 180 degrees.

Condensation heat transfer of vapor flowing through a tube bank crossing them horizontally was experimentally studied by Fujii, et al.(21). The results from two tube banks of inline and staggered arrangements were compared, and the following heat transfer correlation was proposed:

$$N_u = K X_o \left[1 + \frac{0.276}{X_o^4 F_r H} \right]^{0.25} Re^{0.5} \quad \text{------(2.13)}$$

where K=0.8 for inline arrangements and unity for staggered arrangements. Equation (2.13) showed good agreement with the experimental data of other investigators. The patterns of temperature distribution for inline and staggered arrangements seem to be different from each other and also from those on a single tube.

The two phase boundary layer equations of filmwise condensation on a horizontal tube were solved with an approximate method by Fujii,et al. (22). The condensate layer pressure and inertia forces were not accounted for. The theoretical model obtained was in good agreement with the experimental results of other investigators. The temperature distribution on the periphery of the tube was found to be effected by the oncoming vapor velocity, and the local heat transfer coefficient became relatively higher with increasing vapor velocity, but body forces became negligible. It is reported that 80 per cent of the total condensation took place on the upper part of the cylinder.

Ivanov,et al. (23) studied experimentally the heat transfer coefficient of condensing R-12 vapor moving through a bundle of smooth and finned tubes. The study revealed that the average heat transfer coefficient was markedly higher than the values predicted by Nusselt's equation (2.2). The effect of condensate flow from higher tubes to the lower ones in the bundle may be accounted for more exactly by the factor $N^{-0.16}$ rather than $N^{-0.25}$ in Nusselt's theory (4) due to film turbulence formation. This finding agrees with that of Kern (15). It is stated that for a tube bundle the heat transfer coefficient does not vary with $\Delta T^{-0.25}$, as stated by Nusselt's theory.

The condensate film inertia and pressure forces, energy

convection and liquid subcooling were not treated simultaneously by previous investigators, instead, some or all of these parameters were ignored. E.S.Gaddis (24) presented a method for solving the full two phase boundary layer equations for the condensation of flowing vapor on a horizontal tube, taking all these parameters into consideration. The theoretical model obtained was compared with Nusselt's theory. For water, good agreement was found to exist between the theories, but there was a difference when these theories were applied to fluids of a Prandtl number much higher or much lower than unity. The difference in the two theories was attributed to:

1- For low Prandtl number fluids the convection is not effective but ignoring the inertial forces increased the Nusselt number by 30 per cent. Ignoring the shear forces at the liquid vapor interface gave rise to a 20 per cent in Nusselt's number.

2- For high Prandtl number fluids the inertial forces in the condensate layer and the shear force at the liquid vapor interface have an insignificant effect on the Nusselt number, but eliminating energy convection leads to a reduction of 5 per cent.

Kutateladze et al.(25) conducted experimental investigations to determine the effects of the film

temperature drop ($T_v - T_s$), vapor velocity, condensation pressure and position of the tube on the heat transfer coefficient of condensing vapors in a vertical bundle of inline and staggered tube condensers. Refrigerant R-21 was used. It was found that the heat transfer coefficient decreases on both tube arrangements as the vapor flows deeper in the bundle. Decrease of vapor velocity and increase of temperature drop resulted in a decrease of the heat transfer coefficient. The experiments showed that, for stationary vapor, the number of rows has an influence only up to a certain temperature drop above which the heat transfer remains constant and independent of the position of the tube in the bundle. But for the case of high vapor velocity, each tube can be regarded independently.

Experiments of heat transfer in condensation of flowing vapor of Freon-21 were conducted in a vertical stack of ten smooth horizontal tubes by Kutateladze et al.(26). Data were obtained on the dependence of the heat transfer coefficient on the temperature gradient and the vapor velocity. The stationary vapor experiments showed that the heat transfer coefficient, h, of the first and second tube of the bundle varies with $(\Delta T)^{-0.25}$ which is in accordance with Nusselt's theory, but in the lower tubes, h, was found to depend less on ΔT and on the tube location and this was attributed to the change in the mode of flow of the condensate film. In the case of flowing vapor, only the

first tube was reported to follow Nusselt's theory concerning $h \propto (\Delta T)^{-0.25}$. The lower tubes of the bundle ceased to follow this relation. The results of this study revealed the following:

1- In the case of stationary vapors, the tube location was found important to a certain value of ΔT, above which (h) becomes almost constant.

2- At high vapor velocity, the behaviour of each tube can be treated independently due to condensate break-off.

3- The experimental data for flowing vapor were found to be in satisfactory agreement with the Fujii equation quoted in (22).

4- The effects of run-off of condensate onto lower tubes and vapor velocity must be corrected for simultaneously due to turbulance occurring in the condensate layer for the lower tubes.

2.2 - Condensation of oil refrigerant mixture:

Available information on the effect of refrigerant-oil mixtures on condensation heat transfer is very limited. Mirmov,et al.(27,28) investigated experimentally the effects of ammonia-oil mixtures on condensation heat transfer.

Mineral oil was used. Ammonia and mineral oil solution are classified as totally immiscible (29). It was reported that the presence of oil may lead to partial dropwise condensation and may also help reduce fouling. Hence, the heat transfer coefficient for oil-ammonia mixture was higher than that for pure ammonia vapor; but no percentage of oil in the mixture was reported.

William and Sauer (30) studied the effects of R-11 vapor-oil mixtures on condensation heat transfer outside a single plain horizontal tube. Naphthene-based oil with two different viscosities (150 and 500 SUS at 37.7 ℃) were used. R-11 and mineral oil are totaly miscible (29). For each set of test runs conducted, a certain oil flow rate was maintained. Thus, the percentage of oil to refrigerant mass ratios would increase as the film temperature drop ($T_v - T_s$) decreased. They concluded that, for 150 SUS viscosity oil, there was no appreciable change in the heat transfer coefficient for oil concentration less than (6 to 7%); but as the oil concentration was increased above this range, the condensation heat transfer coefficient decreased significantly. For the 500 SUS viscosity oil, they reported that the presence of oil, even at high concentration, had no significant effect.

The experimental method used by William and Sauer has the following limitations:

1- A regulated air supply from a compressed air cylinder was used to inject the oil-refrigerant mixture into the test section. The air pressure applied was 689 kPa (100 psig). Because of the use of high pressure air, a strong possibility exists for air to be dissolved in the oil and be transferred to the condensing surface. It is well known that the presence of a non condensible gas, even in small amounts may result in the reduction of condensation heat transfer;

2- The spray action of the refrigerant-oil mixture directly on the condensing surface used in the experimental apparatus was reported to have a significant effect on the heat-transfer coefficient.

Finally, the survey shows that the available information on the condensation of oil-vapor mixture are not only limited, but contradictory to each other. Neither a real simulation test apparatus, to experimentally investigate the effects of oil on condensation under closely controlled conditions, has been described nor have attempts been made to treat the problem mathematically.

CHAPTER 3

EXPERIMENTAL APPARATUS

3.1- Introduction

To study the effect of oil on the condensation heat transfer rates of refrigerant on the outside surface of single and multiple horizontal tubes, a special test apparatus as shown schematically in Figure (3) was designed and built. The apparatus is so equipped that an actual simulation of the oil carry over into the condenser may be performed.

The highlights of the design of this test apparatus are as follows:

(a)- It is so designed that a predetermined amount of lubricating oil is atomized and mixed with the refrigerant vapor and the mixture is then led to the test condenser under investigation. In fact, any desired amount of oil, carried over by the refrigerant vapor from the compressor into the condenser, can be precisely simulated.

(b)- Condensation results can be accomplished for constant oil to refrigerant mass ratios at varying temperature differences between the refrigerant vapor and tube wall.

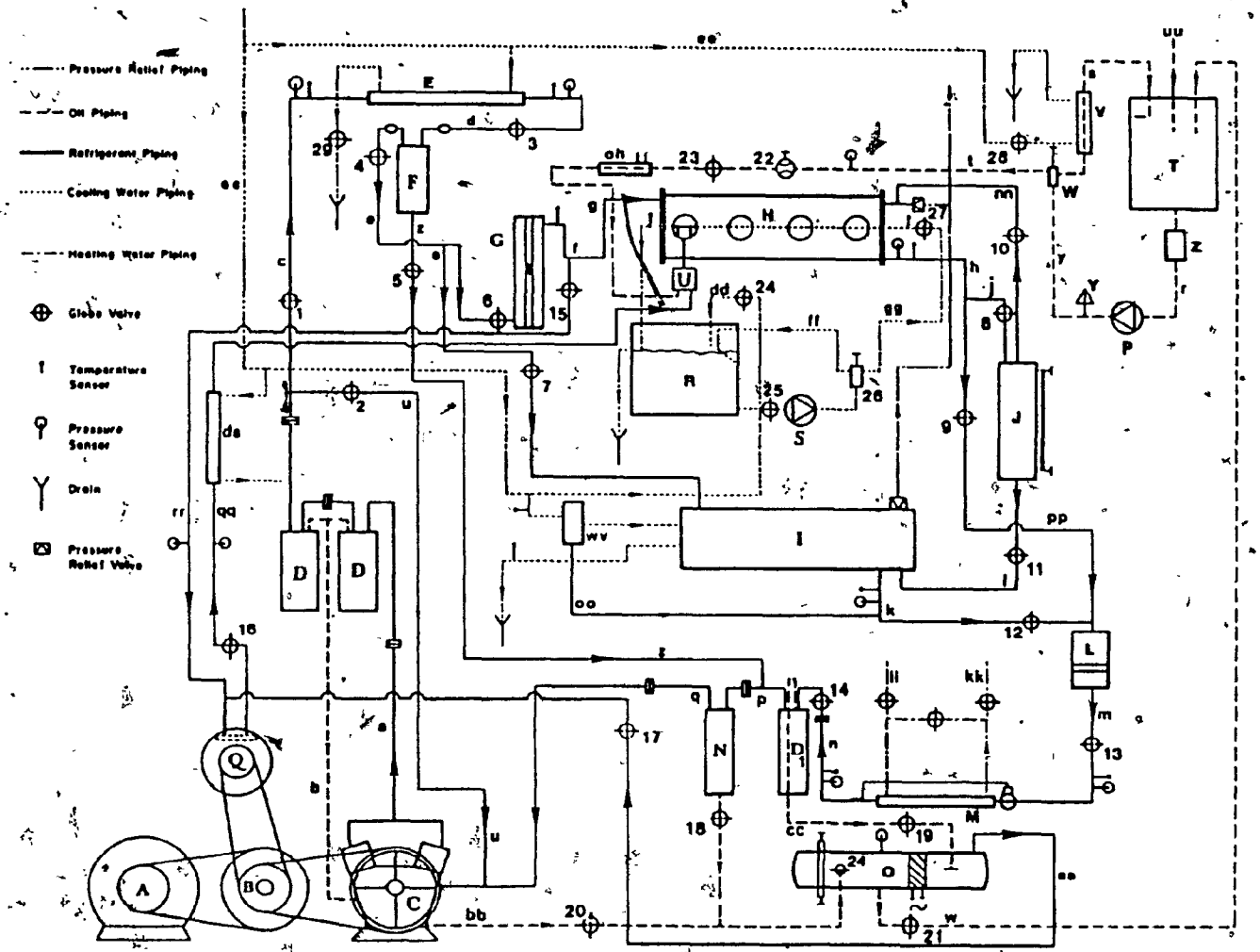

Figure 3 : Test apparatus

LEGEND
(For Figure 3)

A - 15HP Electric Motor

B - Intermediate Pullies

C - Compressor

D - Discharge line oil separators

E - Desuperheater

F - Refrigerant condensate separator

G - Refrigerant vapor flow meter

H - Test condenser

I - Full size condenser

J - Liquid receiver

L - Filter-drier

M - Evaporator

D_1 - Suction line oil separator

N - Suction line accumulator

O - Oil receiver

P - Oil pump

Q - Booster compressor

R - Water Reservoir

S - Water Pump

T - Oil reservoir

U - Oil atomization unit

V - Oil cooler

W - Pressure regulating valve

Y - Pulsation damper

Z = Oil filter

oh= Oil heater

wv= Pressure operated water valve

(c)- The condensing film coefficient can be determined from both the direct method (from heat flux and temperature difference between the refrigerant vapor and tube wall) and the indirect method (from overall and tube side heat transfer).

(d)- It provides clear visual observation of the condensation process in the test condenser.

(e)- It has the capacity of testing the different commonly used refrigerants, namely R-12, R-22 and R-502.

(f)- For a particular refrigerant, a wide range of saturation pressures may be selected.

(g)- Accurate measurements of the refrigerant condensation rates can be obtained.

(h)- Both saturated and superheated vapors can be achieved, and any degree of superheat within the compressor capability may be maintained.

(i)- A wide range of condensation rates may be accomplished for a particular refrigerant at a given saturation pressure.

(j)- A broad selection of cooling water velocities,

inside the condensing tubes, can be provided.

(k)- Different cooling water temperatures may be obtained and a precise constant water temperature may be maintained at the inlet of the condensing tube (s).

(l)- A steady-state condition can be usually maintained.

(m)- It provides good control of pressures and temperatures throughout the different components of the system.

(n)- Easy separation of the oil and refrigerant during the running of tests may be obtained.

(o)- No compressed air is involved in the spray system. Moreover, oil atomization and mixing with the refrigerant vapor can be done at a distance far from the condensing tube, and the portion of the condensing tube right at the spray flow can be made inactive for condensation.

The accuracy of the condensing coefficient obtained depends upon close control of the conditions for a particular test. Such conditions involve superheat temperature, saturation pressure, condensate flow rate, tube

wall surface temperature, and cooling water inlet and outlet temperatures. All these points have been taken care of during both the design and manufacturing stages of the test apparatus. Consequently, it is felt that for the purpose of studying the effects of the refrigerant-oil mixture on condensation, this facility is reasonably accurate and fully reliable.

3.2- Description of the test apparatus

The test apparatus consists of four circuits, namely refrigerant, oil, cooling water and hot water. Details of these ciruits are given below.

3.2.1- REFRIGERANT CIRCUIT:

The refrigerant ciruit is the most important in the entire system. The specifications, functions and special design features of its components are as follows:

3.2.1.a- Compressor: (C)

The compressor is one of the five essential parts of the compression refrigeration system. The compressor used in the test apparatus is a reciprocating, four-cylinder, single acting open type with a capacity of ten refrigeration tons rated at 700 RPM and 5°C suction temperature. An 80 watt crankcase heater is used to warm the lubrication oil and prevent refrigerant condensation inside the compressor during the shutdown period.

3.2.1.b- Discharge line oil separator: (D)

Two oil separators were installed, in series, in the compressor discharge line to prevent the migrating oil which leaves the compressor crankcase with the compressed vapor from reaching the condenser under investigation. A 6.35 mm (0.25 - inch) O.D. tube was used to carry the oil from the separator back to the compressor crankcase. The separators used are serviceable (bolted construction) to allow for draining and flushing when required.

3.2.1.c- Desuperheater: (E)

In this study, only saturated vapor is required to be condensed in the test condenser. Consequently, a desuperheater was designed and fabricated to remove the superheat in the refrigerant vapor on the way to the test condenser. The desuperheater is a double pipe heat exchanger, with the vapor passing through the inner pipe and the cooling water at the annulus.

The heat exchange capacity of the desuperheater is controlled by a 9.5 mm (3/8 inch) throttle valve installed at the water outlet. Any degree of superheat in the vapor may be achieved by admitting the necessary rate of cooling water.

3.2.1.d- Refrigerant condensate separator: (F)

Occasionally, there are cases in which the vapor may contain already condensed refrigerant prior to entering the test condenser. In order to have accurate measurements of the condensation rate in the test condenser, a condensate separator was installed between the desuperheater and the test condenser. Any collected condensate in the separator will be transferred back to the compressor suction line through valve no. 5 and a 12 mm (half-inch) O.D. tube. Two sight glasses were mounted on the inlet and outlet pipes of the condensate separator to monitor the flow situation.

3.2.1.e- Refrigerant vapor flow meter: (G)

This study emphasizes the effect of oil on refrigerant vapor condensation, thus, it is highly desirable to obtain the condensation heat-transfer coefficient at constant oil to refrigerant mass ratios. To keep such a constant ratio, a corresponding refrigerant vapor flow rate is required to match the fixed oil flow rate. The refrigerant vapor can only be measured by a vapor flow meter. A full view, packed gland, glass tube flow meter was installed between the condensate separator and the test condenser. Even though this type of flow meter is usually designed and calibrated for a specific set of fluid conditions, such as specific gravity, viscosity and range of flow, recalibration is still needed for each condensing temperature of the refrigerant vapor to ensure accurate results. This was done with the pure refrigerant vapor condensed at different

vapor-to-surface temperature drops, and calibration curves as shown in Figures (4 , 5) were generated for each refrigerant vapor condition under investigation.

3.2.1.f- Test condensers:

Two horizontal test condensers were built in this study, one for single-tube tests, the other for multi-tube tests. Both are water-cooled shell-and-tube type, and insulated with thermaflex insulation material.

A-Single tube test condenser: (H)

Both 15.8 mm and 25.4 mm (5/8 inch and 1 inch) outside diameter copper tubes, each with 1.65 mm (0.065 inch) thickness, were used in this study. Cooling water flows inside the tubes. Refrigerant 12 single tube tests on the 25.4 and 15.8 mm (1 and 5/8 inch) O.D. tubes were performed in this condenser. The 25.4 mm (1 inch) O.D. tube length was 1620 mm (63.6 inches) for the condensation study of pure refrigerant vapor. For the refrigerant-oil mixture tests, the effective condensing tube length was reduced to 1400 mm (55 inches) due to the fact that the portion of the test tube directly facing the refrigerant vapor-oil mixture inlet was made inactive to heat transfer in order to eliminate the dynamic flow effect of the vapor-oil mixture on the condensation process. The effective length of the single 15.8 mm (5/8 inch) O.D. tube was 1470 mm (58 inches) long. The shell is made of cold drawn seamless mechanical tubing,

with a 203 mm (8 inches) outside diameter and a 6.35 mm (0.25 inch) wall thickness. Three glass windows were attached to the shell to enable visual observation of the condensation process. An oil nebulizer assembly was bolted to the shell close to the cooling water outlet end. The tube end sheets were made of steel plate, 279 mm square and 38.1 mm thick (11 inches square and 1.5 inch thick). Besides the tube connections, the vapor inlet, the condensate outlet, the pressure relief valve and thermocouple passages are all located at the end sheet. Adequate lighting was furnished inside the shell to allow observation of the condensation phenomena through the glass windows.

It should be noted that a sealing method was adopted for the tube to sheet joints to provide easy disassembly as required without causing any damage to the tube.

B- Multitube test condenser: (H)

This is a single-pass condenser comprising four copper tubes, one steel shell and two steel end sheets. The design and specifications are similar to those in the single tube test condenser with the exception that only 15.8 mm (5/8 inch) outside diameter tubes were used and arranged in a vertical row with a spacing of 31.7 mm (1.25 inches). The effective condensing length of each tube is 812 mm (32 inches). Single tube tests with R-22 vapor, pure and mixed

with oil, were performed on the top tube of the bundle while the lower tubes were made inactive for condensation.

3.2.1.g- Full size condenser: (I)

It is a (1 to 4) pass, removable bundle exchanger, designed and fabricated with a capacity of five tons of refrigeration. The tube bundle element consists of 18 X 19 mm (3/4 inch) O.D. plain copper tubes, each 1828 mm (72 inches) long. The full size condenser serves as a system pressure controller and also as a liquid refrigerant reservoir. The system condensing pressure is regulated by the adjustment of the cooling water flow rate through this full size condenser.

3.2.1.h- Liquid receiver: (J)

One of the important features in condensation studies is the determination or measurement of the rate of vapor condensation. In this study, this was achieved by collecting the condensate in a receiver of known cross-sectional area , recording the change of the level, and calculating according to the following equation:

$$M_r = (L_2 - L_1) A_L \rho$$

$$Q = M_r h_{fg}$$

where M_r is the liquid refrigerant flow rate, ρ is the density of the liquid at the condensing temperature, A_L is the cross-sectional area of the receiver and ($L_2 - L_1$) is the change of the liquid level in the receiver per unit time.

A pressure balance tube was connected from the test condenser to the receiver, thereby maintaining a constant liquid level in the test condenser.

3.2.1.i- Liquid line filter drier: (L)

A filter-drier was installed between the liquid receiver and the evaporator to: (a) avoid the moisture freezing problem in the expansion valve; (b) prevent moisture from mixing with oil in the system; and (c) remove dirt or chips.

3.2.1.j- Expansion valve:

A thermostatic type of expansion valve was chosen to control the mass flow rate of the liquid refrigerant entering the evaporator and to keep the unevaporated refrigerant in the evaporator from returning through the suction line to the compressor.

3.2.1.k- Evaporator: (M)

The evaporator is the part of the refrigeration system

where the liquid refrigerant boils or evaporates at constant temperature and pressure, thereby producing a cooling effect on the fluid being circulated. However, there are two types in use today, air cooling and liquid cooling evaporators. In this study, a liquid cooling evaporator is used.

The evaporator was designed and built from four sets of double-pipe heat exchangers. The heating water circulates through the annulus while the refrigerant evaporates inside the inner tube. The outer and inner tubes are 41.2 and 28.5 mm (1.6 inches and 1.1 inches) outside diameters respectively, both made of copper, with an effective length of 1524 mm (5 feet) each.

3.2.1.1- Suction line oil separator: (D_1)

In the study of condensation of the refrigerant vapor mixed with oil, the oil was atomized and added to the pure refrigerant vapor before entering the test condenser. The oil in the refrigerant stream passing from the condenser to the suction line was separated with a separator in order to recycle the oil and to avoid flooding the compressor crankcase. The construction and operating mechanism of the suction line oil separator is exactly the same as that of the compressor discharge line oil separator. The separated oil was carried away, through a float valve, in a 6.35 mm (0.25 inch) O.D. tube back to the oil receiver.

3.2.1.m- Suction line accumulator: (N)

The accumulator is a standard component associated with the compressor. It is a safety device to prevent liquid refrigerant from flowing into the compressor.

3.2.1.n- Refrigerant piping:

The piping design was made according to the refrigeration piping code quoted in Ref.(31) to accomplish the following objectives:

1- Insure proper feed to the evaporator.

2- Provide practical line size without excessive pressure drop.

3- Prevent lubricating oil from being trapped in the system.

3.2.2- OIL CIRCUIT:

In this study, a specially-designed oil circuit was employed to establish the relationship between the condensing coefficient and the temperature difference between the vapor and the tube wall, at a fixed oil-to-refrigerant mass flow ratio. Just before entering the test condenser, the oil-free refrigerant vapor was mixed with the atomized oil at a predetermined mass flow ratio. The mixture was then led to the test condenser under investigation. After travelling through the liquid

receiver, filter-drier, and the evaporator, the oil in the mixture was separated from the refrigerant vapor, then transferred to the oil receiver and returned back to the oil reservoir; and finally to the oil nebulizer, thus completing the circuit. The details of the components of the oil circuits are described in the following:

3.2.2.a- Oil atomization unit: (U)

In the simulation of the oil carried by the refrigerant vapor from a compressor into a condenser we assume a uniform mixture of the two. To achieve this, the oil should be broken down into fine aerosols that can be transported over the distance into the test condenser without settling. For a good simulation, the aerosol generating system for the oil should have the following characteristics:

1- Capable of producing uniform fine particles of oil.

2- Variable flow rate capacity. A wide range of flow rates would allow the investigator to carry out tests at different oil-to- refrigerant mass flow ratios.

3- Ability to operate under varying conditions. Tests at different saturation pressures of the refrigerant vapor are desirable and require the oil to be mixed with the refrigerant vapor at the different corresponding saturation temperatures which, in turn, have an appreciable effect on

the oil viscosity. Consequently, the aerosol generator is expected to have the capability of dealing with different oil viscosities in addition to the different pressures and temperatures;

4- Ability to generate a low velocity aerosol that would not disturb the condensate flow on the condensing-tube surface.

Different atomizing devices such as nozzles and sprays, ultrasonic nebulizers and compressed-vapor nebulizers were tried in this study. It is worthwhile to discuss briefly each of these devices:

a.1- Nozzles and Sprays:

In these type of atomizers, the size of the generated particle is a function of the orifice diameter. If the orifice is too small for a fine degree of atomization, the liquid feed rate and subsequent aerosol concentration will be quite low, Ref.(32).

a.2- Ultrasonic Nebulizers:

These nebulizers utilize high intensity sonic or ultrasonic vibration to break up the liquid. The size of the generated aerosol particle is related to the frequency of vibration Ref.(33). One of the advantages of these nebulizers is that no pressure device is needed to break up

the liquid, hence low speed aerosols are generated. However, there was one limitation which prohibited the use of such a device, and that is the decrease of the rate of atomization with the increase of pressure surrounding the nebulizer.

a.3- Compressed-Vapor Nebulizers:

In this type of nebulizer, compressed vapor is used at high velocity to break up the liquid emerging from a nozzle and plays a predominate part in achieving a fine degree of atomization Ref.(33). Hrubecky, Ref.(34), found that atomization was finest if the liquid was injected parallel to the gas flow inside the nozzle and in a region of maximum gas velocity. In Ref.(32) it is stated that with the use of an inside mixing nozzle a more uniform size distribution of droplets with a diameter less than 20 microns may be accomplished.

In this study, the compressed-vapor nebulizer was found the most suitable device in achieving a fine degree of oil atomization along with the required oil flow rates.

The refrigerant vapor from the refrigerant circuit within the system was used at high velocity to break up the liquid emerging from a nozzle. Thus, the oil was atomized and mixed with the refrigerant vapor.

The refrigerant vapor flow rate was metered before it entered the test condenser. Some of the vapor was then extracted and diverted to the booster compressor.

The rate of vapor extraction was controlled by a manual valve (no. 16) mounted on the suction line "qq". The booster compressor may increase the vapor pressure to (40-60) kPa above the condensing pressure under investigation. It is important to boost the vapor pressure to create a fast moving vapor inside the nozzle, thereby having a proper atomization of the oil. This extra compression work results in a rise of the vapor temperature, thus a desuperheater was installed in the line leading to the atomization nozzle. Inside the nozzle, the oil was brought from the oil circuit through a separate tube and injected in parallel into the flowing vapor at a maximum vapor- velocity zone. Thus a fine mist of oil was generated and mixed with the vapor on the way to the test condenser.

3.2.2.b- Oil Receiver: (O)

The oil receiver is a pressure vessel, 152 mm (6 inches) diameter by 457 mm (18 inches) long. Its three main functions are as follows:

1- receiving and collecting the separated oil from the suction line separator, the liquid accumulator and the compressor crankcase;

2- separating the dissolved liquid refrigerant from the collected oil;

3- returning the separated liquid refrigerant back to the refrigerant circuit and supplying the pure oil to the oil reservoir.

3.2.2.c- Oil Reservoir: (T)

The oil used for simulation and atomization was kept in a see-through reservoir. The reservoir was made of clear plexiglass pipe. The mass flow rate of the oil atomized during each test run can then be easily determined by measuring the rate of oil level drop in the reservoir.

3.2.2.d- Oil Pump: (P)

The oil pressure was raised by the pump from the atmosphere level in the reservoir to the mixing refrigerant vapor pressure. At the outlet of the pump, a pulsation damper was installed to smooth out the piston pump surges and provide a steady oil pressure.

3.2.2.e- Pressure Regulating Valve: (W)

The pressure regulating valve, of the unloader bypass type, was installed in the oil circuit to serve the following purposes:

a- controlling the oil pressure to the atomizing level;

and

b- protecting the oil pump against overheating and wear by maintaining a continuous bypass flow at different oil flow rates.

3.2.2.f- Oil Heater:

A thermostatically controlled electric heater was mounted in the oil circuit, before the atomization unit, to raise the oil temperature to the refrigerant-vapor condensing temperature.

3.2.2.g- Oil Cooler: (V)

Due to the compression of the oil through the oil pump, the temperature of the circulating oil rises gradually. However, it is essential to keep the oil temperature in the oil reservior constant. Consequently, an oil cooler was installed in the oil circulating line to maintain the oil at a desired temperature. The cooler is a small shell and tube heat exchanger, with oil flowing in the tube side and cooling water circulating at the shell side.

3.2.3- MAIN COOLING WATER CIRUIT:

Cooling water was used in this study to achieve the cooling of the condensing tube surface. The design objectives for this cooling water circuit are as follows:

a- to provide a wide range of water velocities;

b- to supply the water at different temperatures for different condensing rates; and

c- to maintain good control over the water temperature.

The cooling water circuit comprises a water reservoir, a water pump, pipe lines and valves. A bypass line and manually operated gate valve were employed to control the water flow rate through the test condenser. Cooling water supply was from a city water main. A manual valve on the supply line to the water reservoir, as well as the bypassed water, served to maintain the required cooling water temperature during the test period. For the multi-tube condenser, each individual condensing tube was supplied with a different branch, and a gate valve was installed in each branch to have a fine adjustment of the cooling water flow rate.

3.2.4- HOT WATER CIRCUIT:

Hot water was the heat source of the evaporator. Circulating in a closed system, hot water absorbed the heat transferred from steam through a heat exchanger. The water temperature supplied to the evaporator was controlled by the amount of water bypassing the heat exchanger, with a thermostat modulator.

3.3-Other Design Features:

Besides the circuits presented above, there are several

several special features in the design of this apparatus worthy of describing as follows:

3.3.1- Pressure control devices:

a- Condensing pressure regulation:

Tests were conducted at different condensing pressures and corresponding saturation temperature on each refrigerant investigated in this study. Means had to be provided in the test apparatus by which the condensing pressure of the system could be verified and controlled for the different refrigerants used. This was achieved with the full size condenser and the aid of a pressure-operated water valve. The valve was mounted on the cooling water inlet to the condenser and the water was supplied from a city main pipe. The capillary tube which transmits the pressure to the valve was connected to the outlet of the condenser close to the condenser pressure gauge.

The condensing pressure regulator (wv) is a two-way pressure operated water valve. Its function was to modulate the quantity of water passing through the condenser in response to the condensing pressure. The water flow rate required depends on condenser performance data, the temperature of available water, the allowable leaving water temperature and the quantity of heat which must be transferred to this water. A constant condensing pressure may be maintained by automatic modulation of the valve to correct for variation in temperature or pressure of the

water supply and variation in the quantity of refrigerant vapor to the condenser.

The pressure-operated water valve has bellows attached to the high pressure side of the system. This valve may be adjusted by means of a heavy spring which presses against the bellows. After the compressor starts, the condenser pressure begins to rise. When the operating pressure setting of the regulator spring is reached, the bellows moves to gradually open the valve disk, thus permitting water to flow in. The regulator continues to open and increase the water flow, until a balance point is reached between the water flow and the heat rejection requirement. At this point, the condensing pressure is stabilized. When the compressor stops, the continuing water flow through the regulator causes the condensing pressure to drop gradually, thereby closing the regulator.

b- High pressure safety cut off:

A high pressure cut-off switch was used to trip off the compressor motor when the head pressure increased over the allowable value. It was connected to the cylinder head on the high pressure side of the system.

The cut-off switch is a safety device to prevent the buildup of dangerous pressure within the system which could, in turn, ruin the compressor and its motor through

overloading and overheating. The rise in head pressure can result from the presence of air in the system or the cooling water being shut off.

In line with the manufacturer's recommendation, the control was set to cut-off about 20% above the normal head pressure. With R-12 the control was set at 1378 kPa (200 psig), while with R-22 the setting was 1929 kPa (280 psig).

c- Pressure relief valves:

A refrigerating system, regardless of its size, is a sealed system acting as a pressure container. In order to prevent high pressure buildup (which can arise during shutdown or in case of fire, extreme temperature conditions or faulty electrical controls), with subsequent risk of explosion, two pressure relief valves were provided, one mounted on the full size condenser, and the other on the test condenser.

3.4- Separation of the atomized oil from the refrigerant:

Upon leaving the evaporator, the mixture of refrigerant vapor and oil entered the suction line oil separator wherein the oil settled and separated from the vapor. The level of the liquid oil in the separator rose until the float valve opened, allowing the oil to flow back to the oil receiver. The flow of the oil was made possible by setting the suction pressure of the compressor higher than the saturated

pressure of the refrigerant at room temperature. Once the oil receiver was full, the oil had to be further separated from the dissolved refrigerant before being delivered to the oil reservoir. This final separation was done by heating the vapor-rich oil at low pressure with an electric heater surrounding the oil receiver. The low pressure was created by the operation of the boosting compressor through the line (aa) with valve no. 15 closed and valve no. 17 open.

It is possible to check that the oil is free of any dissolved refrigerant simply by closing valve no. 17 and observing the rise of pressure in the receiver. When the pressure fails to rise, it indicates that the oil is free of dissolved refrigerant.

3.5- Flow Valves:

As shown in Figure (3), the experimental apparatus contains numerous valves in the different piping with each valve serving a specific function. These valves are described below:

a- Valve no. 1 is mounted in the compressor discharge line and should be kept fully open during system operation. The only time this valve is to be closed is during servicing of the separators.

b- Valve no. 2 is mounted in the hot gas bypass (u) and is partially opened to allow a certain amount of the high pressure hot gas to pass back into the compressor suction pipe (q).

The importance of this valve is to control the compressor suction pressure and the superheat temperature of the refrigerant vapor at the inlet of the compressor.

The adjustment of valve no. 2 depends on the amount of superheat required in the suction line. Three to five degrees C superheated vapor admitted to the compressor is a common practice. This valve should be completely closed when pumping down of the test condenser is required.

c- Valves no. 3 and 4 are installed at the refrigerant-vapor inlet and outlet of the liquid separator respectively. Their functions are similar as those of valve no. 1.

d- Located at the liquid outlet of the liquid separator is valve no. 5. This valve is usually closed, and opened only when there is liquid refrigerant built-up in the liquid separator.

e- Valve no. 6 controlling the vapor flow to the test condenser is usually open, and closed only during pumping

down of the test condenser.

f- Located in the inlet vapor pipe to the liquid reservoir (i.e. the full size condenser) is valve no. 7. This valve is used to achieve a fine adjustment of the condensing pressure required in the test condenser. It also serves to create a pressure difference between the test condenser and the liquid reservoir so that the pressure in the former is a few kPa higher than that in the latter. This pressure difference allows a continuous condensate flow from the test condenser to the reservoir passing through the liquid receiver, thus making it possible to collect and measure the condensate flow leaving the test condenser.

g- Valves no. 8 and 10 are used to isolate the test condenser from the liquid receiver when pumping down of the test condenser is required. Valve no. 10 is mounted in the pressure balance pipe (nn), while valve no. 8 is mounted in the liquid line (j). Both valves are normally fully open during the operation of the system.

h- Valve no. 9 located in the liquid bypass line (pp) is normally closed. This pipe serves to pump down the test condenser and during this operation only is valve no. 9 set fully open.

i- In the liquid line (i) between the liquid receiver

and the liquid reservoir there is a valve no. 11. When the rate of condensation is to be determined in the liquid receiver, this valve should be fully closed. For the other system operation, it may be partially or fully open.

j- Valve no. 12 mounted in the liquid outlet pipe from the liquid reservoir is normally open. It should be fully closed when pumping down of the test condenser or replacing the filter-drier is required.

k- Replacing the filter-drier also requires closing valve no. 13 which is located between the filter-drier and the evaporator. During the normal operation of the system, this valve should be fully open.

l- Valve no. 14 installed in the compressor suction line is usually fully open during the normal operation of the system.

m- When mixing oil with the refrigerant, the refrigerant vapor flow to the booster compressor is controlled by valve no. 15, while no. 16 is used for the returning vapor to the oil atomization chamber. Valve no. 17 serves to transfer the refrigerant vapor trapped in the oil receiver back to the booster compressor.

n- Valve no. 18 is employed for transferring the oil

trapped in the suction-line accumulator to the oil receiver. Usually, it is closed.

o- Valve no. 19 controls the oil flow from the suction line separator to the oil receiver. It is usually fully open except at start up when a temporary closing is required.

p- The oil flow from the compressor crankcase to the oil receiver is controlled by valve no. 20, while the oil flow from the receiver to the oil reservoir is controlled by valve no. 21.

q- Valve no. 23 is mounted in the oil line leading to the atomization nozzle. For test runs of pure refrigerant, this valve is closed. Besides valve no. 23 in this line, there is a fine metering valve no. 22 which accurately controls the oil flow rate. This valve is only operational when valve no. 23 is open.

r- Valves no. 24 through 29 are for controlling water flow.

3.6-Instrumentation

Thermocouples, pressure gauges and a transducer were used to measure temperatures and pressures of the

circulating refigerant, oil and water at various locations in the apparatus. These measurement points are as follows:

1- Before and after the desuperheater, to ensure that the leaving refrigerant vapor has been slightly superheated.

2- At the vapor entrance to the oil atomization unit (U) to check that the vapor is slightly superheated at the boosted condition such that pre-condensation of the vapor is prevented.

3- At the vapor section of the test condenser to measure the condensing pressure with a transducer. A dial pressure gauge was also mounted on the test condenser in parallel with the transducer to provide a quick check for the pressure transducer setting

4- In the single tube condenser, thermocouples were attached to the condenser tube at three equally spaced stations to measure the tube wall surface temperature. At each station, four thermocouples were embedded, at 90 degrees to one another, to measure the tube wall temperature. The average of the twelve local temperatures yielded the mean condensing tube wall temperature. For the multi-tube tests, two thermocouples in horizontal positions at 180 degrees to each other were employed per tube for each station, thus a total of twenty four readings were used to

yield the mean condensing tube wall temperature.

5- At the liquid line leaving the test condenser to measure the subcooling of the condensate so that the condensate rate may be accurately determined in the liquid receiver.

6- At the full size condenser to monitor pressure variation and to determine the vapor condition.

7- At the liquid outlet of the full size condenser to check the subcooling of the condensate.

8- At a point before the expansion valve to indicate any variation in the subcooling and pressure in the liquid line.

9- At a point after the evaporator to record both temperature and pressure.

10- Inside the oil receiver a vacuum gauge was installed to indicate the pressure during separation of the dissolved refrigerant from the oil.

11- In the reservoir, to measure oil temperature used for the calculation of oil mass flow rate.

12- At the inlet to the atomization nozzle, a liquid filled pressure gauge and a thermocouple were mounted. This type of pressure gauge was chosen because pulsation can develop in the fluid during pump operation.

13- At the cooling water inlet for each condensing tube, a thermocouple was installed, while at the outlet three thermocouples were used for the single tube condenser and one for each tube in the multi-tube condenser.

The thermocouples used in this study were of copper-constantan. Two types of pressure gauges were used, with and without a calibration device. For the most sensitive measurements required, such as condensing vapor pressure and liquid pressure, gauges with a calibration device were employed. All the thermocouples and pressure gauges were calibrated before installation.

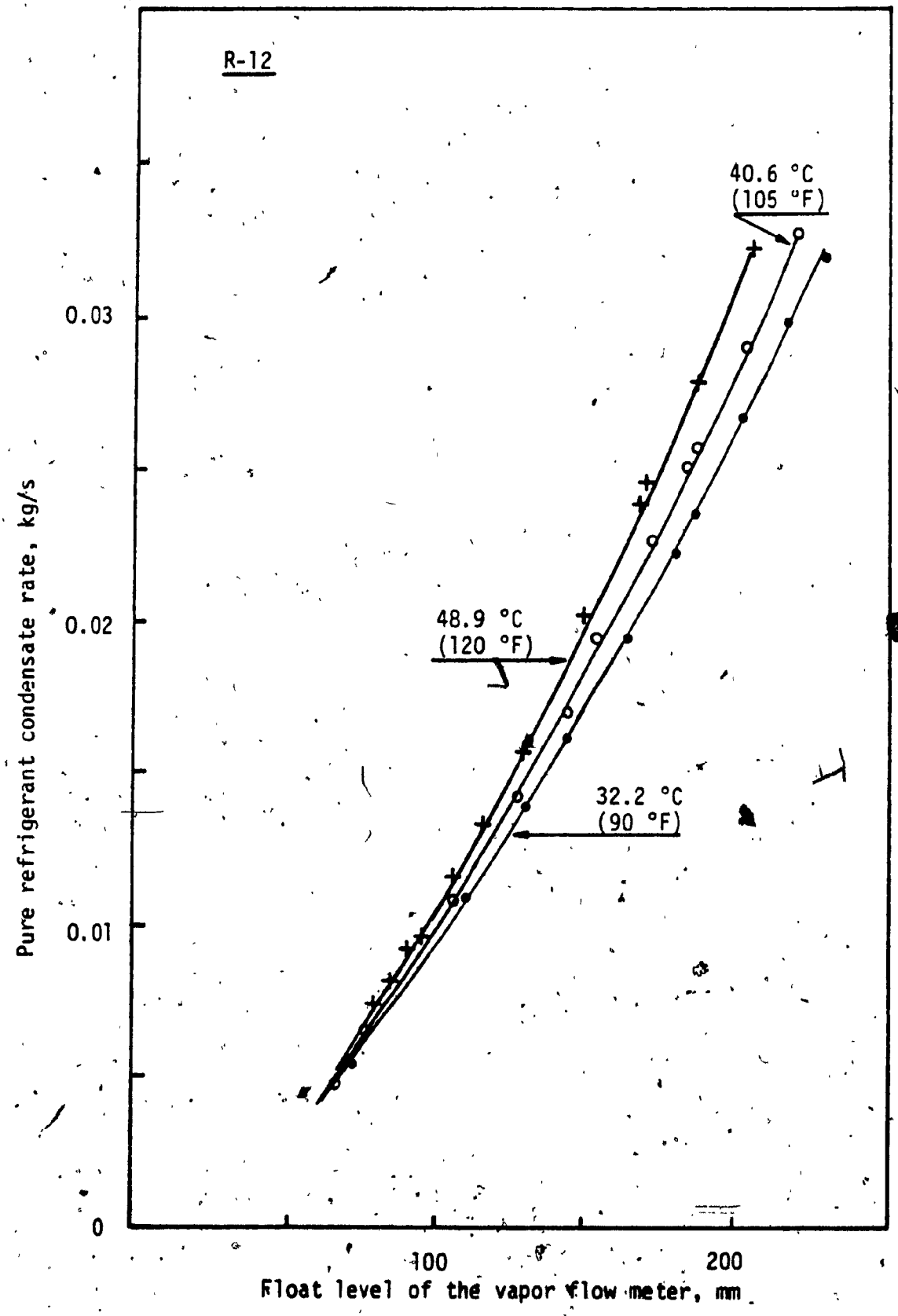

Figure 4: Vapor flow meter calibrations

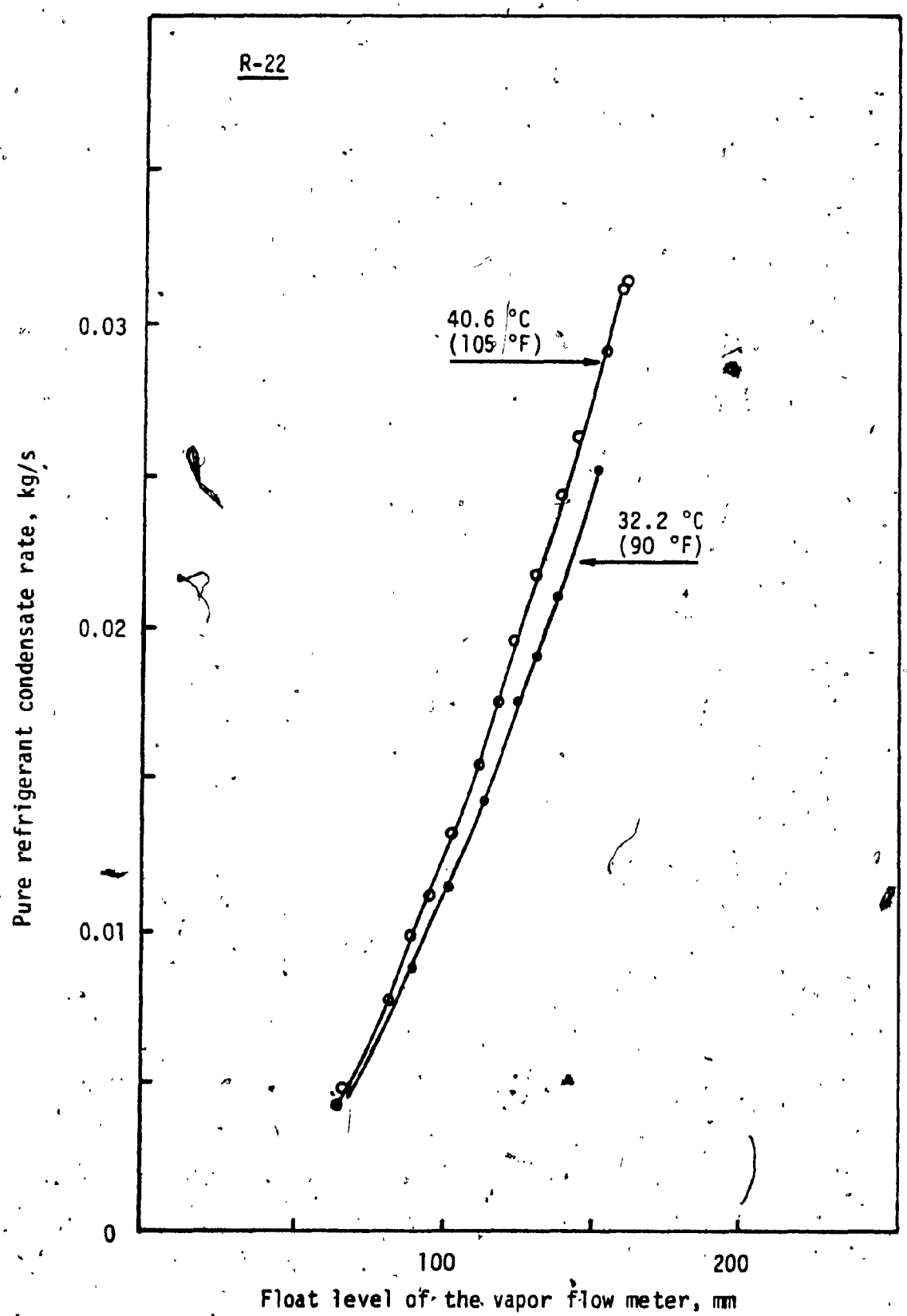

Figure 5: Vapor flow meter calibrations

CHAPTER 4

EXPERIMENTAL PROCEDURE

Generally, the experimental procedure may be divided into two main features:

1- The experimental procedure for the condensation of pure refrigerant vapors; and

2- The condensation of oil vapor mixtures.

4.1-Experimental Procedure for Condensation of Pure Refrigerants:

1- For the 32.2°C (90°F) vapor saturation temperature, all tests were started at the maximum achievable vapor to surface temperature drop, which was limited by the available city water temperature. But for 40.6 and 48.9°C (105 and 120°F) vapor saturation temperatures, the cooling water temperature was raised to obtain a similar temperature drop to that of the low temperature case. In the following consecutive test, the temperature drop was reduced gradually by increasing the cooling water temperature.

At the beginning of each new set of tests the water barrel (R) was filled with fresh cold water. To maintain the lowest possible water temperature for the first run of the 32.2°C (90°F) tests, the water supply valve no. 24 was kept fully open, but for the 40.6 and 48.9°C (105 and 120°F)

tests, the valve was adjusted to deliver the required mass flow of cold water. The water level in the barrel was maintained constant by the overflow.

2- The latent heat required to boil the liquid refrigerant in the evaporator is supplied by hot water circulating between the evaporator and the water heater. The heater and the circulating pump should be switched to the "on" position before putting the experimental set-up into operation. Failure to do this might result in a water freeze and pipe rupture within the evaporator.

3- The water valve no. 26 mounted in the cooling water circulating loop (ff), and the suction line valve no. 22 must be fully open before switching on the cooling water pump. These two valves were examined prior to each pump operation to ensure proper cooling and lubrication of the pump's shaft seal and internal surfaces. It is important to note that the pump must not be run unless the case is full of water.

4- For good practice, water flow inside the condensing tubes should generally be turbulent, in other words, water velocity should be maintained as high as permitted by the water pressure drop, because of its direct influence on the water side heat transfer coefficient. In this study, the range of the water velocity, 1.2 to 2.1 m/s (4 to 7 ft/s),

was selected for the following two reasons:

a- To simulate the water flow condition in the water-cooled condenser of a refrigerant system.

b- To achieve a reasonable cooling water temperature rise inside the condensing tube.

The required velocity was set with valve no. 27. With the opening and closing of this valve, the water mass flow rate, through the condensing tube, was varied. After each setting the water was collected in a designated bucket per unit time and weighed. When a mass flow rate, with water velocity between 1.2-2.1 m/s (4-7) ft/s., had been achieved, the valve setting was held constant and four additional water flow measurements were taken. The average water velocity was then determined based on the five measurements taken.

5- As the oil level of the compressor crankcase might rise due to refrigerant migration from the system components and condensed in the crankcase when the crankcase heater is off, the oil level should be observed before putting the compressor into operation. It should be noted that during a shut-down period the heater must always be kept energized. If, however, the oil level is higher than the normal level seen through the sight glass provided in the crankcase, the

heater should be examined and switched on. Any attempt to operate the compressor with too high a liquid level in the crankcase may result in compressor valve damage.

6- The compressor is started after having adjusted the system components as described above.

7- Adjustment of system test pressure:

Having started the compressor, the desired test pressure may be obtained in the test condenser by adjusting valves no. 7, 11, and valve wv. The cooling water valve wv, installed at the inlet to the full size condenser (liquid reservoir), controls the pressure of the entire system automatically. The valve is set to open at a definite condensing pressure. If, after start- up of the compressor, the system pressure is considerably less than the required condensing pressure, the cooling water flow rate through the full scale condenser should be decreased by turning the valve adjustment knob. The decrease in the flow rate of the cooling water causes the system pressure to rise. Pressure should be applied gradually so as to give the system time to achieve a steady-state condition. The highest pressure which may be reached by adjusting valve (wv) should be between 34.5-68.9 kPa (5-10 psi) lower than the desired condensing pressure in the test condenser.

The desired condensing pressure in the test condenser may be achieved by obstructing the vapor flow through valve no. 7, while keeping the cooling water temperature constant and valve no. 11 fully closed. Consequently, the pressure will rise and may be observed in the gauge until the desired test pressure is reached. Extra care should be taken when adjusting valve no. 7 as pressure variation is highly sensitive to the valve setting.

It is important that the test pressure remains constant whether valve no. 11 is closed or partially open. To achieve this, a certain liquid level should be maintained in the liquid refrigerant receiver to prevent vapor from escaping to the evaporator. This requires trial and error adjustment of valve no. 11 so that the rate of liquid condensate received from the test condenser is equal to the rate at which it passes to the full size condenser.

8- The vapor admitted to the test condenser is required to be 1-2°C superheated. This was found important because any condensation in the vapor supply line can result in a high liquid accumulation rate in the liquid receiver, thus causing an over estimation of the refrigerant side heat transfer rate and a poor heat balance between the refrigerant and water sides.

The superheated vapor temperature is controlled by

adjusting the cooling water flow rate through the desuperheater with valve no. 29. If any liquid condensate is present within the vapor leaving the desuperheater, it can be monitored visually through the sight glass installed at the liquid separator. Valve no. 5 may be kept slightly open so that any separated liquid would be expanded into the compressor suction line.

9- Having finished all the adjustments required as described above, and before taking any measurements, the system should be left operating until steady state conditions are reached. These conditions may be identified by (a) the constant inlet and outlet cooling water temperatures, (b) the constant superheated vapor temperature and, (c) the constant saturation pressure.

10- After steady state conditions have reached at a certain temperature drop between the vapor and the wall surface, measurements may then be taken in the following sequence:

a) Rate of condensation was obtained by collecting the condensate in the liquid receiver with valve no. 11 completely closed. With the aid of a stop watch, the rate of liquid rise in the receiver may be recorded. To repeat the readings, valve no. 11 should be reopened partially until the liquid level drops slowly back to its initial

level. After each condensate collection, it is important to check the stability of the saturation pressure and the inlet water temperature. For each test run, four readings are required and their average will be used as the rate of condensation.

b) The thermocouple temperature measurements (in millivolts) were manually recorded. It was found important that when switching from one thermocouple to the other, several seconds of time interval were needed for the measurement to stabilize before recording it.

c) The next test runs were carried out at the same condensing pressure but with reduced temperature drops across the condensate film. For each subsequent temperature drop, the same procedures as discussed in (a) and (b) were repeated.

To reduce the temperature drop across the condensate film, the cooling water temperature was raised while the condensing temperature was held constant. By closing valve no. 24 in the water supply line, the water temperature inside the reservoir tank can be raised, thus the water entering the test condenser becomes warmer. Once having obtained the desired inlet water temperature to the condenser, it should be maintained constant by controlling valve no. 24.

d) While adjusting the cooling water flow rate for the next run, the pressure in the test condenser fluctuates due to the change of the vapor surface temperature drop, (ΔT). For any temperature drop the pressure must be regulated by adjusting valve no. 7 so that a constant pressure may be maintained throughout the test.

e) Before taking measurements at new vapor surface temperature drop, the steady state conditions must be examined again.

4.1.1- Calibration of the flow meter:

As previously stated, the float type flow meter is only accurate when it is operated under similar conditions to those at which it was calibrated. Therefore, for each refrigerant tested in this study and at each saturation condition, the flow meter was calibrated. Thus relations between the flow meter float level and the condensation rate were developed. These relations made it possible to achieve the desired condensate rate. Hence, constant oil to refrigerant mass ratios can be maintained during the various tests.

Calibration of the flow meter was made during the condensation of the pure refrigerant. For a certain vapor state, the float level indication was recorded for each condensation rate at a constant temperature difference

between the vapor and the tube wall.

It is important when recording the float level, that the liquid condensate in the liquid receiver is maintained.

4.2- Experimental Procedure for Condensation of Oil Vapor Mixture:

The experimental procedure described above may be considered as the starting procedure for the tests conducted with the refrigerant oil mixture. After completion of the start up procedure, the experimental apparatus should be allowed to achieve steady state condition. The rate of condensation may then be determined by starting with the largest vapor to surface temperature drop (Δ T) similar to those obtained for the pure vapor condensation. The rate of condensation is obtained by observing the float level in the flow meter and then referring to the developed calibration figures. Thus, the maximum oil flow rate required may be calculated for the desired oil to refrigerant mass ratios.

With the oil pump (P) running, the oil pressure is controlled by setting the pressure regulating valve (W) so that a pressure of 200-275 kPa above the refrigerant condensing pressure is maintained in the oil piping. The oil heater is then switched on and the temperature controller is set 2-4 ° C higher than the refrigerant

condensing temperature.

The most suitable procedure for obtaining an accurate mass ratio was found to be that of first randomly setting the oil flow rate and then adjusting the refrigerant mass flow rate accordingly. This was applied to all the runs for a group of tests, but in addition, and only for the starting run where a (ΔT) similar to that of the pure refrigerant condensation, was maintained, the oil mass flow rate for the largest rate of condensation had to be fixed first. However, it was found difficult to achieve the right mass ratio when the refrigerant flow rate is fixed first and then the corresponding oil flow rate second. Instead, the oil metering valve no. 22 was randomly set so that any oil flow rate obtained could be used as long as it was close to the calculated value required for the largest rate of condensation. This approximate flow rate was obtained by a trial and error method.

The oil mass flow rate measurement procedure is as follows:

1- Having a steady pressure in the oil pipe, the pressure in the condenser is maintained, at the saturation pressure;

2- Opening of the shut valve no. 23 allows the oil to pass from the reservoir to the atomization nozzle. The rate of fall of the oil level in the oil reservoir indicates the

rate of oil mass flow rate.

Having measured the oil mass flow rate for the first run, the required percentage of refrigerant mass flow rate may then be calculated. The refrigerant flow rate thus calculated, is the rate of condensation which should be obtained by varying the cooling water inlet temperature to the condensing tube. The variation in the rate of condensation can be monitored by observing the float level in the refrigerant vapor flow meter and referring that to the calibration figures. When the float reaches a level that matches the calculated refrigerant mass flow rate, the corresponding cooling water temperature should then be maintained.

Next, when valve no. 15 is in a closed position, the pressure boosting compressor (Q) is switched on. The amount of refrigerant drawn from the main circuit by the boosting compressor to achieve atomization of the oil is controlled by setting the valve no. 15. This valve has to be set such that the boosting compressor discharge pressure is 40-60 kPa above the test condensing pressure.

Before attempting to take any measurement, the following points have to be rechecked:

1- Constant oil pressure and constant condensing pressure.

2- Refrigerant vapor temperature within 1-2 °C superheat at the inlet of the test condenser.

3- Inlet cooling water temperature.

4- Float level in the flow meter.

Having checked these points, the following measurements can be taken:

1- Surface temperature of the tube.

2- Inlet and outlet cooling water temperature.

3- Rate of liquid rise in the liquid accumulator.

4- Refrigerant vapor temperature.

5- Oil level drop rate in the oil reservoir.

6- Float level in the flow meter.

For the next run, the oil metering valve is slightly closed, then the rate of oil flow and the corresponding refrigerant condensation rate are determined by the same procedure outlined above.

CHAPTER 5

THEORETICAL PREDICTION

It is desirable for designers to be able to predict the heat transfer coefficient encountered during filmwise condensation of refrigerant vapors mixed with oil. The analysis presented here attempts to obtain theoretical models for the heat transfer coefficient for a single horizontal tube and a vertical bank of horizontal tubes.

5.1- Single horizontal tube model:

In the physical model Figure (6), a cross sectional view of the condensing tube of radius (r) is shown. A condensate-oil mixture of thickness (δ) covers the surface of the tube and runs down under the influence of gravity with velocity (v). The (x) coordinate measures the distance normal to the surface while the (y) coordinate measures the distance along the circumference of the tube. The condensing tube is assumed to be situated in a quiescent mixture of oil fog and refrigerant vapor. The mixture is at the refrigerant saturation temperature (T_v). The surface temperature of the tube (T_s) is uniform and $T_v > T_s$.

THEORETICAL PREDICTION:

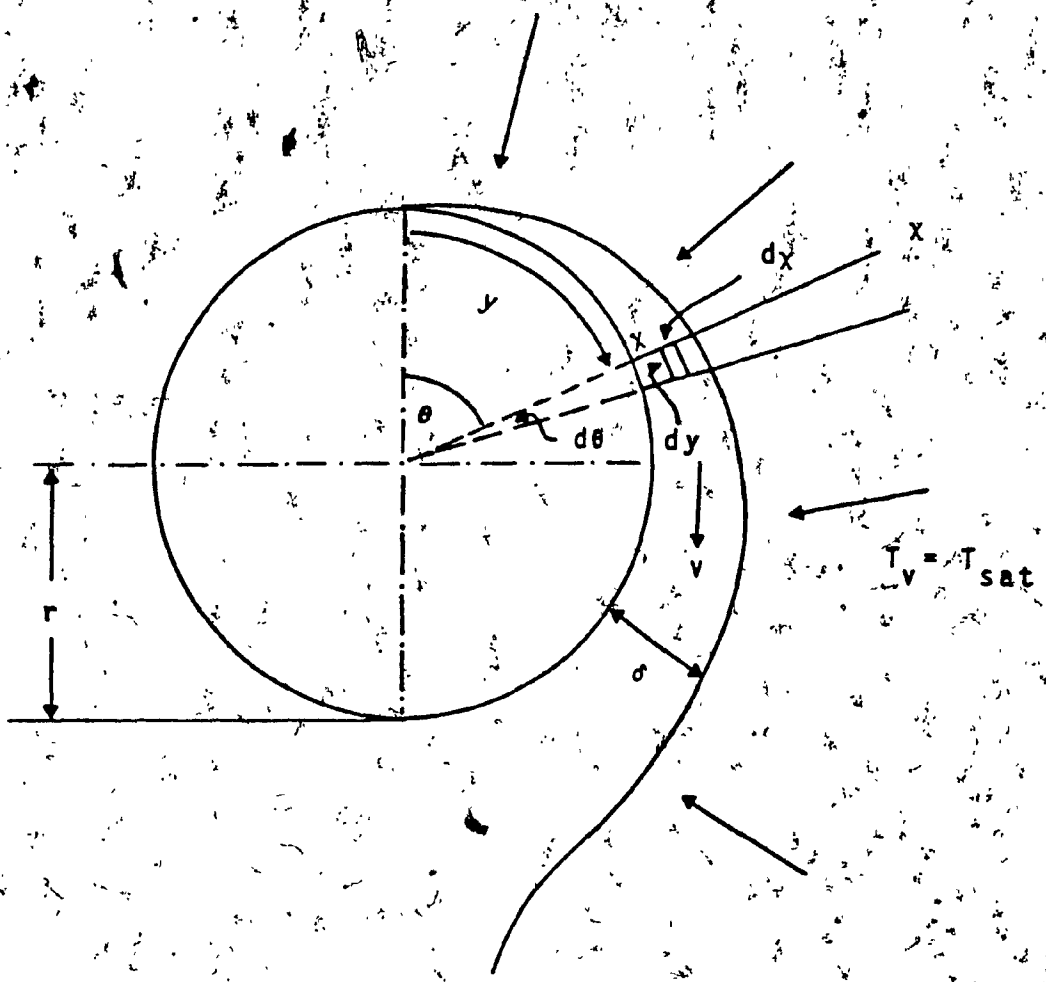

Figure 6: Physical model and co-ordinate system

When a completely miscible oil and refrigerant vapor mixture is admitted to the condenser, a single phase liquid layer mixture of thickness (δ) is formed on the condensing surface on which further oil particles arrive and more vapor condenses at the liquid vapor interface between the oil particles. Thus, the liquid layer increases in thickness until it runs down under the influence of gravity.

As a result of the high solubilities of halogenated refrigerant in the lubricating oil, the liquid layer on the condensing surface can no longer be treated as a pure refrigerant condensate, but rather as an oil-refrigerant solution whose properties are different from those of the pure refrigerant and are dependent on the oil to refrigerant mass ratios.

5.1.1- Assumptions

The following assumptions have been made:

1- A uniform mixture of oil and vapor is entering the condenser.

2- The liquid layer flow is laminar on the periphery of the tube.

3- The effect of the liquid surface tension near the bottom of the condensing tube is neglected.

4- Uniform tube surface temperature.

5- Physical properties are constant.

6- Entering vapor velocity is small so that standstill

vapors are considered.

7- The static pressure gradient across the liquid film is neglected relative to the gravity force.

8- Uniform oil particle size.

9- Acceleration of the liquid film on the periphery of the tube has insignificant effects, therefore it is neglected.

10- The vapor is saturated.

11- There is no appreciable vapor shear stress existing at the liquid vapor interface.

12- Non condensible gas is not present.

13- No thermal resistance at the vapor-liquid interface.

14- No slip at the wall.

15- linear temperature distribution across the condensate film is assumed, because the actual condensate film is very thin.

5.1.2- SINGLE TUBE ANALYSIS

Neglecting the static pressure gradient and the inertia forces the momentum equation becomes; (Ref. 16)

$$g \sin\theta + \frac{\mu_m}{\rho_m}\left[\frac{\partial^2 v}{\partial x^2}\right] = 0 \qquad \text{----------(5.1)}$$

where

μ_m = dynamic viscosity of the mixture liquid layer, kg/ms

ρ_m = density of the mixture liquid layer.

v = mixture liquid velocity in the (y) direction, m/s

rearrange (5.1)

$$\frac{\partial^2 v}{\partial x^2} = - g \sin \theta_1 \frac{\rho_m}{\mu_m} \qquad \text{----------(5.2)}$$

integrate (5.2)

$$\frac{\partial v}{\partial x} = - g \sin \theta \frac{\rho_m}{\mu_m} x + C_1 \qquad \text{--------(5.3)}$$

integrate (5.3)

$$v = - g \sin \theta \frac{\rho_m}{\mu_m} \frac{x^2}{2} + C_1 x + C_2 \qquad \text{--------(5.4)}$$

Boundary conditions are:

a- At $x = 0$ $\quad v = 0$ and $C_2 = 0$

b- At $x = (\delta)$ $\quad \left.\frac{dv}{dx}\right|_{x=\delta} = 0$, $C_1 = g \sin\theta \frac{\rho_m}{\mu_m} \delta$.

substituting of the constants, C_1 and C_2 in Eq. (5.4), we get

$$v = -g \sin\theta \frac{\rho_m x^2}{\mu_m^2} + g \sin\theta \frac{\rho_m}{\mu_m} \delta x$$

The velocity distribution in the liquid film is;

$$v = \frac{\rho_m}{\mu_m} g \sin\theta \left(\delta x - \frac{x^2}{2} \right) \qquad \text{----------(5.5)}$$

The liquid mass flow rate per unit width at any (y), would be

$$M_t = \rho_m \int_0^{\delta} v \, dx \qquad \text{--------(5.6)}$$

where M_t is the sum of oil and refrigerant mass flow rates

$$M_t = M_o + M_r \qquad \text{----------(5.7)}$$

by substitution of (5.5) in (5.6)

$$M_t = \rho_m \int_0^{\delta} \frac{\rho_m}{\mu_m} g \sin\theta \left(\delta\chi - \frac{\chi^2}{2}\right) d\chi \qquad \text{------(5.8)}$$

integrate (5.8)

$$M_t = \frac{\rho_m^2}{\mu_m} g \sin\theta \left[\frac{\delta\chi^2}{2} - \frac{\chi^3}{6}\right]_0^{\delta}$$

$$M_t = \frac{\rho_m^2}{\mu_m} g \sin\theta \left[\frac{\delta^3}{2} - \frac{\delta^3}{6}\right]$$

the liquid mass flow rate is

$$M_t = \frac{\rho_m^2}{\mu_m} g \sin\theta \frac{\delta^3}{3} \qquad \text{---------(5.9)}$$

let the oil to refrigerant mass ratios, $M_o / M_r = Z$, so

$$Z\ M_r = M_o \qquad \text{---------(5.10)}$$

by substitution of (5.10) into (5.7), the liquid flow rate is

$$M_t = M_r + M_r\ Z$$

$$M_t = M_r\ (1 + Z) \qquad \text{---------(5.11)}$$

substitute (5.11) in (5.9)

$$M_r\ (\ 1 + Z\ ) = \frac{\rho_m^2}{\mu_m} g \sin\theta \frac{\delta^3}{3}$$

the refrigerant mass flow rate at any angle (θ) per unit width is

$$M_r = \frac{\rho_m^2 \, g \, \sin\theta \, \delta^3}{3 \, \mu_m \, (1+Z)} \qquad \text{--------(5.12)}$$

Energy Equation:

Figure (7) is a three dimensional physical model representing a condensing tube sector of unity length and of radius (r). The condensing vapor approaching the elemental liquid layer contains uniform oil particles which are at the vapor condensing temperature.

At the tube surface, the oil particles cover a certain area($d A_o$) of the element, while the vapor condenses on the remaining exposed area($d A_r$), where the latent heat is released. Taking the liquid subcooling into consideration, the total heat transfer to the cooling surface would be the sum of the latent heat released plus the heat of liquid subcooling. Thus the energy equation is: (Ref. 14)

$$k_m \left.\frac{\partial T}{\partial x}\right|_{x=0} dy = h_{fg} \, dM_r - \frac{\partial}{\partial \delta}\left[\int_{x=0}^{x=\delta} -\rho_m \, C_{pm} \, (T-T_v) \, v \, dx\right] d\delta$$

--------(5.13)

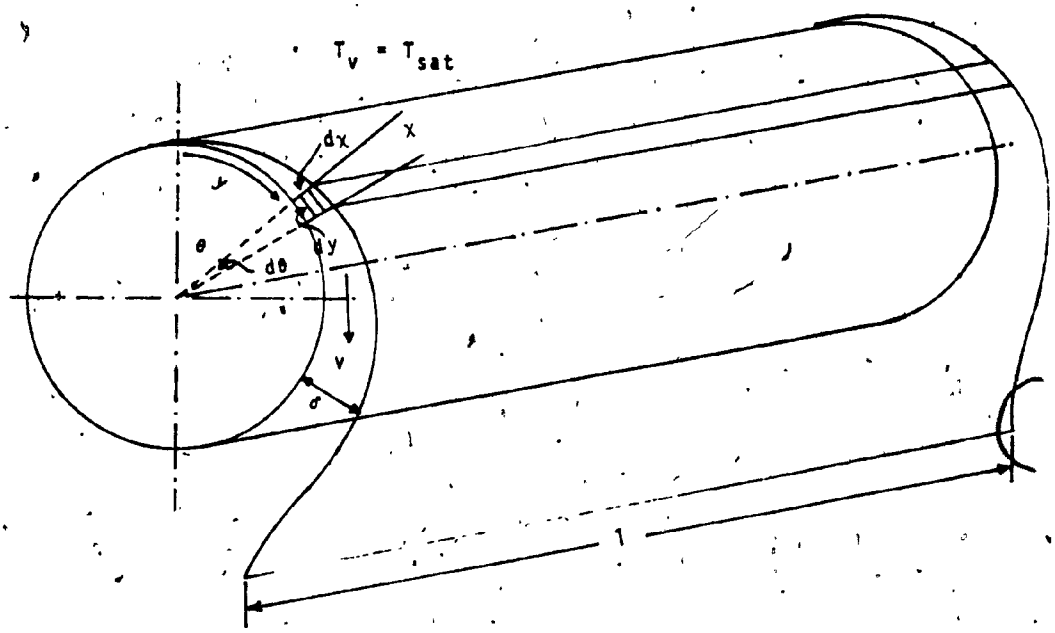

Figure 7 : Physical model and co-ordinate system

Where the left hand term represents the total heat transfer rate through the cooling surface. On the right hand side, the first term represents the latent heat transfer in the fractional area (A_{fr}) and the second term represents the liquid subcooling.

Assuming a linear temperature distribution across the condensate film, then

$$\frac{T - T_v}{T_v - T_s} = \frac{x - \delta}{\delta} \qquad \text{---------(5.14)}$$

The temperature gradient at the tube wall

$$\left.\frac{dT}{dx}\right|_{x=0} = \frac{\Delta T}{\delta} \qquad \text{----------(5.15)}$$

where

$$\Delta T = T_v - T_s$$

substitute (5.15) in the energy equation, to obtain

$$k_m \frac{\Delta T}{\delta} dy = h_{fg} dM_r - \frac{\partial}{\partial \delta}\left[\int_{x=0}^{x=\delta} \rho_m C_{pm} (T - T_v) v \, dx\right] d\delta$$

$$\text{---(5.16)}$$

substitute equations (5.5) and (5.14) in the second term of eq. (5.16) to obtain

$$\frac{\partial}{\partial \delta}\left[\int_{\chi=0}^{\chi=\delta} \rho_m C_{pm}\left[\Delta T\left(\frac{\chi-\delta}{\delta}\right)\right]\left[g\frac{\rho_m}{\mu_m}\left(\delta\chi-\frac{\chi^2}{2}\right)\sin\theta \; d\chi\right]\right] d\delta$$

taking the constants out of the integration

$$\frac{\Delta T\, \rho_m^2\, C_{pm}\, g}{\mu_m}\frac{\partial}{\partial \delta}\left[\sin\theta \int_0^{\delta}\left(\frac{\chi}{\delta}-1\right)\left(\delta\chi-\frac{\chi^2}{2}\right) d\chi\right] d\delta$$

simplify the second term

$$\frac{\Delta T\, \rho_m^2\, C_{pm}\, g}{\mu_m}\frac{\partial}{\partial \delta}\left[\sin\theta \int_0^{\delta}\left(\chi^2-\frac{\chi^3}{2\delta}-\delta\chi+\frac{\chi^2}{2}\right) d\chi\right] d\delta$$

integrate w.r.t.(x)

$$\frac{\Delta T\, \rho_m^2\, C_{pm}\, g}{\mu_m} \quad \frac{\partial}{\partial \delta}\left[\sin\theta \quad \left[\frac{x^3}{3} - \frac{x^4}{8\delta} - \frac{\delta x^2}{2} + \frac{x^3\,\delta}{6}\right]_0\right] d\delta \quad \text{-----(5.17)}$$

let

$$K = \frac{\Delta T\, \rho_m^2\, C_{pm}\, g}{\mu_m} \qquad \text{----------(5.17 a)}$$

substitute boundaries to get

$$K \frac{\partial}{\partial \delta}\left[\sin\theta\left[\frac{\delta^3}{3} - \frac{\delta^3}{2} - \frac{\delta^4}{8\delta} + \frac{\delta^3}{6}\right]\right] d\delta \qquad \text{----(5.18)}$$

simplify to get

$$-\frac{K}{8}\ \frac{\partial}{\partial \delta}\ [\sin\theta\ \delta^3]\ d\delta \qquad \text{----------(5.19)}$$

let

$$-\frac{K}{8} = P \qquad \text{----------(5.19 a)}$$

the second term becomes

$$P\ \ \partial\ (\sin\theta\ \delta^3)$$

or

$$P\ \ (3\ \delta^2 d\delta\ \sin\theta\ +\ \cos\theta\ d\theta\ \ \delta^3)$$

substitute in energy equation (5.16), the energy equation becomes;

$$k_m\ \frac{\Delta T}{\delta}\ dy\ =\ h_{fg}\ dM_r\ -\ P\ (3\ \delta^2\ d\delta\ \sin\theta + \cos\theta\ d\theta\ \delta^3)$$

------(5.20)

differentiate (5.12)

$$dM_r = \frac{\rho_m^2 g\, d(\sin\theta \cdot \delta^3)}{3\,\mu_m (1 + Z)}$$

$$dM_r = \frac{\rho_m^2 g}{3\,\mu_m (1 + Z)} \left(3\,\delta^2 d\delta \sin\theta + \cos\theta\, d\theta\, \delta^3 \right)$$

---------(5.21)

substitute (5,21) in (5.20)

$$k_m \frac{\Delta T}{\delta} dy = \frac{h_{fg}\ \rho_m^2\ g}{3\ \mu_m (1 + Z)} \left(3\,\delta^2 d\delta \sin\theta + \cos\theta\, d\theta\, \delta^3 \right) -$$

$$P \left(3\,\delta^2 d\delta \sin\theta + \cos\theta\, d\theta\, \delta^3 \right)$$

---------(5.22)

simplify

$$k_m \frac{\Delta T}{\delta} dy = \left[\frac{h_{fg}\ \rho_m^2\ g}{3\,\mu_m (1 + Z)} - P \right] \left(3\,\delta^2 d\delta \sin\theta + \cos\theta\, d\theta\, \delta^3 \right)$$

-------(5.23)

let

$$\frac{h_{fg}\ \rho_m^2\ g}{3\ \mu_m\ (1 + Z)} - P = A \qquad \text{------ (5.23 a)}$$

let

$$B = k_m\ \Delta T \qquad \text{------- (5.23 b)}$$

equation (5.23) becomes

$$\frac{B}{\delta^4}\ dy = A\ (\ 3\ \delta^2\ d\delta\ \sin\theta + \cos\theta\ d\theta\ \delta^3\ ) \qquad \text{------(5.24)}$$

multiply by (δ) and divide by (A)

$$\frac{B}{A}\ dy = 3\ \delta^3\ d\delta\ \sin\theta + \cos\theta\ d\theta\ \delta^4 \qquad \text{------(5.25)}$$

let

$$\frac{B}{A} = E \qquad \text{---------(5.25 a)}$$

substitute in equation (5.25)

$$E\,dy = -3\delta^{3}\,d\delta \sin\theta + \cos\theta\, d\theta\, \delta^{4}$$

-----(5.26)

but

$$y = r\,\theta$$

differentiate

$$dy = r\,d\theta$$

equation (5.26) becomes

$$E\,r\,d\theta = -3\delta^{3}\,d\delta \sin\theta + \cos\theta\, d\theta\, \delta^{4}$$

--------(5.27)

divide by

$$E\,r\,d\theta$$

to get

$$\frac{3\delta^{3}\,d\delta\,\sin\theta}{E\,r\,d\theta} + \frac{\cos\theta\, d\theta\, \delta^{4}}{E\,r\,d\theta} - 1 = 0$$

----(5.28)

let

$$F = \frac{\delta^{4}}{Er}$$

-----(5.29)

differentiate

$$\frac{dF}{d\delta} = \frac{4\,\delta^3}{E\,r} \qquad \text{----------(5.30)}$$

so,

$$E\,r = 4\,\delta^3 \frac{d\delta}{dF} \qquad \text{----------(5.31)}$$

substitute (5.29) and (5.31) in (5.28)

$$\frac{3\,\delta^3\,d\delta\,\sin\Theta\,dF}{4\,\delta^3\,d\delta\,d\Theta} + \frac{\cos\Theta\,d\Theta\;F}{d\Theta} - 1 = 0 \qquad \text{----------(5.32)}$$

equation (5.32) is transferred to ordinary differential equation

$$\frac{3}{4}\sin\Theta\frac{dF}{d\Theta} + F\cos\Theta - 1 = 0$$

the solution of this differential equation was given by Nusselt (Ref. 4) as:

$$F = \frac{\frac{4}{3}\int_{\Theta_1}^{\Theta_2} \sin^{\frac{1}{3}}\Theta\; d\Theta}{\sin^{\frac{4}{3}}\Theta} \qquad \text{----------(5.33)}$$

from equation (5.29)

$$\text{let} \quad F = \frac{\delta^4}{E r} = \Psi^4 \qquad \text{----------(5.34)}$$

so

$$\delta = [\, E\, r \,]^{0.25}\ \Psi \qquad \text{----------(5.34a)}$$

by substitution of equation (5.34) in equation (5.33), we get

$$\Psi = \left[\frac{\frac{4}{3} \int_{\theta_1}^{\theta_2} \sin^{\frac{1}{3}} \theta \, d\theta}{\sin^{\frac{4}{3}} \theta} \right]^{0.25} \qquad \text{----------(5.34b)}$$

substitute equation (5.34 b) in equation (5.34 a), the film thickness (δ) will be

$$\delta = (E\, r)^{\frac{1}{4}} \left[\frac{\frac{4}{3} \int_{\theta_1}^{\theta_2} \sin^{\frac{1}{3}} \theta \, d\theta}{\sin^{\frac{4}{3}} d\theta} \right]^{0.25} \qquad \text{---------(5.35)}$$

but

$$hx = \frac{k_m}{\delta} \qquad \text{----------(5.36)}$$

substitute (5.35) in (5.36)

$$hx = \frac{k_m}{(E\,r)^{\frac{1}{4}} \left\{ \frac{\frac{4}{3} \int_{\Theta_1}^{\Theta_2} \sin^{\frac{1}{3}} d\Theta}{\sin^{\frac{4}{3}} \Theta} \right\}^{0.25}}$$

the mean heat transfer coefficient is

$$h_m \Big|_{\Theta_1}^{\Theta_2} = \frac{k_m}{(E\,r)^{0.25}\,(\Theta_2 - \Theta_1)} \int_{\Theta_1}^{\Theta_2} \frac{d\,\Theta}{\Psi}$$

$$h_m \Big|_{\Theta_1}^{\Theta_2} = \frac{k_m}{(E\,r)^{0.25}\,(\Theta_2 - \Theta_1)} \int_{\Theta_1}^{\Theta_2} \frac{d\theta}{\left\{ \frac{\frac{4}{3} \int_{\Theta_1}^{\Theta_2} \sin^{\frac{1}{3}}\Theta\, d\Theta}{\sin^{\frac{4}{3}}\Theta} \right\}^{0.25}}$$

simplify

$$h_m\Big|_{\theta_1}^{\theta_2} = \frac{k_m}{(E\,r)^{0.25}\,(\theta_2-\theta_1)} \int_{\theta_1}^{\theta_2} \frac{\sin^{\frac{1}{3}}\theta\, d\theta}{\left[\frac{4}{3}\int_{\theta_1}^{\theta_2} \sin^{\frac{1}{3}}\theta\, d\theta\right]^{0.25}} \qquad \text{------(5.37)}$$

the programme (Omar) in appendix (1) evaluate the integration numerically

$$\int_0^{\pi} \frac{\sin^{\frac{1}{3}}\theta\, d\theta}{\left[\frac{4}{3}\int_0^{\pi} \sin^{\frac{1}{3}}\theta\, d\theta\right]^{0.25}} = 2.52 \qquad \text{------(5.37a)}$$

substitute equation (5.37 a) in equation (5.37), to get

$$h_m\Big|_0^{\pi} = \frac{k_m}{[E\,r]^{0.25}\,\pi}\,2.52 \qquad \text{----------(5.37b)}$$

but,

$$r = \frac{D}{2}$$

substitute in equation (5.37.b)

$$h_m = \frac{0.954\ k_m}{E^{0.25}\ D^{0.25}} \qquad \text{----------(5.38)}$$

substitute back for

$$E = \frac{B}{A}$$

the mean heat transfer coefficient becomes

$$h_m = \frac{0.954\ k_m\ A^{0.25}}{[\,B\ D\,]^{0.25}}$$

substitute back for A and B to obtain

$$h_m = \frac{0.954\ k_m \left[\frac{h_{fg}\ g\ \rho_m^2}{3\ \mu_m\ (1+Z)} + \frac{\Delta T\ \rho_m^2\ C_{pm}\ g}{8\ \mu_m} \right]^{0.25}}{[k_m\ \Delta T\ D]^{0.25}}$$

Finally, the mean heat transfer coefficient for condensation of oil-vapor mixture on a single horizontal tube is:

$$h_m = \frac{0.725\, k_m^{0.75} \left[\frac{h_{fg}\, g\, \rho_m^2}{\mu_m\,(1+Z)} + \frac{3\,\Delta T\, \rho_m^2\, C_{pm}\, g}{8\,\mu_m} \right]^{0.25}}{[\, D\, \Delta T\,]^{0.25}} \qquad \text{----------(5.39)}$$

5.2- VERTICAL ROW OF HORIZONTAL TUBES ANALYSIS:

The same argument discussed for the condensation on a single horizontal tube in section (5.1) may be applied for the vertical row of (N) horizontal tubes.

5.2.1- Assumptions

All the assumptions used in section 5.11 are applied to the case of multitube condensation, in addition, the following assumptions are also considered:

1- The condensate rate between the tubes is neglected.

2- No rippling occurs in the condensate layer when the liquid descends from a top tube to the lower one.

3- Subcooling of the liquid layer is neglected.

4- No condensate splash takes place, i.e. all the condensate leaving a tube is received by the lower one.

5.2.2- Multitube analysis : (Ref. 4)

From the analysis of the single tube, the liquid flow on one side of the tube per unit length was found;

$$M_r = \frac{\rho_m^2 \, g \sin\theta \, \delta^3}{3 \, \mu_m \, (1 + Z)}$$

For heat transfer by conduction through the liquid film, the film coefficient (h) is defined by;

$$h = \frac{k_m}{\delta} \qquad \text{----------(5.40)}$$

since

$$\delta = \left[\frac{3 \, M_r \, \mu_m \, (1+Z)}{\rho_m^2 \, (g \sin\theta)} \right]^{\frac{1}{3}} \qquad \text{----------(5.41)}$$

and by substitution of (5.41) in (5.40), the heat transfer coefficient will be

$$h = 0.693 \left[\frac{k_m^3 \rho_m^2 \; g \sin \theta}{\mu_m M_r (1 + Z)} \right]^{\frac{1}{3}} \qquad \text{------(5.42)}$$

Neglecting the subcooling of the refrigerant and assuming a linear temperature drop across the liquid film, the energy balance over a single tube section is

$$h_{fg} \, dM_r = h \, \Delta T \, \frac{D}{2} \, d\theta \qquad \text{-------(5.43)}$$

but equation (5.42) is

$$h = \left[\frac{k_m^3 \rho_m^2 \, g \sin \theta}{3 \mu_m M_r (1+Z)} \right]^{\frac{1}{3}}$$

substitute (5.42) in (5.43)

$$h_{fg} \, dM_r = \left[\frac{k_m^3 \rho_m^2 \, g \sin \theta}{3 \mu_m M_r (1+Z)} \right]^{\frac{1}{3}} \frac{\Delta T}{2} \, D \, d\theta \qquad \text{---------(5.44)}$$

$$h_{fg} \, (M_r)^{\frac{1}{3}} \, dM_r = \left[\frac{k_m^3 \rho_m^2 \, g}{3 \mu_m (1+Z)} \right]^{\frac{1}{3}} \frac{\Delta T}{2} \, D \sin^{\frac{1}{3}} \theta \, d\theta \qquad \text{---------(5.45)}$$

integrate (5.45) from 0 to π

$$2\,h_{fg}\int_{M_{r_0}}^{M_{r\pi}} (M_r)^{\frac{1}{3}}\,dM_r = \left[\frac{k_m^3 \rho_m^2\, g}{3\mu_m (1+Z)}\right]^{\frac{1}{3}} \Delta T\, D \int_0^{\pi} \sin^{\frac{1}{3}}\theta\, d\theta$$

----------(5.46)

integrate the left hand side of equation (5.46), to get

$$2\,h_{fg}\,\frac{3}{4}\left[(M_r)^{\frac{4}{3}}\right]_{M_{r_0}}^{M_{r\pi}} = \left[\frac{k_m^3 \rho_m^2\, g}{3\mu_m\,(1+Z)}\right]^{\frac{1}{3}} \Delta T\, D \int_0^{\pi} \sin^{\frac{1}{3}}\theta\, d\theta$$

----------(5.47)

but

$$\frac{4}{3}\int_0^{\pi} \sin^{\frac{1}{3}}\theta\, d\theta = 3.42 \qquad \text{----------(5.48)}$$

Equation (5.47) becomes

$$2\, h_{fg}\left[M_{r\pi}^{\frac{4}{3}} - M_{r_0}^{\frac{4}{3}}\right] = 3.42\left[\frac{k_m^3\,\rho_m^2\,g}{3\mu_m\,(1+Z)}\right]^{\frac{1}{3}}\Delta T\, D \qquad \text{-----(5.49)}$$

The refrigerant flow over both sides of the condensing tube, is

$$M_{rt} = 2\,M_r \qquad \text{----------(5.50)}$$

or

$$M_r = \frac{M_{rt}}{2} \qquad \text{----------(5.51)}$$

raise to the power 4/3

$$[M_r]^{\frac{4}{3}} = \frac{[M_{rt}]^{\frac{4}{3}}}{[2]^{\frac{4}{3}}} \qquad \text{----------(5.52)}$$

substitute (5.52) in (5.49)

$$2\left[\frac{M_{rt\pi}^{\frac{4}{3}}}{2^{\frac{4}{3}}} - \frac{M_{rt_0}^{\frac{4}{3}}}{2^{\frac{4}{3}}}\right] = 3.42\left[\frac{k_m^3\,\rho_m^2\,g}{3\mu_m\,(1+Z)}\right]^{\frac{1}{3}}\frac{D\,\Delta T}{h_{fg}} \qquad \text{----(5.53)}$$

$$M_{rt_1}^{\frac{4}{3}} - M_{rt_0}^{\frac{4}{3}} = 2^{\frac{1}{3}}(3.42)\left[\frac{k_m^3 \rho_m^2 g}{3\mu_m(1+Z)}\right]^{\frac{1}{3}} \frac{\Delta T\, D}{h_{fg}} \quad \text{----(5.54)}$$

For a vertical bank of (N) horizontal tubes, the condensate leaving a top tube is the condensate received by the tube below. This permits a simple consecutive addition by neglecting the condensate rates between tubes, the result will be

$$M_{rtn}^{\frac{4}{3}} - M_{rto}^{\frac{4}{3}} = N\, 2^{\frac{1}{3}}(3.42)\left[\frac{k_m^3 \rho_m^2 g}{3\mu_m(1+Z)}\right]^{\frac{1}{3}} \frac{\Delta T\, D}{h_{fg}} \quad \text{----(5.55)}$$

where

M_{rto} = saturated liquid unit rate entering at the top of the top tube.

M_{rtn} = condensate unit rate leaving the bottom of the bottom tube n.

raise equation (5.55) to power 3/4 to obtain

$$[M_{rtn}^{\frac{4}{3}} - M_{rto}^{\frac{4}{3}}]^{\frac{3}{4}} = [N]^{\frac{3}{4}} \, 2^{\frac{1}{4}} \, (3.42)^{\frac{3}{4}} \, [\frac{k_m^3 \, \rho_m^2 \, g}{3 \, \mu_m \, (1+Z)}]^{\frac{1}{4}} \, [\frac{\Delta T \, D}{h_{fg}}]^{\frac{3}{4}}$$

--------(5.56)

A mean coefficient can be introduced by the energy balance

$$h_{fg} \, [\, M_{rtn} - M_{rto} \,] = h_m \, \Delta T \, (\, N \, D \, \pi \,) \qquad \text{----------(5.57)}$$

where hm is to be the mean coefficient for the vertical bank of (N) tubes.

Multiply equation (5.56) by

$$h_{fg} \, [\, M_{rtn} - M_{rto} \,]$$

to get

$$h_{fg}\left(M_{rtn}-M_{rto}\right)\left(M_{rtn}^{\frac{4}{3}}-M_{rto}^{\frac{4}{3}}\right)^{\frac{3}{4}}$$

$$=h_{fg}\left(M_{rtn}-M_{rto}\right)N^{\frac{3}{4}}2^{\frac{1}{4}}(3.42)^{\frac{3}{4}}$$

$$\times\left[\frac{k_m^3\,\rho_m^2\,g}{3\mu_m\,(1+Z)}\right]^{\frac{1}{4}}\left[\frac{\Delta T\,D}{h_{fg}}\right]^{\frac{3}{4}}$$

rearrange to get

$$h_{fg}\left(M_{rtn}-M_{rto}\right)=N^{\frac{3}{4}}2^{\frac{1}{4}}(3.42)^{\frac{3}{4}}\left[\frac{k_m^3\,\rho_m^2\,g}{3\mu_m\,(1+Z)}\right]^{\frac{1}{4}}$$

$$\times\left[\frac{\Delta T\,D}{h_{fg}}\right]^{\frac{3}{4}}\times\frac{h_{fg}\left(M_{rtn}-M_{rto}\right)}{\left(M_{rtn}^{\frac{4}{3}}-M_{rto}^{\frac{4}{3}}\right)^{\frac{3}{4}}}$$

------(5.60)

By analogy with equation (5.57), which is

$$h_{fg} [M_{rtn} - M_{rto}] = h_m \Delta T (N D \pi)$$

$$h_m \Delta T (N D \pi) = N^{\frac{3}{4}} 2^{\frac{1}{4}} (3.42)^{\frac{3}{4}} \left[\frac{k_m^3 \rho_m^2 g}{3 \mu_m (1+Z)}\right]^{\frac{1}{4}}$$

$$\times \left[\frac{D \Delta T}{h_{fg}}\right]^{\frac{3}{4}} \times \frac{h_{fg} [M_{rtn} - M_{rto}]}{[M_{rtn}^{\frac{4}{3}} - M_{rto}^{\frac{4}{3}}]^{\frac{3}{4}}}$$

the mean heat transfer coefficient is

$$h_m = \frac{N^{\frac{3}{4}} 2^{\frac{1}{4}} (3.42)^{\frac{3}{4}}}{N \pi} \left[\frac{k_m^3 \rho_m^2 g}{3 \mu_m (1+Z)}\right]^{\frac{1}{4}} \times \left[\frac{h_{fg}}{\Delta T D}\right]$$

$$\times \left[\frac{D \Delta T}{h_{fg}}\right]^{\frac{3}{4}} \times \frac{[M_{rtn} - M_{rto}]}{[M_{rtn}^{\frac{4}{3}} - M_{rto}^{\frac{4}{3}}]^{\frac{3}{4}}}$$

simplify

$$h_m = \frac{2^{\frac{1}{4}}\,(3.42)^{\frac{3}{4}}}{\pi}\left[\frac{k_m^3\,\rho_m^2\,g}{3\,\mu_m\,(1+Z)}\right]^{\frac{1}{4}} \times \left[\frac{h_{fg}}{\Delta T\;D}\right]^{\frac{1}{4}} \times \left[\frac{1}{N}\right]^{\frac{1}{4}}$$

--------(5.61)

$$\times \frac{\left[M_{rtn} - M_{rto}\right]}{\left[M_{rtn}^{\frac{4}{3}} - M_{rto}^{\frac{4}{3}}\right]^{\frac{3}{4}}}$$

The refrigerant mass flow rate (M_{rto}) entering the top of the top tube = 0, then equation (5.61) is reduced to

$$h_m = \frac{2^{\frac{1}{4}}\,(3.42)^{\frac{3}{4}}}{\pi}\left[\frac{k_m^3\,\rho_m^2\,g}{3\,\mu_m\,(1+Z)}\right]^{\frac{1}{4}} \times \left[\frac{h_{fg}}{\Delta T\;D}\right]^{\frac{1}{4}} \left[\frac{1}{N}\right]^{\frac{1}{4}} \quad --(5.62)$$

Finally, the average heat transfer coefficient for (N) number of tubes during oil-vapor condensation is

$$h_m = 0.725\left[\frac{k_m^3\,\rho_m^2\,g}{\mu_m\,(1+Z)}\right]^{\frac{1}{4}} \left[\frac{h_{fg}}{\Delta T\;D}\right]^{\frac{1}{4}} \left[\frac{1}{N}\right]^{\frac{1}{4}} \quad ----(5.63)$$

5.3- Liquid mixture thermo-physical properties

The thermal and physical properties of the oil-refrigerant condensate mixture used in this study were obtained and calculated from published figures and formulas as follows;

5.3.1- mixture density ρ_m:

For the estimation of the density of the oil-refrigerant solution, the following formula quoted in Ref. (35) was used ,

$$\rho_m = \frac{\rho_o}{1 + W_r \left(\frac{\rho_o}{\rho_r} - 1 \right)} \qquad \text{----------(5.64)}$$

where

ρ_m = oil-refrigerant solution density.

ρ_o = pure oil density at the vapor surface average temperature, (obtained from Fig. 8).

ρ_r = pure refrigerant density.

5.3.2- Mixture viscosity μ_m:

The mixture viscosity was estimated from viscosity-temperature figures quoted in Ref.(35). In the range of solution temperatures and oil percentages used in this study, i.e. 15.5 °C (60°F) < T < 54.4 °C (130°F) and 0 < Z < 20%, part of these figures were enlarged and redrawn on ordinary scale, as shown in Figures (9 and 10). To establish the viscosity lines for concentrations ranging from 2 to 8 per cent, the oil concentration range between 0 to 20 % was divided into ten equal spaces, and parallel lines were drawn.

5.3.3- Mixture thermal conductivity k_m :

A formula given in Ref. (36) was used to calculate the oil-condensate solution thermal conductivity. The formula is;

$$k_m = k_r w_r + k_o w_o - 0.72 [k_o - k_r] w_r w_o \qquad \text{---------(5.65)}$$

where

k_r = Pure refrigerant thermal conductivity at the

vapor-surface average temperature.

k_o = Pure oil thermal conductivity at vapor-surface average temperature, Figure (11).

w_r and w_o are weight fraction of refrigerant and oil in the solution.

5.3.4- Mixture specific heat C_{pm} :

Reference (36) has quoted a formula by which a mixture specific heat may be estimated; the formula is

$$C_{pm} = C_{pr}\, w_r + C_{po}\, w_o \qquad \text{-------(5.66)}$$

where

C_{po} = specific heat of alkylbenzene based refrigeration oil, (obtained from Fig. 12), kJ/kg. C.

C_{pr} = specific heat of liquid refrigerant kJ/kg. C.

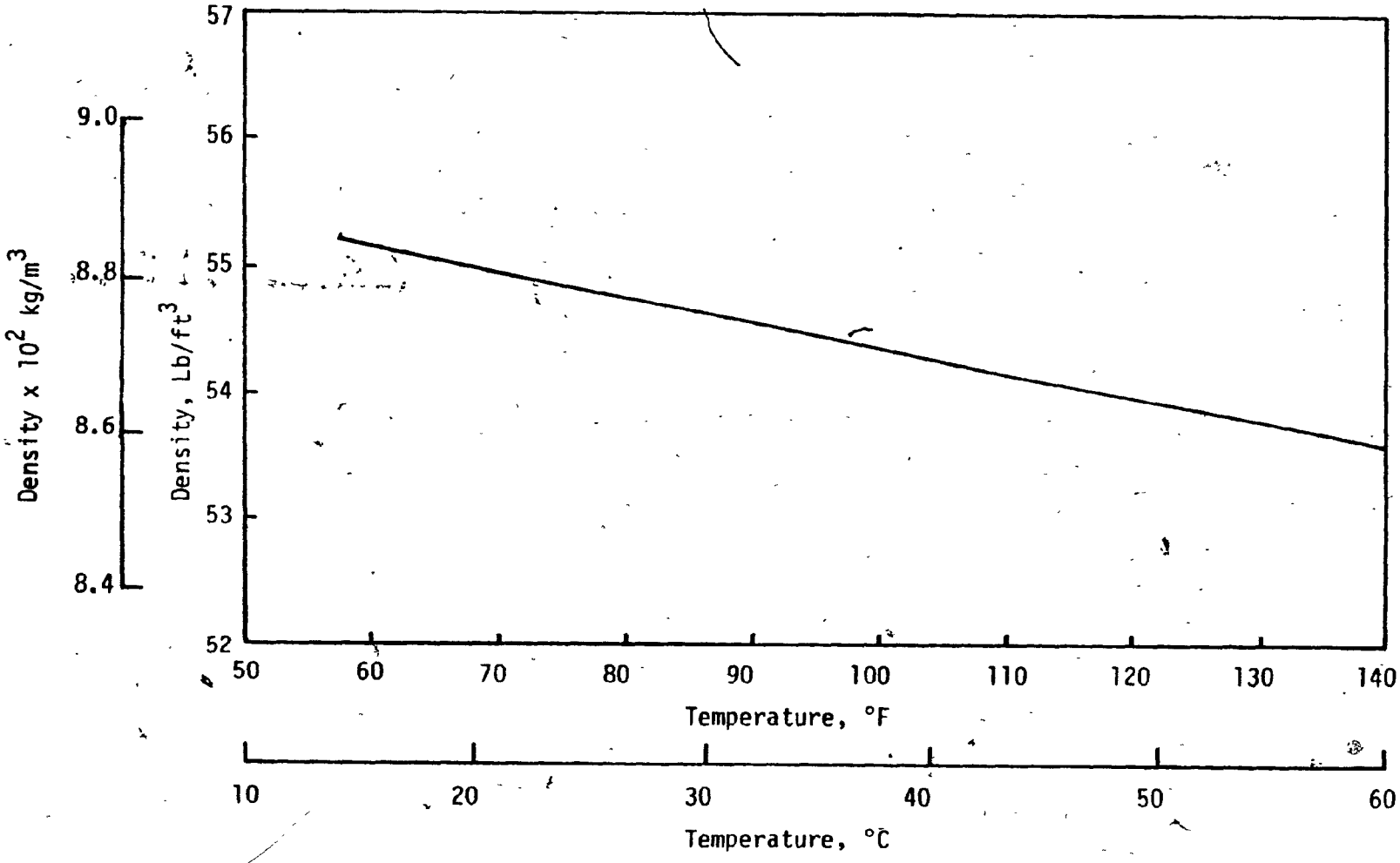

Figure 8: Density of alkylbenzene refrigeration oil of viscosity 150 SSU at 37.7 °C (100 °F). (from oil manufacturer)

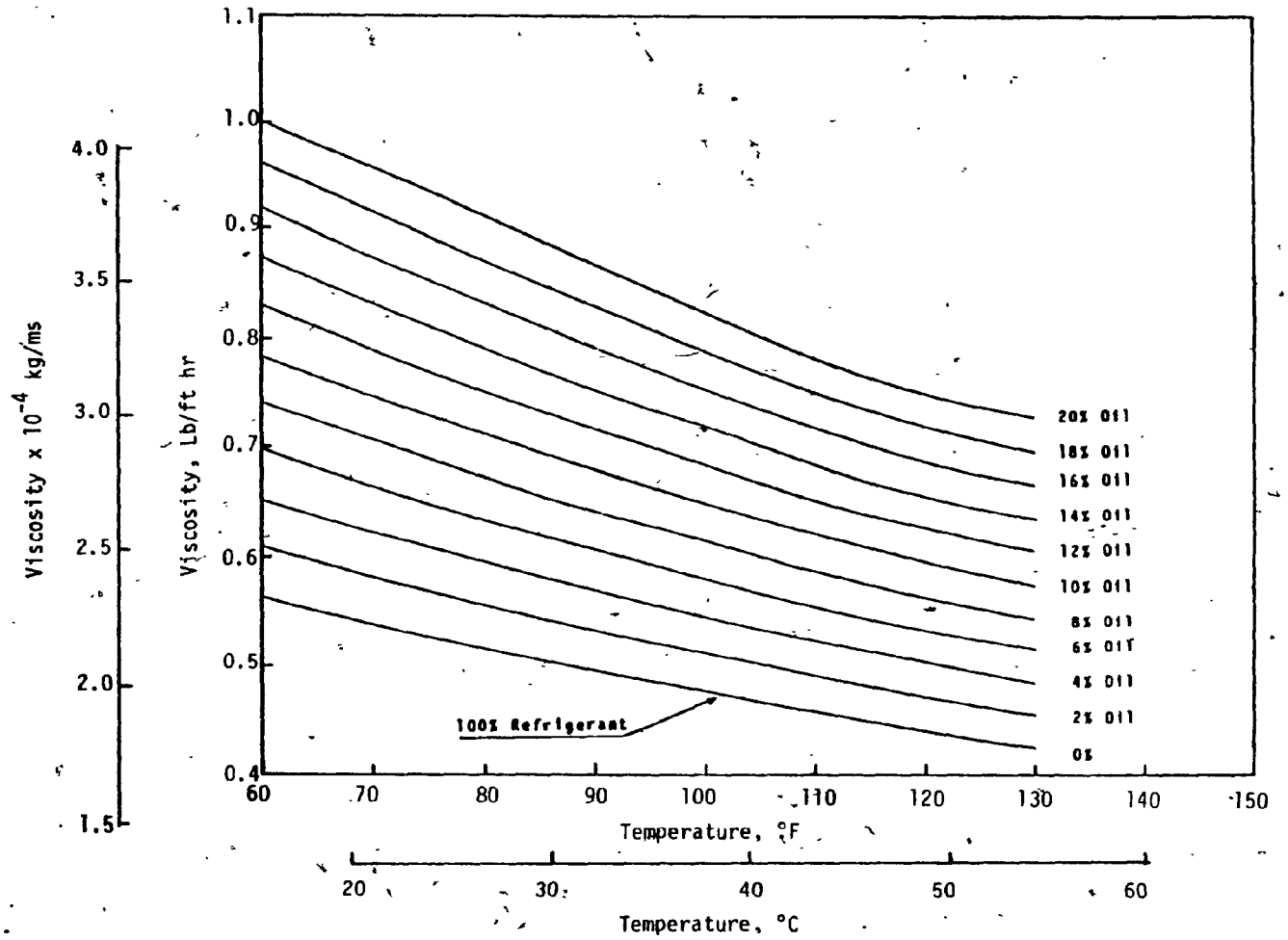

Figure 9: Viscosity of solution R-12 with a 150 SSU at 37.7 °C alkylbenzene oil, (Ref.35).

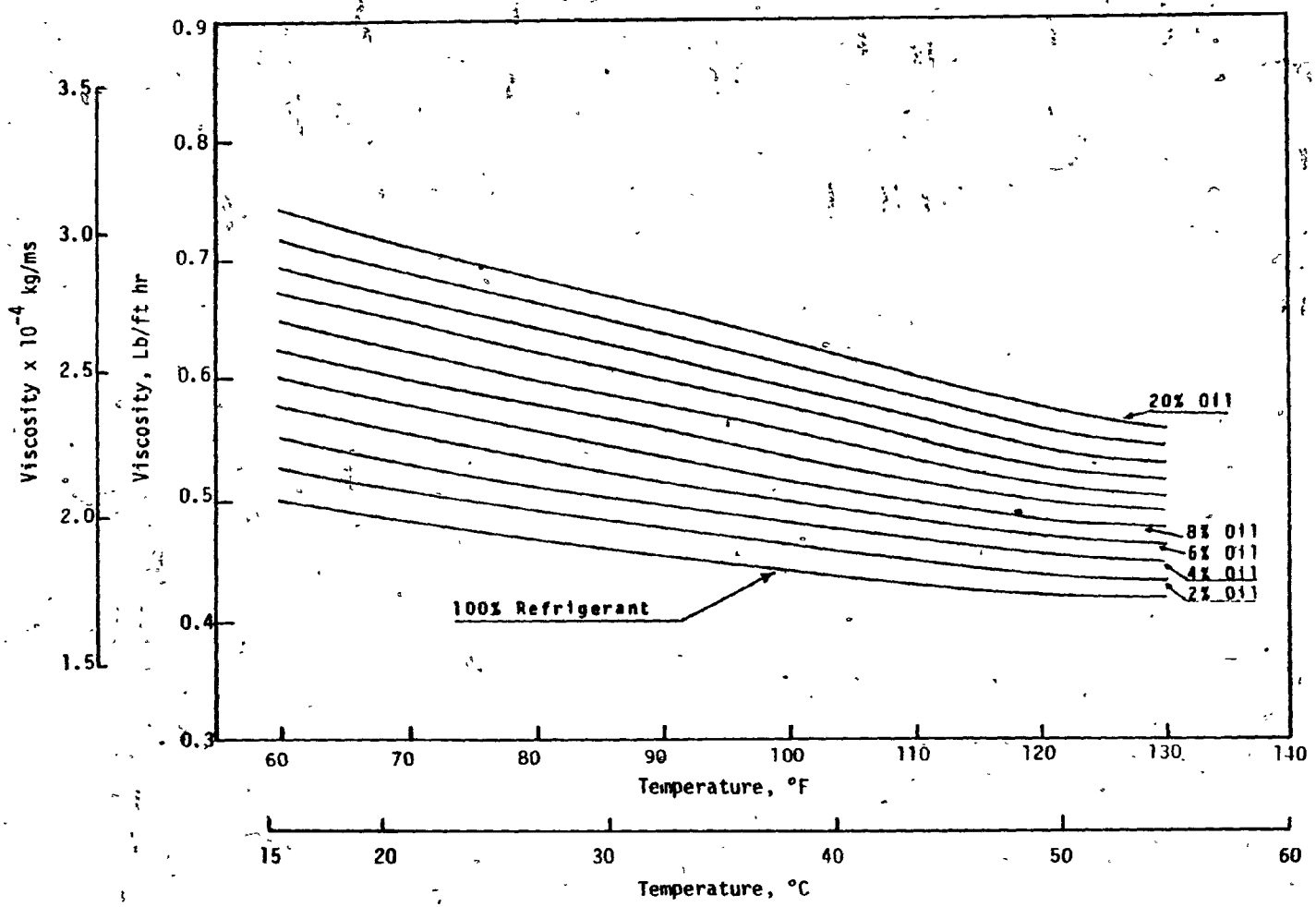

Figure 10: Viscosity of solution R-22 with a 150 SSU at 37.7 °C alkylbenzene oil. (Ref.35).

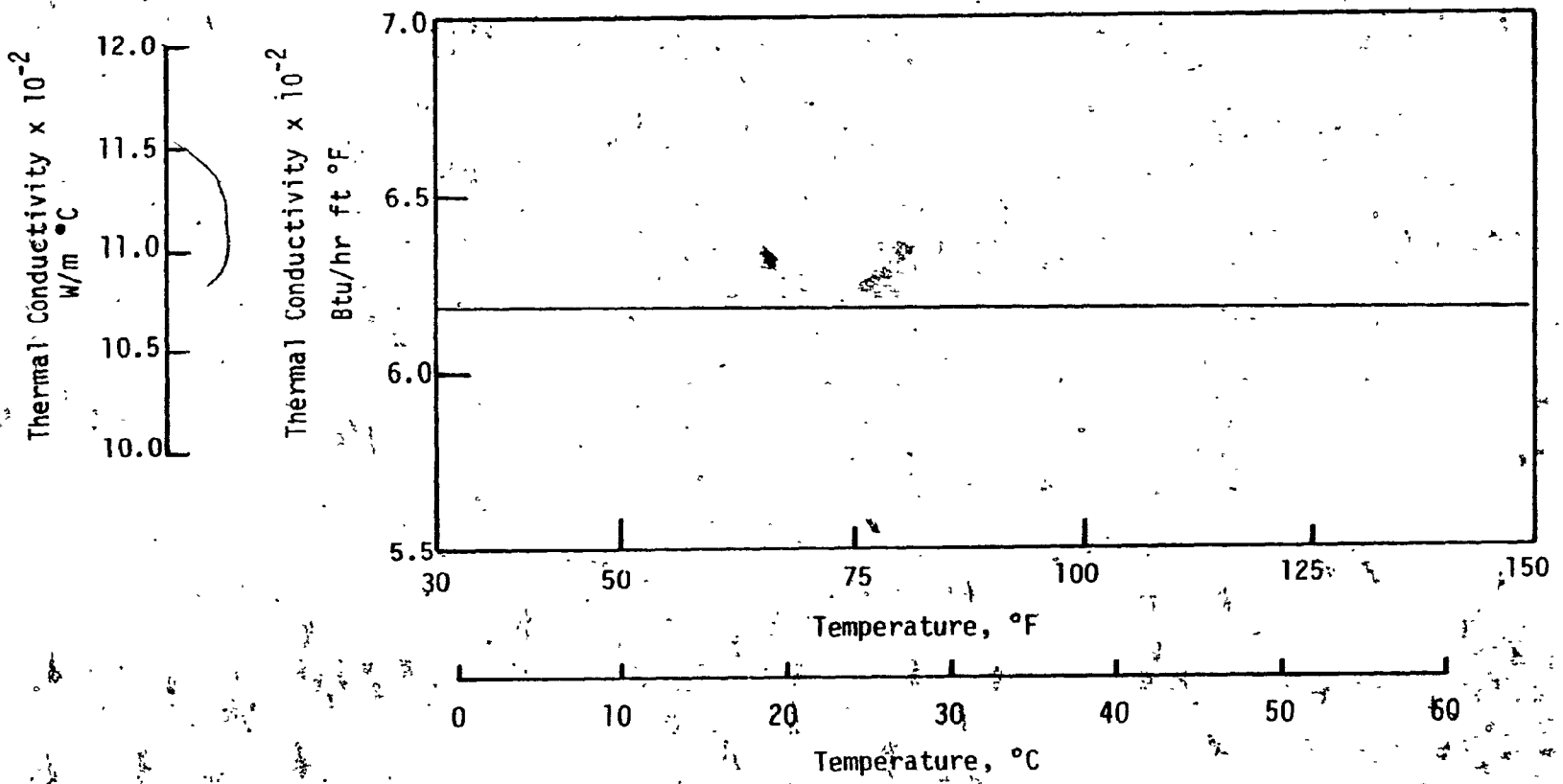

Figure 11: Thermal conductivity of alkylbenzene refrigeration oil of viscosity 150 SSU at 37.7 °C (100 °F). (from oil manufacturer)

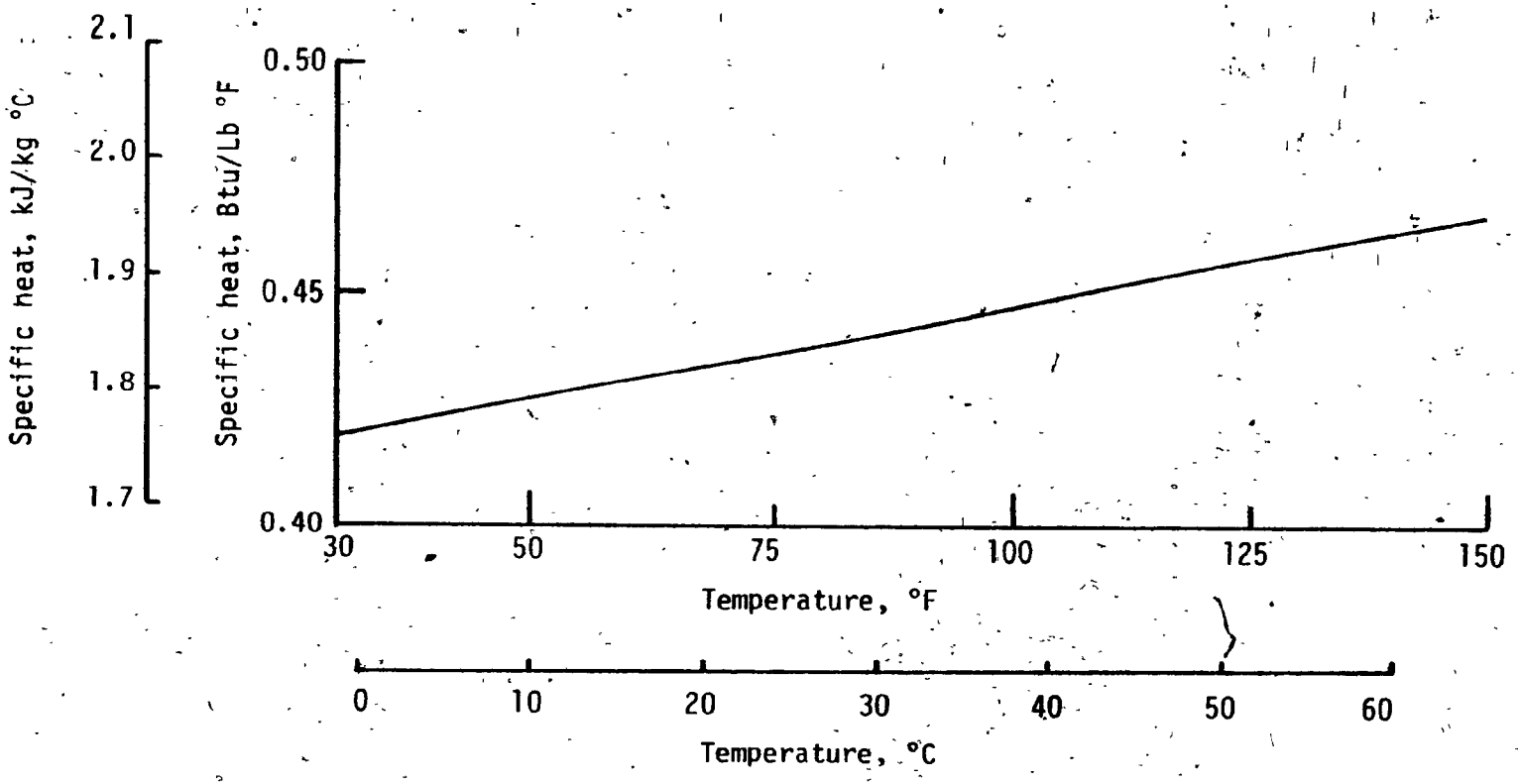

Figure 12: Specific heat of alkylbenzene refrigeration oil of viscosity 150 SSU at 37.7 °C (100 °F). (from oil manufacturer)

CHAPTER 6

RESULTS AND DISCUSSION

6.1- Experimental results and correlations;

In this study R-12 and R-22 vapors, pure and mixed with oil, were condensed on horizontal plain single and 4 tubes stacked in a vertical bank. Condensation tests in the presence of oil were conducted at oil to refrigerant mass ratios of 2, 4, 6 and 8 percentages by weight.

R-12 was condensed on a single 25.4 mm O.D., 15.8mm O.D. and a vertical bank of 4 horizontal 15.8 mm O.D. tubes. Pure vapor and vapor-oil mixtures were condensed at three different vapor saturation temperatures, namely 32.2, 40.6 and 48.9 °C (90, 105 and 120 °F). The experimental data obtained for pure vapor condensation of R-12 on the single and multi-tube cases are listed in Tables (1-3) for each saturation temperature. The data obtained for the condensation of vapor-oil mixture at the different oil percentages used in this study and at each saturation temperature are listed in Tables (4-7), (8-11) and (12-15) for the single 25.4 mm tube, the single 15.8 mm tube and the multi-tube case respectively.

Another refrigerant, R-22, was condensed on a single 15.8 mm O.D. horizontal tube and a vertical bank of 4

horizontal tubes, 15.8 mm O.D. each. Pure vapors and vapor-oil mixtures were condensed at 32.2°C and 40.6°C (90°F and 105°F) saturation temperatures. Condensation in the presence of oil was conducted at the same oil to refrigerant mass ratios as those used for R-12. For both single tube and multi-tube cases, the pure vapor condensation data are listed in tables (16) and (17) and the vapor-oil mixture condensation data are listed in Tables (18-25).

For each refrigerant, the saturation temperatures (T_v) were determined by controlling the corresponding condensing pressure precisely in the test condenser. This was made possible by the application of a pressure transducer.

The tube surface temperature, used to obtain the temperature drop across the liquid film layer, ($\Delta T = T_v - T_s$); was the average of the total thermocouple measurements at different points of the condensing surface.

The heat transfer rate during the condensation process was obtained by measuring the rate of liquid condensate mass entering the liquid receiver and the temperature rise of the cooling water passing through the condensing tube. In the case of pure vapor condensation, the liquid entering the receiver is a pure refrigerant condensate, hence, the heat transfer obtained by the two methods is:

$$Q = h_{fg} M_r$$

and

$$Q = M_w C_{pw} (T_{wo} - T_{wi})$$

In the case of oil-refrigerant condensation, the rate of liquid condensate as a part of the mixture entering the liquid receiver was obtained as follows:

$$\rho_m = \frac{\rho_o}{1 + w_r \left[\frac{\rho_o}{\rho_r} - 1 \right]} \qquad \text{----------(6.1)}$$

(Ref.35)

where

ρ_m = Mixture density at the saturation temperature T_v .

ρ_o = Density of pure oil at the saturation temperature T_v .

ρ_r = Density of pure refrigerant at the saturation temperature T_v .

w_r = Weight fraction of refrigerant in the mixture.

The liquid mixture volume flow rate entering the receiver was estimated by measuring the rate of liquid rise:

$$V = [L_2 - L_1]\, A_L \qquad \text{----------(6.2)}$$

where

$(L_2 - L_1)$ = Rate of change of liquid level in the receiver, m/s.

A_L = Receiver cross sectional area, m^2.

If M_t is the mass flow rate of the liquid mixture entering the receiver, then:

$$M_t = \rho_m V \qquad \text{----------(6.3)}$$

At a steady state condition, the mixture mass flow rate to the receiver is equal to the sum of mass rates of the refrigerant and oil entering the test condenser:

$$M_t = M_r + M_o \qquad \text{----------(6.4)}$$

where

M_r = Refrigerant mass flow rate, kg/s

M_o = Rate of oil mass atomized, kg/s

If the oil to refrigerant mass ratio $M_o / M_r = Z$, then

$$M_o = Z \; M_r \qquad \text{--------(6.5)}$$

by combining equations (6.6), (6.4) and (6.5) and solving for (ρ_m):

$$\rho_m = \frac{M_r}{V} \; (1 + Z) \qquad \text{----------(6.6)}$$

substitution of equation (6.6) in equation (6.1) yields the liquid condensate mass flow rate to the liquid receiver:

$$M_r = \left(\frac{V}{1 + Z} \right) \left\{ \frac{\rho_o}{1 + w_r \left[\frac{\rho_o}{\rho_r} - 1 \right]} \right\} \qquad \text{-------(6.7)}$$

Neglecting the subcooling, the heat transfer rate is then:

$$Q = M_r \; h_{fg}$$

where

h_{fg} = Latent heat, kJ/kg

The heat transfer coefficient (h), of condensing vapors, pure and mixed with oil, were then calculated by Newton's equation:

$$h_m = \frac{Q}{A_s[\, T_v - T_s \,]}$$

where Q and T_s are measured, T_v is the condensing temperature and A_s is the condensing surface area. (see computer programme in Appendix 2).

6.1.1- R-12 Pure vapor condensation

Film coefficients for condensing R-12 pure vapor on the external surface of a single horizontal 15.8, 25.4 mm O.D. tubes and vertical bank of 4 horizontal 15.8 mm O.D. tubes, at the condensing temperatures 32.2, 40.6 and 48.9 °C (90, 105 and 120 °F) are plotted in Figure (13). Nusselt's equations derived for these cases were solved at 32.2 °C saturation and the results are shown in the same figure. Nusselt's equation for multi-tube condensation modified by Kern Ref.(15) is plotted. Also White's data Ref.(10) based on 32.2 °C saturation temperature are shown for comparison.

The experimental data for the condensation of R-12 on both 25.4 mm O.D. and 15.8 mm O.D. single tubes were correlated by one empirical relation:

$$h = C \left[\frac{1}{D \ \Delta T} \right]^{0.25} \qquad \text{----------(6.8)}$$

in which (D) is the tube outside diameter and (C) is a constant calculated for each test point and tube diameter. The average (C) is calculated and, hence, the empirical equation deduced for the single tube is:

$$h = 1010 \left[\frac{1}{D \ \Delta T} \right]^{0.25} \qquad \text{----------(6.9)}$$

Equation (6.9) is plotted in Figure (13) and seems to represent the experimental data for both tube diameters quite accurately.

By comparing the experimental results for both single and multi-tube condensation with Nusselt's equations for the same cases, it can be said that , for the single tube case, the data have the same pattern as that of Nusselt's theory, i.e. $h \propto (\Delta T)^{-0.25}$. But the data obtained from the multi-tube condensation tend to rise when (ΔT) gets larger and thus deviating from the theory pattern, i.e. $h \propto (\Delta T)^{-e}$ where (e) is less than 0.25.

In order to find the actual exponent of (ΔT), the multi-tube results were plotted on a log scale as shown in Figure (14) and a straight line of slope (-0.25) was drawn through. By inspection of Figure (14) it was found that this line does not represent the average of the data; therefore another line of slope (-0.2) was drawn and found to better weigh and average these data.

In deducing an empirical equation to correlate the multi-tube pure vapor condensation results, an attempt was made to modify equation (6.9) by keeping the same constant (C = 1010) but changing the exponent of (ΔT) from (-0.25) to (-0.2) and introducing (N) the number of tubes. The equation thus found is:

$$h = 1010 \left[\frac{1}{D}\right]^{0.25} \left[\frac{1}{\Delta T}\right]^{0.2} \left[\frac{1}{N}\right]^{\beta} \qquad \text{----------(6.10)}$$

with N=4, the exponent (β) thus calculated was 0.171. This equation (6.10) was found not to represent the experimental data satisfactorily. Since $N^{-0.167}$ was recommended by Kern Ref.(15) and Ivanov Ref.(23), it was used in equation (6.10) and the constant (C) for each point was calculated. The average constant (C) was obtained and the empirical equation for the multi-tube

case is as follows:

$$h = 898 \left[\frac{1}{D}\right]^{0.25} \left[\frac{1}{\Delta T}\right]^{0.2} \left[\frac{1}{N}\right]^{0.167} \qquad \text{---------(6.11)}$$

Equation (6.11) is plotted in Figure (13) and seems to well represent the average of the multi-tube pure vapor condensation results. Also, Nusselt's equation for multi-tube condensation, and Nusselt's equation modified by Kern, are plotted in the same figure for comparison.

6.1.2.- R-12 vapor-oil mixture condensation

The experimental heat transfer coefficient versus film temperature drop of condensing oil-vapor mixture on a single horizontal 25.4 mm and 15.8 mm O.D. tubes are shown in Figures (15) and (16) respectively. In these two figures the data obtained at different oil concentrations, namely 2, 4, 6 and 8 per cent are plotted and compared with the pure vapor condensation. These results indicate that the presence of oil mixed with the condensing vapor affects the heat transfer coefficient. The higher the oil concentration the lower the coefficient. From Figure (13) the comparison of the pure vapor data pattern with Nusselt's prediction confirms that $h \propto (\Delta T)^{-0.25}$. In Figures (15) and (16) the patterns generated by the experimental points for the

various oil concentrations are the same as those for the pure vapor data, which indicate that for single tube oil-vapor condensation, the heat transfer coefficient, also, varies with $(\Delta T)^{-0.25}$.

Since it was possible to correlate the pure vapor condensation data, generated by the 25.4 mm and 15.8 mm O.D. tubes by a single equation as shown in Figure (13), this equation was modified to include the oil-refrigerant mass ratio (Z) so that it can be applied for the oil-vapor condensation. The modified equation is:

$$h_m = [\, 1010 - C\, Z \,] \left[\frac{1}{D\, \Delta T} \right]^{0.25} \qquad \text{----------(6.12)}$$

All the data for oil-vapor condensation plotted in Figures (15) and (16) were used to evaluate the constant (C). The deduced empirical equation is:

$$h_m = [\, 1010 - 1460\, Z \,] \left[\frac{1}{D\, \Delta T} \right]^{0.25} \qquad \text{----------(6.13)}$$

Equation (6.13) was plotted in Figures (15) and (16)

showing a good correlation of the experimental results for both 15.8 and 25.4 mm O.D. tubes at various oil percentages.

The heat transfer coefficient obtained for the oil-vapor condensation on the vertical bank of 4 tubes are shown in Figure (17). Data of 2, 4, 6 and 8 per cent oil concentration are plotted and compared with the pure component results. As for the single tube, the results show that the presence of oil reduces the heat transfer coefficient.

The empirical equation developed for the pure vapor condensation (equation 6.11) was modified to predict the oil-vapor mixture condensation on a vertical bank of 4 tubes. The equation is:

$$h_m = [\ 898 - 1550\ Z\ ]\ [\ \frac{1}{D}\ ]^{0.25}\ [\ \frac{1}{\Delta T}\ ]^{0.2}\ [\ \frac{1}{N}\ ]^{0.167} \quad ---(6.14)$$

Equation (6.14) is plotted in Figure (17) and seems to reasonably represent the average of the test data.

6.1.3- R-22 Pure vapor condensation results

The heat transfer coefficient of condensing R-22 pure vapor is plotted against vapor-surface temperature drop (T_v - T_s) in Figure (18). Nusselt's equation for the condensation of R-22 on a horizontal 15.8 mm O.D. tube is also plotted for comparison.

The experimental data listed in Tables (22) and (23) are correlated by the following empirical equation:

$$h = C \left[\frac{1}{\Delta T}\right]^{0.25} \qquad \text{----------(6.15)}$$

in which the constant (C) is calculated for each test point and the average is obtained. The empirical equation thus deduced is:

$$h = 3560 \left[\frac{1}{\Delta T}\right]^{0.25} \qquad \text{----------(6.16)}$$

Equation (6.16) is plotted in Figure (18) and seems to represent the experimental data at the saturation temperatures 32.2 and 40.6 °C (90 and 105 °F) quite

accurately.

As for R-12, the data obtained from the single tube tests form a pattern similar to that generated by Nusselt's theory, i.e. $h \propto (\Delta T)^{-0.25}$.

The experimental data obtained from pure R-22 condensation on a vertical bank of 4 horizontal, 15.8 mm O.D. tubes are plotted in Figure (19) along with Nusselt's theory for multi-tube condensation. The pattern generated by the data was found to be different from that of the theory, hence the data were plotted on a log scale, Figure (20). By direct measurement, the actual slope of (ΔT) was found to be (-0.2) rather than (-0.25), which is same as that found for R-12.

With the exponent of (ΔT) thus found, and the exponent of (N) as suggested by Kern and Ivanov, Ref.(15) and (23) respectively, the following empirical equation was deduced:

$$h = 3340 \left[\frac{1}{\Delta T}\right]^{0.2} \left[\frac{1}{N}\right]^{0.167} \qquad \text{----------(6.16 a)}$$

where the constant is the average of all the constants evaluated at each test point.

Equation (6.16 a) is plotted in Figure (19), where it shows a good agreement with the experimental results.

6.1.4- R-22 vapor-oil mixture condensation

The experimental data obtained from the condensation of oil-vapor mixture on a 15.8 mm O.D. single tube are shown in Figure (21). The heat transfer coefficient obtained at different oil concentrations, namely, 2, 4, 6 and 8 per cent are plotted versus ΔT and compared with the pure vapor condensation.

The empirical equation (6.16) deduced for the pure vapor condensation was modified to predict the heat transfer coefficient of oil-vapor mixture condensation. The modified equation is:

$$h_m = [\, 3560 - C\,Z \,]\, [\, \frac{1}{\Delta T} \,]^{0.25} \qquad \text{----------(6.17)}$$

All the data for oil-vapor condensation plotted in Figure (21) were used to evaluate the constant (C). The average value of (C) was calculated and the deduced empirical equation is:

$$h_m = [\ 3560 - 3550\ Z\ ]\ [\ \frac{1}{\Delta T}\ ]^{0.25} \qquad \text{---------(6.18)}$$

Equation (6.18) is plotted in Figure (21) and shows a good correlation with the experimental data.

The heat transfer coefficients obtained for the oil-vapor condensation on the vertical bank of 4 tubes are plotted in Figure (22). The empirical equation developed for the pure vapor condensation, equation (6.11), was modified to predict the oil-vapor mixture condensation on a vertical bank of 4 tubes. The equation is:

$$h_m = [\ 3340 - 3390\ Z\ ]\ [\ \frac{1}{\Delta T}\ ]^{0.2}\ [\ \frac{1}{N}\ ]^{0.167} \qquad \text{--------(6.18a)}$$

Equation (6.18 a) is plotted in Figure (22) and it shows a good agreement with the experimental data.

6.2- Theoretical results

The derived theoretical model for the condensation on a single tube is:

$$h_m = \frac{0.725\ k_m^{0.75} \left\{ \frac{h_{fg}\ g\ \rho_m^2}{\mu_m\ [1 + Z]} + \frac{3\ \Delta T\ \rho_m^2\ C_{pm}\ g}{8\ \mu_m} \right\}^{0.25}}{[\ D\ \Delta T\ ]^{0.25}} \qquad \text{-----(6.19)}$$

and for the multi-tube condensation is

$$h_m = 0.725 \left[\frac{k_m^3\ \rho_m^2\ g}{\mu_m\ (1 + Z)} \right]^{0.25} \left[\frac{h_{fg}}{\Delta T\ D} \right]^{0.25} \left[\frac{1}{N} \right]^{0.25} \qquad \text{----------(6.20)}$$

To solve these two equations, the physical and thermal properties of the condensate-oil solutions at oil percentages used in this study and at the average film temperature, must be determined.

Equations (6.19) and (6.20) were solved at the vapor saturation temperature 32.2 °C (90°F), and accordingly all the physical and thermal properties were calculated at the average film temperature $T_f = (T_v + T_s)/2$. Density, thermal conductivity, viscosity and specific heat of pure

R-12 and R-22 are listed in Table (26), while oil-refrigerant mixtures properties at 2, 4, 6 and 8 percentages of oil to refrigerant mass ratios are listed in tables (27 to 30), respectively.

Equation (5.64) was used to calculate the oil-refrigerant mixture density for the different oil concentrations. The pure refrigerant and oil densities required to solve the equation were taken from Table (26) and Figure (8), respectively.

R-12 and R-22 oil solution viscosities, at the average film temperatures were taken from Figures (9) and (10) respectively at the desired oil percentages.

Equation (5.65) was used to calculate the refrigerant-oil solution thermal conductivity. The pure refrigerant solution for R-12 and R-22 were taken from Table (26) and the pure oil thermal conductivity was taken from Figure (11).

The specific heat of the oil-refrigerant solution for different oil concentrations and at different film temperature were calculated by using equation (5.66). The required pure refrigerant specific heat values were taken from Table (26) and the pure oil specific heat values were found from Figure (12).

The theoretical heat transfer coefficients for the condensation of pure R-12 and R-22 vapors and vapor-oil mixtures on a single tube calculated by equation (6.19) and listed in Tables (31 to 33), are plotted in Figures (23) and (24) for R-12 and Figures (25) for R-22.

For multi-tube condensation, the oil-vapor condensation coefficient calculated by equation (6.20), for both R-12 and R-22, are listed in tables (34) and (35) respectively. These results are plotted in Figures (26) and (27) and compared with Nusselt's equation for multi-tube condensation.

To predict closer results to the actual condensing coefficient, the analytical equation (6.20) was modified. The exponent of (N) was changed from (- 0.25) to (- 0.167), and this modified equation was evaluated at different vapor-surface temperature drop and different oil percentages, for both refrigerants used in this study. The results obtained are listed in tables (36) and (37) and plotted in Figures (28) and (29) respectively. The modified analytical equation is:

$$h_m = 0.725 \left[\frac{k_m^3 \rho_m^2 g}{\mu_m (1 + Z)} \right]^{0.25} \left[\frac{h_{fg}}{\Delta T D} \right]^{0.25} \left[\frac{1}{N} \right]^{0.167} \qquad \text{--------(6.20a)}$$

6.3- Discussion of the experimental results:

A synthetic alkylbenzene refrigeration oil (150 SSU. at 37.7°C) was used to study the effects of oil presence during the condensation of refrigerants R-12 and R-22 on the outside surface of a single and a vertical bank of plain horizontal tubes. Both refrigerants are completely miscible with the alkylbenzene refrigeration oil.

R-12, pure and mixed with oil vapors, were condensed at 32.2, 40.6 and 48.9 °C (90, 105 and 120 °F) saturation temperatures, while R-22 was condensed at 32.2 and 40.6°C (90 and 105 °F) only. At each condensing temperature, besides the pure vapor, tests were conducted at 4 different oil to refrigerant mass ratios, namely 2, 4, 6 and 8 per cent.

6.3.1- Single tube tests

a- Pure refrigerant condensation

R-12 and R-22 pure vapor condensation test results shown in Figures (13), (18) and (19) were used as the base reference for the condensation of oil-refrigerant mixtures and to generate the flow meter calibration curves as shown in Figures (4) and (5).

In Figure (13), the data obtained from the condensation

of pure R-12 vapor on the external surface of a single horizontal 25.4 mm and 15.8 mm O.D. tubes at the saturation temperatures 32.2, 40.6 and 48.9°C, are plotted.

The test data obtained from the condensation of pure R-22 vapor on a horizontal 15.8 mm O.D. tube at the saturation temperatures 32.2 and 40.6 °C are plotted in Figure (18). Close examination of Figures (13) and (18), shows that there is no appreciable difference between the data obtained at the condensing temperature range used in this study for both refrigerants. Although most of the data follows Nusselt's theory so that the lower the saturation temperature, the higher is the heat transfer coefficient for the same ΔT, the experimental difference is much less than that predicted by the theory. Nusselt's theory based on 32.2 °C condensing temperature, for both refrigerants, is plotted in Figures (13) and (18). If the other two curves based on 40.6 and 48.9 °C were to be plotted, they would be lower than the one based on 32.2 °C. This indicates that Nusselt's theory based on 32.2 °C, for both refrigerants, predicts results closer to the actual heat transfer coefficients than that based on higher temperatures.

Based on these results, and for engineering practice where a simple relation may be used that can deal with different cases, the results obtained from each refrigerant condensation tests at the different saturation temperatures

were successfully correlated by a single relation. Equation (6.9) plotted in Figure (13) is a good representative for the condensation of R-12 vapor on both 25.4 mm and 15.8 mm O.D. tubes and at the condensing temperatures 32.2, 40.6 and 48.9 °C. Also equation (6.16), plotted in Figure (18), correlates the data taken at the condensing temperatures 32.2 and 40.6 °C for refrigerant-22 vapor condensation on the outside surface of a 15.8 mm O.D. tube, quite accurately.

The consistency of R-12 pure vapor condensation results was checked by a comparison made with other investigator's results. For R-22 vapor condensation, experimental data are not available in the open literature.

White's data, Ref.(10), obtained from the condensation of R-12 vapor on a 15.8 mm O.D. tube at 32.2 °C condensing temperature, are plotted in Figure (13). The comparison yields a good agreement between these data and those obtained in this study. On the 25.4 mm O.D. tube condensation, test data were not found in the literature, therefore, the results obtained were compared with the data obtained from the 15.8 mm O.D. tube which is already confirmed, using Nusselt's relation

$$h \propto [\, D \,]^{-0.25}$$

By transformation of the results obtained from the 25.4 mm O.D. tube to the 15.8 mm tube using Nusselt's relation, a good agreement was found to exist, from which it was concluded that the data obtained from the 25.4 mm O.D. tube are also consistent.

By comparing the experimental results of R-12 and R-22 vapor condensation with the predictions of Nusselt's theory, as shown in Figures (13) and (18), it is interesting to note that the experimental results for both refrigerants are about 3 per cent higher than those predicted by the theory. The two figures indicate that for both refrigerants, the experimental data have the same pattern as Nusselt's theory and for the same ΔT, R-22 results are higher than those of R-12 due to the relatively lower viscosity and higher thermal conductivity.

In Figure (13), White's data are also higher than the theoretical results, which is in contradiction with his article where Nusselt's theory was reported to be higher than the experimental results. Young's results Ref.(9) for the condensation of R-12, were also reported to be higher than the prediction of Nusselt's theory.

In this study as well as that of Young, the physical and thermal properties of the tested refrigerants were evaluated at an average between the condensing tube and the

condensing vapor temperature. Although White did not indicate at what conditions the properties were evaluated, he indicated that his results fall 13 per cent below the Nusselt lines for all condensing temperatures and the results of Young fall 9.6 per cent below. By comparing the results obtained in this study and those of White, it is concluded that the physical and thermal properties used by those investigators are different from the properties available at the present time.

b- Oil-vapor mixture condensation

In this study the rate of oil atomized and mixed with the vapor was always in a fixed mass proportion for a set of runs. This procedure allowed the study of the variation of the heat transfer coefficient with varying vapor to surface temperature drop while keeping the oil-vapor mixture constant throughout the set of runs.

Inspection of Figures (15), (16) and (18) indicate that the presence of oil affects the smooth tube condensation and that the heat transfer coefficient is dependent on the oil-refrigerant mass ratio. These results are in agreement with the conclusions arrived at by Sauer, Ref.(30). The heat transfer coefficient was found to vary inversely with the oil to refrigerant mass ratios.

Generally, in the literature, experimental data for the

condensation of R-12 and R-22 vapor-oil mixtures are not available, therefore, a comparison with the data obtained here cannot be made. The only experimental data available in the literature are those presented by Sauer, with which a comparison on an absolute values cannot be made for the following reasons:

1- Different test apparatus;

2- Different refrigerants;

3- Different condensing tube diameter;

4- Different experimental procedure.

The only comparison which possible between these two tests, is that both refrigerants i.e R-12 and R-22, used in this study as well as R-11 used in Sauer's study, are completely miscible in the refrigeration oil and that the presence of oil in both studies caused a reduction in the heat transfer coefficients. The results of Sauer as well as the results obtained here show that the higher the oil percentage is, the lower is the heat transfer coefficient.

In this study, the heat transfer coefficients, for both refrigerants, were found to be affected by the presence of oil in any proportion, while Sauer stated that for oil percentages lower than 6-7 %, the presence of oil has no appreciable effect. This difference in the results between the two studies for the small oil percentages may be due to the difference in the experimental apparatus and procedure.

In this study, for each set of a fixed oil to refrigerant mass ratio test runs, twelve or more test points were generated. Thus, for a 2 per cent oil to refrigerant mass ratio difference between two consecutive tests, some test points may interfere with each other which may reflect an impression of a non-appreciable effect, but averging of the total generated test points shows a distinct reduction in the heat transfer coefficient as shown in Figures (15), (16) and (18).

6.3.2- Multi-tube condensation

a- Pure refrigerant condensation

Both refrigerants, R-12 and R-22, pure vapor and oil-vapor mixture were condensed on a vertical bank of four 15.8 mm O.D. horizontal tubes. The pure vapor tests shown in Figures (13) and (19) were used as the base reference for the condensation of oil-refrigerant mixtures on the multi-tubes, and to generate the required flow meter calibration curves, Figures (4) and (5). Nusselt's equation for multi-tube condensation, based on 32.2 °C condensing temperature, is also plotted in Figures (13) and (19). The comparison shows that the heat transfer coefficient for R-12 and R-22 are much higher than those predicted by the theory. The difference between the theory and the experiments was attributed to the momentum gain by the liquid descending

from the top tube to the lower and the rippling of the condensate layer on the individual tube, neither of which is taken care of by Nusselt's theory. To modify the theory, Kern, Ref.(15), and Ivanov, Ref.(23), suggested that the exponent of (N), where (N) is the number of tubes in a bank, should be (-1/6) and (-0.16) respectively instead of (-0.25) which was obtained analytically by Nusselt. The modification of Nusselt's equation for multi-tube case will be:

$$h_c = 0.725 \left[\frac{\rho^2 k^3 h_{fg} g}{\mu \Delta T D} \right]^{0.25} \left[\frac{1}{N} \right]^{\frac{1}{6}} \qquad \text{-----(6.21)}$$

Equation (6.21) is plotted in Figures (13) and (29) and seems to represent the experimental data quite accurately at ΔT up to 8 °C. This, however, confirms that the experimental results are consistent and agree with the findings of Kern and Ivanov. It is of interest to note that as ΔT gets larger, the deviation between the modified Nusselt theory and the experimental results increases. When ΔT becomes larger than 8 °C, the theory begins to underestimate the heat transfer coefficient and this is due to the increase of turbulence in the condensate layer as a

result of the increase in the rate of condensation. By visual observation through the shell windows, it was noticed that as the rate of condensation increases, due to the increase of ΔT, the turbulence in the liquid layer increases and this causes the heat transfer coefficient to rise.

The deviation between Nusselt's equation and the experiments was taken care of by the empirical equation (6.11) plotted in Figure (13) and equation (6.16 a) plotted in Figure (19), for R-12 and R-22 respectively. By comparison, these empirical equations seem to correlate the pure vapor results more accurately than Nusselt's equation based on $(N)^{-0.25}$ and , $(N)^{-1/6}$, at all ΔT. This was made possible by finding the actual exponent of ΔT from Figures (14) and (20) as (-0.2) instead of (-0.25) which was found analytically by Nusselt. Ivanov, Ref.(23), results from a ten tube vertical row bundle condensation were correlated by $(\Delta T)^{-0.148}$ and he concluded that $h \propto (\Delta T)^{-0.25}$ does not hold for a tube bundle. His conclusion agrees well with the finding of this study, and the difference in the exponent of (ΔT) can be attributed to the difference in the number of tubes in a row used in both studies.

By comparing the results obtained from the single tube and 4 tube tests conducted in this study, and the ten tube

bundle results obtained by Ivanov, Ref.(23), it can be found that the exponent of (ΔT) has increased from (-0.25) for the single tube to (-0.2) for the 4 tube bundle and up to (-0.148) for the ten tube bundle. Within this range, the variation of the exponent of ΔT can give the impression that it depends on the number of tubes in a tube bundle. The larger the number of tubes, the larger the exponent.

b- Oil vapor mixture condensation

Like the single tube tests, the rate of oil atomized and mixed with the condensing vapor was always in a fixed mass ratio for a certain set of runs. This permitted the study of the behaviour of the heat transfer coefficient when an oil-vapor mixture is condensed on a multi-tube condenser. The results shown in Figures (17) and (22) indicate that the effect of oil presence on the multi-tube condensation is the same as that for a single tube, in the sense that, the higher the oil percentage the lower the heat transfer coefficient. Also, the presence of oil in any proportion was found to affect the condensation and this is clearly shown when the data for different oil percentages tests were averaged.

In Figures (17) and (22), the results obtained from the condensation of R-12 and R-22 vapors mixed with different oil percentages, seem to follow the same pattern as that of the pure vapor condensation. For ΔT higher than 8 °C the

rate of drop of the heat transfer coefficient with the increase of ΔT, decreases for the same reasons as in the case of pure vapor condensation, i.e. the turbulence within the liquid film, whose effect was found to increase with the increase of ΔT and cause a considerable rise of the heat transfer coefficient.

6.4- Discussion of the theoretical results

6.4.1-Single tube condensation

a- Pure refrigerant results

By evaluating the physical and thermal properties of R-12 and R-22 at the average film temperature, Nusselt's theory was plotted in Figures (13) and (18) and found to fall about 3 per cent below the experimental data for both refrigerants. This deviation may occur partly due to the rippling of the condensate film on the cooling surface and the assumption made by Nusselt concerning the linearity of the temperature distribution.

In this study, the analysis revealed equation (6.19) which takes into account the subcooling of the condensate film and was based on a linear temperature distribution. The theoretical pure vapor condensation heat transfer coefficients calculated by equation (6.19) are plotted in Figures (23) and (24) for R-12 and Figure (25) for R-22.

The oil to refrigerant mass ratio Z was set to zero and all other parameters were taken from Table (26).

For both refrigerants, the analysis indicates that the effect of liquid subcooling is appreciable only at high ΔT (i.e. high rate of condensation), and this effect diminishes as ΔT get smaller. Equation (6.19) predicts the heat transfer coefficient about 3.5 per cent higher than Nusselt's equation at $\Delta T = 22\ ^{\circ}C$, and this deviation drops to 0.8 per cent at $\Delta T = 3\ ^{\circ}C$. This means that this analytical equation can predict the actual condensing heat transfer coefficients only at large ΔT, but at low ΔT, it underestimates the results by about 2.2 per cent.

By comparing the results obtained by the analytical equation (6.19) plotted in Figures (23), (24) and (25) and the results of the empirical equations (6.9) and (6.16) as plotted in Figures (13) and (18), it was found that these empirical equations represent most of the experimental data more accurately than the analytical equation at all ΔT.

b- Oil-vapor mixture condensation

By selecting the appropriate values of the thermal and physical properties of the condensate-oil mixtures from Tables (27) to (30), and applying them in equation (6.19) the heat transfer coefficients for the condensation of R-12

and R-22 vapor mixed with 2, 4, 6 and 8 per cent by weight oil were calculated and plotted in Figures (23), (24) and (25). In these figures the theoretical results were found to have a good agreement with the experimental data.

Like the pure vapor condensation, the oil-vapor mixture heat transfer coefficients calculated by equation (6.19) seem to fit the experimental results at large ΔT where the effect of subcooling is appreciable, and underestimates the data at low ΔT where the effect of subcooling diminishes.

By examining Figures (23), (24) and (25), a good agreement is found to exist between the theoretical and the experimental results. In any case, within the oil percentages used in this study, the average decrease in the condensing heat transfer coefficient of R-12, for each 2% increase of oil mixed with the vapor, is about 3%, but for R-22 the average decrease is about 1.9%. Theoretically, this decrease is due to the variation of the liquid properties on the periphery of the tube.

The experimental and the theoretical studies show that the condensing coefficient for R-22 is less affected by the presence of oil than that of R-12. By comparing the percentage changes in the properties of the two refrigerants when oil is present, Tables (32) and (33) show that the presence of a 2% oil by weight , will have a different

effect on the properties of the two refrigerants. R-12-oil mixture density decreases by an average of 0.9% while the thermal conductivity and the viscosity increase by an average of 0.3% and 6.5% respectively. However, for R-22-oil mixture, the density decreases by an average of 0.62% while the thermal conductivity and the viscosity increases by 0.13% and 3% respectively. It can be pointed out that the controlling parameter is the viscosity which is less affected in the case of R-22 than that of R-12.

6.4.2. Theoretical multi-tube condensation

Equation (6.20) was derived to predict the heat transfer coefficient of condensing vapor-oil mixtures on a vertical bank of multiple tubes. The required parameters are listed in Tables (26) to (30). Pure vapor and vapor-oil mixture condensation results obtained by this equation, are plotted in Figures (26) and (27) for refrigerants R-12 and R-22 respectively. Results of 2, 4, 6 and 8 per cent oil-vapor mixtures are shown. Pure condensation results were obtained from equation (6.20) where Z was set to zero and the pure refrigerant properties were used.

For pure condensation, equation (6.20) is the same as Nusselt's equation for multi-tube condensation. This equation is known to underestimate the actual heat transfer coefficient. The experimental data for both refrigerants

are higher than Nusselt's theory by an average of 15 per cent. The deviation between the data and the theory was found to get larger as ΔT increases. This increase of the deviation from small ΔT to large ΔT is due to the increase of turbulence of the liquid film as the rate of condensation rises resulting in a relative increase of the heat transfer coefficient.

In general, the deviation from Nusselt's theory for multi-tube condensation was attributed to the rippling of the condensing film, turbulence and momentum gained by the liquid when descending from a higher tube to the lower one.

By comparing equation (6.20) with the results of Nusselt's modified equation (6.21) plotted in Figures (13 , 29) and the deduced empirical equations (6.14) and (6.18 a) plotted in Figures (17 and 22), it was found that the analytical equation applied for pure vapor condensation; underestimates the heat transfer coefficient by an average of 15 per cent, while the modified equation is good only at small ΔT, i.e.less than 8 °C, above which it also underestimates the results because of the turbulence of the liquid film associated with larger condensation rates. The deduced empirical equations were found to be the best to fit the experimental results and for all the ranges of ΔT.

Similar to the single tube case, the condensing heat

transfer coefficient predicted by equation (6.20) and (6.21) for oil-vapor mixtures was found to decrease with the increase of the oil to refrigerant mass ratio. For an increase of a 2 per cent oil, the average decrease of the coefficient is about 3 per cent for R-12 and 1.9 per cent for R-22. The patterns of the curves for oil-vapor mixtures are the same as that for pure condensation.

6.5- Visual observations

a- Single tube tests

The condensation process was observed through the windows provided in the condenser shell. In the range of the vapor-surface temperature drop used in this study, the condensate liquid formed a smooth laminar layer flowing downward on the periphery of the tube. At ΔT larger than 8 °C it was possible to observe the formation of condensate waves on the condensing tube, see plates (1 to 3) , but below this temperature, these waves seem to vanish, plate (4). The deviation between Nusselt's theory and the experimental data may be partially attributed to the formation of these waves.

Along the lower part of the condensing tube, and due to the liquid surface tension, a thick condensate layer forms

from which continuous individual streams or occasional drops, depending on the condensation rate, flow down. To study the thickness of this condensate layer and the length of the tube perimeter subtended with it, end view photographs, plates (5 to 9) were taken for a 15.8 mm O.D. condensing tube at various rates of condensation. The thick layer was found to start to grow at an angle $\theta = 170$ degrees and by direct measurements, the maximum thickness of the liquid layer at angle $\theta = 180$ degrees was found to be about 1.1 millimeter. It is of interest to note that, for various condensation rates, the liquid layer thickness at the bottom of the tube and the length of the perimeter covered are the same.

b- Multitube condensation

In the case of multi-tube condensation, the first top tube of a tube bundle can be considered as a single tube condenser where a smooth laminar condensation takes place. On the lower tubes, however, part of the condensate layer area is disturbed by the falling condensate from higher tubes. As mentioned in the single tube case, the condensate liquid leaving a higher tube to the one below can take a form of continuous individual streams or occasional drops depending on the rate of condensation. In both cases, the descending liquid affects the laminar condensate layer of the tube below, thus forming disturbed or turbulent regions in the areas where it arrives. By moving a way from the

touching point, the turbulence decreases gradually, changing to ripples. Then it vanishes and a smooth laminar layer is observed to take place.

The distance between the descending streams reaching a lower tube depends on the rate of condensate flow. The higher it is, the smaller is the distance. However, as ΔT gets higher, and the condensate flow increases, the percentage of disturbed surface area of a lower tube increases, thus giving a considerable rise to the average heat transfer coefficient for this tube. At a certain ΔT, the disturbed area on the individual tube decreases when going from a lower tube to a higher one in the bundle. This may explain the increased deviation between the data and Nusselt's theory as number of tubes increases.

TABLE 1

TEST RESULTS OF CONDENSATION OF PURE R-12 VAPOR

ON A HORIZONTAL PLAIN TUBE 25.4 mm OD 1620 mm LONG

TEST RUN NO.	VAPOR-SURFACE TEMPERATURE DROP		HEAT TRANSFER RATE		CONDENSING COEFFICIENT	
	°C	°F	W x 10^3	Btu/hr x 10^3	W/m^2K x 10^3	$Btu/hr.ft^2.°F$
AT CONDENSING TEMPERATURE 32.2°C (90°F)						
1	16.2	29.3	2.65	9.05	1.26	222
2	11.6	20.9	2.06	7.04	1.37	242
3	8.0	14.5	1.55	5.29	1.48	262
4	3.8	6.9	0.869	2.96	1.74	307
5	5.5	10.0	1.16	3.97	1.61	284
6	6.7	12.1	1.34	4.60	1.55	273
7	9.7	17.5	1.79	6.13	1.43	252
8	13.1	23.6	2.29	7.81	1.35	238
9	14.7	26.5	2.50	8.56	1.31	231
10	13.6	24.5	2.29	7.82	1.30	230
11	6.3	11.4	1.31	4.50	1.60	283
12	4.2	7.6	0.973	3.32	1.78	314
AT CONDENSING TEMPERATURE 40.6°C (105°F)						
1	21.9	39.4	3.38	11.5	1.19	210
2	19.1	34.4	3.00	10.2	1.21	214
3	13.6	24.4	2.31	7.91	1.32	232
4	8.5	15.3	1.62	5.53	1.48	260
5	4.6	8.3	1.05	3.59	1.75	308
6	20.5	37.0	3.20	10.9	1.20	213
7	19.2	34.7	3.04	10.3	1.22	215
8	18.0	32.4	2.87	9.81	1.23	218
9	15.7	28.4	2.57	8.77	1.26	222
10	11.8	21.4	2.11	7.22	1.38	243
11	9.7	17.6	1.78	6.09	1.41	249
12	5.7	10.3	1.20	4.11	1.63	287
13	14.1	25.5	2.41	8.25	1.32	233
14	8.7	15.7	1.63	5.57	1.45	255
15	5.5	10.0	1.17	4.00	1.62	287
16	20.6	37.2	3.23	11.0	1.21	213
17	17.7	31.9	2.83	9.67	1.23	218

TABLE 1 (cont'd)

TEST RESULTS OF CONDENSATION OF PURE R-12 VAPOR

ON A HORIZONTAL PLAIN TUBE OF 25.4 mm OD X 1620 mm LONG

TEST RUN NO.	VAPOR-SURFACE TEMPERATURE DROP		HEAT TRANSFER RATE		CONDENSING COEFFICIENT	
	°C	°F	W x 10^3	Btu/hr x 10^3	W/m^2K x 10^3	Btu/hr.ft^2.°F
AT CONDENSING TEMPERATURE 48.9°C (120°F)						
1	18.4	33.1	2.93	10.0	1.23	218
2	14.1	25.4	2.40	8.19	1.31	231
3	8.6	15.4	1.60	5.48	1.44	255
4	11.2	20.3	1.99	6.81	1.37	241
5	4.5	8.1	0.98	3.36	1.69	298
6	16.6	29.9	2.73	9.31	1.27	224
7	14.3	25.8	2.39	8.16	1.29	228
8	10.7	19.3	1.92	6.57	1.38	244
9	5.4	9.8	1.17	4.01	1.66	292
10	17.8	32.0	2.85	9.73	1.24	218
11	15.2	27.3	2.84	9.69	1.27	225
12	12.8	23.0	2.18	7.46	1.32	233
13	9.4	17.0	1.75	6.00	1.43	253
14	6.5	11.8	1.34	4.57	1.58	278
15	8.0	14.4	1.53	5.24	1.48	261
16	2.2	4.0	0.60	2.07	2.11	373

TABLE 2

TEST RESULTS OF CONDENSATION OF PURE R-12 VAPOR

ON A HORIZONTAL PLAIN TUBE OF 15.9 mm OD X 1470 mm LONG

TEST RUN NO.	VAPOR-SURFACE TEMPERATURE DROP		HEAT TRANSFER RATE		CONDENSING COEFFICIENT	
	°C	°F	W x 10^3	Btu/hr x 10^3	W/m^2K x 10^3	$Btu/hr.ft^2.°F$
AT CONDENSING TEMPERATURE 32.2°C (90°F)						
1	17.0	30.6	1.78	6.10	1.43	251
2	13.1	23.6	1.41	4.83	1.49	263
3	10.2	18.4	1.19	4.06	1.57	278
4	5.2	9.44	0.74	2.53	1.92	339
5	6.8	12.3	0.91	3.10	1.80	318
6	8.4	15.2	1.07	3.65	1.72	303
7	12.1	21.9	1.35	4.61	1.51	266
8	14.6	26.4	1.57	5.36	1.45	256
9	20.1	36.2	2.01	6.89	1.36	240
10	23.5	42.4	2.17	7.40	1.25	220
11	20.7	37.3	1.99	6.81	1.31	230
12	17.5	31.5	1.76	6.01	1.36	241
13	12.6	22.7	1.37	4.70	1.48	261
14	6.6	12.0	0.84	2.88	1.72	303
15	4.5	8.2	0.66	2.25	1.97	347
AT CONDENSING TEMPERATURE 40.6°C (105°F)						
1	26.4	47.6	2.37	8.10	1.22	215
2	23.2	41.7	2.18	7.44	1.27	225
3	18.2	32.7	1.87	6.38	1.39	246
4	13.4	24.2	1.46	4.98	1.47	260
5	20.9	37.7	2.05	6.99	1.32	233
6	15.8	28.5	1.66	5.67	1.42	251
7	11.1	20.1	1.27	4.35	1.55	273
8	7.9	14.3	1.00	3.42	1.71	301
9	20.6	37.1	1.97	6.74	1.30	229
10	17.3	31.2	1.75	5.99	1.37	242
11	13.8	24.9	1.48	5.06	1.45	256
12	11.2	20.3	1.27	4.36	1.54	271
13	9.2	16.6	1.13	3.88	1.67	295
14	6.0	10.9	.834	2.84	1.86	328

TABLE 2 (cont'd)

TEST RESULTS OF CONDENSATION OF PURE R-12 VAPOR

ON A HORIZONTAL PLAIN TUBE OF 15.9 mm X 1470 mm LONG

TEST RUN NO.	VAPOR-SURFACE TEMPERATURE DROP		HEAT TRANSFER RATE		CONDENSING COEFFICIENT	
	°C	°F	W x 10^3	Btu/hr x 10^3	W/m^2K x 10^3	$Btu/hr.ft^2.°F$
AT CONDENSING TEMPERATURE 48.9°C (120°F)						
1	25.6	46.1	2.31	7.90	1.22	216
2	22.4	40.3	2.09	7.15	1.27	224
3	18.6	33.5	1.86	6.36	1.36	240
4	14.4	25.9	1.51	5.15	1.42	251
5	12.0	21.7	1.34	4.58	1.51	266
6	8.3	15.1	1.03	3.52	1.67	295
7	6.0	10.8	.816	2.78	1.84	324
8	21.9	39.5	2.09	7.15	1.29	228
9	19.6	35.3	1.93	6.59	1.33	235
10	15.6	28.1	1.65	5.63	1.43	253
11	11.2	20.3	1.33	4.54	1.60	282
12	3.8	6.8	.772	2.63	1.91	337

TABLE 3

TEST RESULTS OF CONDENSATION OF PURE R-12 VAPOR ON FOUR HORIZONTAL PLAIN TUBES, 15.9 mm OD X 812 mm LONG, IN A VERTICAL BANK

TEST RUN NO.	VAPOR-SURFACE TEMPERATURE DROP		HEAT TRANSFER RATE		CONDENSING COEFFICIENT	
	°C	°F	W x 10^3	Btu/hr x 10^3	W/m^2K x 10^3	Btu/hr.ft^2.°F
AT CONDENSING TEMPERATURE 32.2°C (90°F)						
1	20.4	36.7	3.71	12.6	1.12	197
2	14.5	26.2	2.76	9.44	1.17	206
3	9.8	17.7	2.00	6.85	1.25	221
4	6.1	11.0	1.36	4.64	1.36	240
5	3.9	7.1	.995	3.39	1.53	270
6	21.6	38.8	3.98	13.5	1.13	200
7	17.8	32.0	.333	11.3	1.15	203
8	12.0	21.6	2.42	8.26	1.24	218
9	8.0	14.5	1.74	5.95	1.32	234
10	2.3	4.2	.672	2.29	1.73	306
AT CONDENSING TEMPERATURE 40.6°C (105°F)						
1	21.7	39.1	3.91	13.3	1.11	195
2	18.9	34.1	3.46	11.8	1.12	198
3	16.5	29.7	3.06	10.4	1.14	201
4	14.2	25.6	2.71	9.27	1.17	206
5	11.6	21.0	2.32	7.93	1.22	216
6	8.2	14.8	1.70	5.81	1.27	224
7	5.8	10.4	1.29	4.42	1.37	242
8	3.1	5.7	.781	2.66	1.50	265
9	2.1	3.8	.585	1.99	1.69	298
AT CONDENSING TEMPERATURE 48.9°C (120°F)						
1	20.6	37.1	3.67	12.5	1.09	193
2	17.8	32.0	3.19	10.8	1.10	194
3	14.9	26.8	2.80	9.58	1.15	204
4	11.6	20.9	2.30	7.85	1.21	214
5	8.5	15.4	1.80	6.15	1.29	228
6	5.8	10.4	1.32	4.53	1.41	248
7	4.3	7.8	1.06	3.62	1.49	263
8	2.8	5.0	.766	2.61	1.67	295

TABLE 4

TEST RESULTS OF CONDENSATION OF 2% OIL AND R-12 MIXTURE ON A HORIZONTAL PLAIN TUBE OF 25.4 mm OD X 1400 mm LONG

TEST RUN NO.	VAPOR-SURFACE TEMPERATURE DROP		HEAT TRANSFER RATE		CONDENSING COEFFICIENT	
	°C	°F	W x 10^3	Btu/hr x 10^3	W/m^2K x 10^3	Btu/hr.ft^2.°F
AT CONDENSING TEMPERATURE 32.2°C (90°F)						
1	16.8	30.3	2.27	7.76	1.21	213
2	14.9	26.8	2.05	7.01	1.23	218
3	11.1	20.0	1.64	5.62	1.32	234
4	9.0	16.3	1.42	4.85	1.40	247
5	7.1	12.8	1.18	4.02	1.48	261
6	4.5	8.2	.843	2.87	1.64	290
AT CONDENSING TEMPERATURE 40.6°C (105°F)						
1	20.6	37.1	2.66	9.10	1.15	204
2	17.8	30.6	2.32	7.92	1.22	215
3	12.5	22.6	1.84	6.28	1.31	231
4	7.6	13.7	1.25	4.29	1.48	260
5	6.3	11.3	1.08	3.71	1.54	272
6	5.0	9.0	.902	3.08	1.60	283
AT CONDENSING TEMPERATURE 48.9°C (120°F)						
1	18.2	32.8	2.43	8.31	1.19	210
2	14.9	26.8	2.05	7.02	1.23	217
3	9.1	16.4	1.42	4.86	1.40	246
4	7.3	13.2	1.19	4.06	1.45	256
5	5.4	9.8	0.94	3.23	1.56	275

TABLE 5

TEST RESULTS OF CONDENSATION OF 4% OIL AND R-12 MIXTURE ON A HORIZONTAL PLAIN TUBE OF 25.4 mm OD X 1400 mm LONG

TEST RUN NO.	VAPOR-SURFACE TEMPERATURE DROP		HEAT TRANSFER RATE		CONDENSING COEFFICIENT	
	°C	°F	W x 10^3	Btu/hr x 10^3	W/m^2K x 10^3	$Btu/hr.ft^2.°F$
AT CONDENSING TEMPERATURE 32.2°C (90°F)						
1	16.1	29.1	2.21	7.56	1.22	216
2	13.3	24.0	1.90	6.50	1.28	225
3	6.9	12.4	1.12	3.83	1.45	256
4	5.2	9.4	.914	3.11	1.55	274
5	4.5	8.1	.806	2.75	1.59	281
6	10.9	19.8	1.66	5.66	1.35	238
7	12.8	23.2	1.85	6.31	1.28	227
8	15.4	27.7	2.12	7.25	1.23	217
AT CONDENSING TEMPERATURE 40.6°C (105°F)						
1	8.0	14.5	1.28	4.39	1.42	251
2	6.5	11.7	1.08	3.71	1.49	263
3	5.0	9.1	.886	3.02	1.56	274
4	18.2	32.8	2.41	8.25	1.18	209
5	13.2	23.9	1.88	6.43	1.27	224
6	15.1	27.3	2.06	7.05	1.22	215
7	10.5	19.0	1.57	5.37	1.33	234
AT CONDENSING TEMPERATURE 48.9°C (120°F)						
1	17.9	32.2	2.32	7.92	1.16	204
2	15.7	28.4	2.10	7.18	1.19	210
3	11.7	21.1	1.69	5.77	1.29	227
4	9.4	17.0	1.41	4.83	1.34	236
5	7.0	12.7	1.14	3.91	1.45	256
6	5.1	9.2	.877	2.99	1.53	270
7	4.3	7.8	.780	2.66	1.60	282

TABLE 6

TEST RESULTS OF CONDENSATION OF 6% OIL AND R-12 MIXTURE ON A HORIZONTAL PLAIN TUBE OF 25.4 mm OD X 1400 mm LONG

TEST RUN NO.	VAPOR-SURFACE TEMPERATURE DROP		HEAT TRANSFER RATE		CONDENSING COEFFICIENT	
	°C	°F	W x 10^3	Btu/hr x 10^3	W/m^2K x 10^3	Btu/hr.ft^2.°F
AT CONDENSING TEMPERATURE 32.2°C (90°F)						
1	7.3	13.2	1.16	3.98	1.41	249
2	9.8	17.7	1.46	4.99	1.32	234
3	11.5	20.7	1.65	5.66	1.29	227
4	14.7	26.6	1.96	6.70	1.19	209
5	13.4	24.2	1.81	6.20	1.21	213
6	5.4	9.7	.91	3.10	1.50	264
7	2.5	4.5	.49	1.67	1.74	307
AT CONDENSING TEMPERATURE 40.6°C (105°F)						
1	4.4	8.0	.783	2.674	1.57	278
2	16.3	29.4	2.14	7.312	1.17	206
3	10.8	19.5	1.56	5.328	1.28	227
4	7.8	14.1	1.20	4.125	1.38	243
5	6.7	12.1	1.04	3.560	1.39	245
6	12.5	22.5	1.75	5.973	1.25	221
AT CONDENSING TEMPERATURE 48.9°C (120°F)						
1	16.8	30.3	2.19	7.479	1.16	205
2	13.8	24.9	1.87	6.413	1.21	214
3	10.4	18.7	1.49	5.106	1.29	227
4	7.6	13.7	1.18	4.040	1.38	244
5	4.8	8.7	.813	2.776	1.50	264
6	3.3	6.1	.625	2.134	1.65	290

TABLE 7

TEST RESULTS OF CONDENSATION OF 8% OIL AND R-12 MIXTURE ON A HORIZONTAL PLAIN TUBE OF 25.4 mm OD X 1400 mm LONG

TEST RUN NO.	VAPOR-SURFACE TEMPERATURE DROP		HEAT TRANSFER RATE		CONDENSING COEFFICIENT	
	°C	°F	W x 10^3	Btu/hr x 10^3	W/m^2K x 10^3	Btu/hr.ft^2.°F
AT CONDENSING TEMPERATURE 32.2°C (90°F)						
1	5.2	9.3	.855	2.91	1.47	259
2	6.6	11.9	1.05	3.58	1.41	249
3	8.0	14.4	1.22	4.17	1.36	240
4	10.2	18.5	1.45	4.96	1.26	223
5	12.1	21.9	1.68	5.74	1.23	218
6	15.5	27.9	2.04	6.96	1.18	207
AT CONDENSING TEMPERATURE 40.6°C (105°F)						
1	11.8	21.3	1.66	5.68	1.25	221
2	13.7	24.7	1.82	6.21	1.18	209
3	9.0	16.2	1.32	4.53	1.32	232
4	3.1	5.6	.606	2.07	1.72	303
5	7.9	14.3	1.20	4.11	1.35	238
6	5.7	10.4	.924	3.15	1.43	252
7	16.3	29.3	2.07	7.07	1.14	200
AT CONDENSING TEMPERATURE 48.9°C (120°F)						
1	17.2	31.0	2.20	7.52	1.14	201
2	13.2	23.9	1.79	6.12	1.21	213
3	9.4	16.9	1.36	4.65	1.29	228
4	7.7	13.8	1.17	4.01	1.36	240
5	4.7	8.5	.794	2.71	1.50	265
6	2.8	5.1	.544	1.85	1.71	301

TABLE 8

TEST RESULTS OF CONDENSATION OF 2% OIL AND R-12 MIXTURE ON A HORIZONTAL PLAIN TUBE OF 15.9 mm OD X 1470 mm LONG

TEST RUN NO.	VAPOR-SURFACE TEMPERATURE DROP		HEAT TRANSFER RATE		CONDENSING COEFFICIENT	
	°C	°F	W x 10^3	Btu/hr x 10^3	W/m^2K x 10^3	Btu/hr.ft^2.°F
AT CONDENSING TEMPERATURE 32.2°C (90°F)						
1	16.0	28.8	1.59	5.45	1.35	239
2	12.1	21.8	1.30	4.44	1.45	256
3	8.9	16.0	1.02	3.50	1.56	275
4	6.7	12.2	.842	2.87	1.68	297
5	3.8	6.8	.540	1.84	1.91	338
6	21.3	38.3	1.99	6.79	1.27	224
AT CONDENSING TEMPERATURE 40.6°C (105°F)						
1	23.2	41.8	2.11	7.20	1.23	217
2	17.7	31.9	1.74	5.95	1.33	235
3	8.7	15.8	1.03	3.51	1.59	281
4	4.9	8.8	.668	2.27	1.85	326
5	6.8	12.3	.856	2.92	1.69	298
6	12.7	22.9	1.32	4.53	1.41	249
7	20.2	36.3	1.88	6.43	1.26	223
AT CONDENSING TEMPERATURE 48.9°C (120°F)						
1	23.9	43.0	2.19	7.48	1.24	219
2	17.5	31.5	1.71	5.86	1.33	234
3	12.3	22.2	1.34	4.57	1.47	259
4	10.9	19.7	1.23	4.19	1.52	268
5	8.9	16.0	1.04	3.55	1.59	280
6	6.4	11.5	.836	2.85	1.76	311

TABLE 9

TEST RESULTS OF CONDENSATION OF 4% OIL AND R-12 MIXTURE ON A HORIZONTAL PLAIN TUBE OF 15.9 mm OD X 1470 mm LONG

TEST RUN NO.	VAPOR-SURFACE TEMPERATURE DROP		HEAT TRANSFER RATE		CONDENSING COEFFICIENT	
	°C	°F	W x 10^3	Btu/hr x 10^3	W/m^2K x 10^3	Btu/hr.ft^2.°F
AT CONDENSING TEMPERATURE 32.2°C (90°F)						
1	21.0	37.8	1.94	6.62	1.25	221
2	17.1	30.7	1.64	5.61	1.31	230
3	11.0	19.9	1.18	4.05	1.46	257
4	14.7	26.5	1.45	4.97	1.34	236
5	7.8	14.1	.906	3.09	1.56	275
6	6.3	11.3	.753	2.56	1.62	285
7	4.3	7.8	.593	2.02	1.85	326
AT CONDENSING TEMPERATURE 40.6°C (105°F)						
1	20.1	36.2	1.86	6.37	1.26	222
2	14.6	26.4	1.47	5.02	1.36	240
3	16.7	30.0	1.63	5.56	1.32	233
4	10.2	18.5	1.11	3.82	1.48	261
5	3.4	6.2	.494	1.68	1.94	341
6	5.6	10.1	.716	2.44	1.72	303
7	7.7	13.9	.884	3.01	1.55	274
AT CONDENSING TEMPERATURE 48.9°C (120°F)						
1	10.6	19.1	1.16	3.97	1.49	262
2	23.5	42.4	2.08	7.11	1.20	212
3	18.9	34.0	1.81	6.17	1.30	229
4	13.9	25.1	1.43	4.89	1.39	246
5	9.0	16.2	1.02	3.50	1.55	273
6	7.3	13.1	.876	2.99	1.63	287
7	6.0	10.8	.755	2.57	1.70	300

TABLE 10

TEST RESULTS OF CONDENSATION OF 6% OIL AND R-12 MIXTURE ON A HORIZONTAL PLAIN TUBE OF 15.9 mm OD X 1470 mm LONG

TEST RUN NO.	VAPOR-SURFACE TEMPERATURE DROP		HEAT TRANSFER RATE		CONDENSING COEFFICIENT	
	°C	°F	W x 10^3	Btu/hr x 10^3	W/m^2K x 10^3	Btu/hr.ft^2.°F
AT CONDENSING TEMPERATURE 32.2°C (90°F)						
1	20.8	36.0	1.84	6.28	1.25	220
2	17.6	31.7	1.64	5.60	1.26	223
3	14.5	26.2	1.43	4.88	1.33	235
4	12.7	22.8	1.29	4.43	1.39	244
5	8.2	14.8	.918	3.13	1.51	266
6	5.8	10.5	.715	2.43	1.65	291
7	4.4	8.0	.578	1.97	1.77	311
AT CONDENSING TEMPERATURE 40.6°C (105°F)						
1	24.0	43.2	2.16	7.37	1.22	215
2	20.3	36.7	1.86	6.37	1.24	219
3	16.3	29.4	1.56	5.34	1.30	229
4	12.3	22.2	1.28	4.39	1.41	249
5	9.4	17.0	1.02	3.49	1.47	259
6	6.8	12.3	.808	2.75	1.60	281
7	4.6	8.3	.600	2.04	1.75	309
AT CONDENSING TEMPERATURE 48.9°C (120°F)						
1	17.4	31.3	1.68	5.76	1.31	232
2	11.5	20.8	1.19	4.06	1.40	246
3	14.8	26.6	1.45	4.95	1.33	235
4	9.5	17.1	1.04	3.56	1.49	263
5	7.6	13.7	.889	3.03	1.58	279
6	5.5	9.9	.716	2.44	1.76	310

TABLE 11

TEST RESULTS OF CONDENSATION OF 8% OIL AND R-12 MIXTURE ON A HORIZONTAL PLAIN TUBE OF 15.9 mm OD X 1470 mm LONG

TEST RUN NO.	VAPOR-SURFACE TEMPERATURE DROP		HEAT TRANSFER RATE		CONDENSING COEFFICIENT	
	°C	°F	W x 10^3	Btu/hr x 10^3	W/m^2K x 10^3	Btu/hr.ft^2.°F
AT CONDENSING TEMPERATURE 32.2°C (90°F)						
1	20.8	37.5	1.81	6.20	1.18	208
2	12.2	22.0	1.22	4.17	1.35	238
3	9.7	17.5	1.05	3.58	1.46	257
4	7.9	14.2	.884	3.01	1.51	267
5	4.5	8.1	.561	1.91	1.69	298
6	5.7	10.3	.712	2.43	1.68	296
AT CONDENSING TEMPERATURE 40.6°C (105°F)						
1	17.2	31.0	1.56	5.33	1.23	217
2	14.3	25.9	1.39	4.75	1.31	231
3	9.3	16.7	1.00	3.43	1.46	258
4	7.6	13.7	.857	2.92	1.53	269
5	6.0	10.9	.723	2.46	1.62	285
6	4.7	8.5	.605	2.06	1.73	305
AT CONDENSING TEMPERATURE 48.9°C (120°F)						
1	22.5	40.5	1.92	6.55	1.15	204
2	19.3	34.7	1.73	5.91	1.22	214
3	13.5	24.4	1.34	4.58	1.34	236
4	10.2	18.4	1.06	3.64	1.41	249
5	6.3	11.3	.747	2.55	1.61	283
6	4.9	8.8	.635	2.16	1.76	310

TABLE 12

TEST RESULTS OF CONDENSATION OF 2% OIL AND R-12 MIXTURE ON FOUR HORIZONTAL PLAIN TUBES, 15.9 mm OD X 812 mm LONG, IN A VERTICAL BANK

TEST RUN NO.	VAPOR-SURFACE TEMPERATURE DROP		HEAT TRANSFER RATE		CONDENSING COEFFICIENT	
	°C	°F	W x 10^3	Btu/hr x 10^3	W/m^2K x 10^3	Btu/hr.ft^2.°F
AT CONDENSING TEMPERATURE 32.2°C (90°F)						
1	18.6	33.4	3.35	11.4	1.11	195
2	15.7	28.3	2.88	9.85	1.13	199
3	11.7	21.0	2.21	7.57	1.16	205
4	8.0	14.5	1.65	5.64	1.26	222
5	4.7	8.5	1.10	3.77	1.43	252
6	2.7	4.9	.710	2.42	1.58	279
AT CONDENSING TEMPERATURE 40.6°C (105°F)						
1	10.5	18.9	2.08	7.11	1.21	214
2	8.6	15.5	1.73	5.93	1.23	218
3	4.8	8.7	1.11	3.80	1.41	249
4	7.1	12.8	1.48	5.06	1.28	225
5	11.6	20.9	2.21	7.55	1.17	206
6	15.0	27.1	2.64	9.03	1.08	190
7	19.2	34.6	3.35	11.4	1.07	189
AT CONDENSING TEMPERATURE 48.9°C (120°F)						
1	17.6	31.7	3.06	10.4	1.07	189
2	14.6	26.3	2.66	9.07	1.12	197
3	9.7	17.4	1.96	6.68	1.24	219
4	7.2	13.0	1.50	5.15	1.28	226
5	4.8	8.6	1.12	3.83	1.43	253
6	2.6	4.7	.688	2.34	1.60	282

TABLE 13

TEST RESULTS OF CONDENSATION OF 4% OIL AND R-12 MIXTURE ON FOUR HORIZONTAL PLAIN TUBES, 15.9 mm OD X 812 mm LONG, IN A VERTICAL BANK

TEST RUN NO.	VAPOR-SURFACE TEMPERATURE DROP		HEAT TRANSFER RATE		CONDENSING COEFFICIENT	
	°C	°F	W x 10^3	Btu/hr x 10^3	W/m^2K x 10^3	$Btu/hr.ft^2.°F$
AT CONDENSING TEMPERATURE 32.2°C (90°F)						
1	18.7	33.7	3.26	11.1	1.07	189
2	15.9	28.6	2.83	9.66	1.09	193
3	15.8	28.5	2.90	9.90	1.12	198
4	12.1	21.8	2.25	7.70	1.14	201
5	9.0	16.2	1.76	6.00	1.20	212
6	6.8	12.4	1.42	4.86	1.27	224
AT CONDENSING TEMPERATURE 40.6°C (105°F)						
1	17.0	30.6	2.99	10.2	1.08	191
2	14.2	25.5	2.57	8.79	1.11	196
3	9.8	17.7	1.89	6.47	1.18	209
4	7.7	13.9	1.55	5.29	1.23	217
5	5.7	10.3	1.26	4.30	1.29	228
6	3.9	7.0	.912	3.11	1.43	252
7	2.1	3.9	.580	1.98	1.63	287
AT CONDENSING TEMPERATURE 48.9°C (120°F)						
1	12.4	22.4	2.31	7.90	1.14	201
2	10.8	19.4	2.03	6.94	1.15	204
3	7.7	14.0	1.56	5.34	1.23	218
4	6.9	12.4	1.38	4.73	1.23	218
5	5.0	9.1	1.08	3.69	1.31	231
6	3.3	6.0	.779	2.66	1.43	252
7	15.5	28.0	2.80	9.56	1.11	195

TABLE 14

TEST RESULTS OF CONDENSATION OF 6% OIL AND R-12 MIXTURE ON FOUR HORIZONTAL PLAIN TUBES, 15.9 mm OD X 812 mm LONG, IN A VERTICAL BANK

TEST RUN NO.	VAPOR-SURFACE TEMPERATURE DROP		HEAT TRANSFER RATE		CONDENSING COEFFICIENT	
	°C	°F	W x 10^3	Btu/hr x 10^3	W/m^2K x 10^3	Btu/hr.ft^2.°F
AT CONDENSING TEMPERATURE 32.2°C (90°F)						
1	20.4	36.8	3.46	11.80	1.04	183
2	13.5	24.3	2.38	8.12	1.08	191
3	10.9	19.6	1.97	6.73	1.11	196
4	8.0	14.4	1.54	5.26	1.18	208
5	4.4	8.0	.962	3.28	1.32	234
6	16.2	29.2	2.75	9.39	1.04	183
AT CONDENSING TEMPERATURE 40.6°C (105°F)						
1	6.7	12.1	1.30	4.45	1.18	209
2	3.8	6.8	.812	2.77	1.30	230
3	9.8	17.7	1.82	6.24	1.14	200
4	14.3	25.9	2.50	8.54	1.07	189
5	17.3	31.2	2.98	10.1	1.06	186
6	2.8	5.0	.658	2.24	1.43	253
AT CONDENSING TEMPERATURE 48.9°C (120°F)						
1	11.9	21.4	2.13	7.27	1.10	194
2	13.0	23.5	2.38	8.15	1.12	198
3	18.2	32.8	3.12	10.6	1.05	185
4	7.5	13.5	1.43	4.88	1.17	206
5	6.6	11.9	1.28	4.40	1.20	211
6	5.2	9.5	1.07	3.65	1.25	220
7	3.3	6.0	.730	2.49	1.34	237

TABLE 15

TEST RESULTS OF CONDENSATION OF 8% OIL AND R-12 MIXTURE ON FOUR HORIZONTAL PLAIN TUBES, 15.9 mm OD X 812 mm LONG, IN A VERTICAL BANK

TEST RUN NO.	VAPOR-SURFACE TEMPERATURE DROP		HEAT TRANSFER RATE		CONDENSING COEFFICIENT	
	°C	°F	$W \times 10^3$	Btu/hr $\times 10^3$	$W/m^2K \times 10^3$	$Btu/hr.ft^2.°F$
AT CONDENSING TEMPERATURE 32.2°C (90°F)						
1	10.8	19.4	1.97	6.72	1.12	198
2	7.7	13.9	1.44	4.91	1.14	201
3	6.6	11.9	1.25	4.26	1.16	205
4	5.7	10.3	1.13	3.87	1.22	215
5	4.6	8.4	.947	3.23	1.25	220
6	3.5	6.4	.759	2.59	1.31	231
AT CONDENSING TEMPERATURE 40.6°C (105°F)						
1	10.6	19.1	1.90	6.49	1.10	194
2	7.3	13.2	1.38	4.73	1.16	204
3	6.2	11.2	1.19	4.07	1.17	207
4	4.5	8.1	.928	3.16	1.26	223
5	3.7	6.6	.760	2.59	1.26	222
6	5.2	9.4	1.03	3.53	1.21	214
AT CONDENSING TEMPERATURE 48.9°C (120°F)						
1	10.2	18.4	1.81	6.18	1.09	192
2	8.4	15.1	1.54	5.28	1.13	200
3	6.3	11.3	1.20	4.11	1.17	207
4	4.5	8.2	.904	3.08	1.21	214
5	8.2	14.9	1.49	5.09	1.11	195

TABLE 16

TEST RESULTS OF CONDENSATION OF PURE R-22 VAPOR ON A HORIZONTAL TUBE OF 15.9 mm OD X 812 mm LONG

TEST RUN NO.	VAPOR-SURFACE TEMPERATURE DROP		HEAT TRANSFER RATE		CONDENSING COEFFICIENT	
	°C	°F	W x 10^3	Btu/hr x 10^3	W/m^2K x 10^3	$Btu/hr.ft^2.°F$
AT CONDENSING TEMPERATURE 32.2°C (90°F)						
1	14.3	25.8	1.08	3.68	1.85	327
2	9.8	17.7	0.79	2.72	2.00	352
3	6.2	11.1	.566	1.93	2.24	396
4	3.8	6.8	.390	1.33	2.51	443
5	20.3	36.6	1.42	4.87	1.72	304
6	17.6	31.7	1.26	4.31	1.76	311
7	14.7	26.5	1.09	3.72	1.82	321
8	12.4	22.4	.957	3.26	1.89	333
9	9.7	17.5	.788	2.68	1.99	351
10	5.8	10.5	.538	1.83	2.26	398
11	2.6	4.6	.283	.968	2.68	473
12	20.8	37.5	1.43	4.89	1.69	299
13	19.5	35.1	1.37	4.69	1.73	306
14	19.1	34.5	1.33	4.56	1.71	302
15	16.7	30.1	1.20	4.10	1.76	311
16	10.0	18.0	.806	2.75	1.99	350
17	8.9	16.0	.740	2.52	2.05	361
18	7.2	13.0	.628	2.14	2.14	378
19	4.4	8.0	.437	1.49	2.39	422
AT CONDENSING TEMPERATURE 40.6°C (105°F)						
1	20.8	37.5	1.42	4.86	1.68	297
2	18.9	34.1	1.33	4.54	1.72	304
3	17.1	30.8	1.22	4.17	1.76	310
4	15.0	27.0	1.10	3.77	1.81	319
5	12.9	23.2	.978	3.34	1.86	328
6	10.3	18.6	.829	2.82	1.97	347
7	8.0	14.5	.688	2.35	2.10	371
8	5.2	9.3	.493	1.68	2.33	411
9	2.2	4.1	.259	.884	2.80	493

TABLE 17

TEST RESULTS OF CONDENSATION OF PURE R-22 VAPOR ON FOUR HORIZONTAL PLAIN TUBES, 15.9 mm OD X 812 mm LONG, IN A VERTICAL BANK

TEST RUN NO.	VAPOR-SURFACE TEMPERATURE DROP		HEAT TRANSFER RATE		CONDENSING COEFFICIENT	
	°C	°F	W x 10^3	Btu/hr x 10^3	W/m^2K x 10^3	Btu/hr.ft^2.°F
CONDENSING TEMPERATURE 32.2°C (90°F)						
1	9.8	17.6	2.73	9.34	1.71	302
2	8.6	15.5	2.44	8.35	1.74	306
3	6.9	12.5	2.01	6.85	1.78	314
4	5.3	9.5	1.62	5.55	1.89	333
5	3.5	6.2	1.16	3.97	2.05	362
6	13.7	24.8	3.57	12.2	1.60	281
7	11.3	20.4	2.99	10.2	1.62	286
8	9.5	17.1	2.65	9.05	1.72	303
9	7.7	13.8	2.24	7.66	1.79	316
10	5.8	10.5	1.78	6.07	1.87	329
11	4.1	7.5	1.30	4.45	1.93	340

TABLE 17 (cont'd)

TEST RESULTS OF CONDENSATION OF PURE R-22 VAPOR ON FOUR HORIZONTAL PLAIN TUBES, 15.9 mm OD X 812 mm LONG, IN A VERTICAL BANK

TEST RUN NO.	VAPOR-SURFACE TEMPERATURE DROP		HEAT TRANSFER RATE		CONDENSING COEFFICIENT	
	°C	°F	W x 10^3	Btu/hr x 10^3	W/m^2K x 10^3	Btu/hr.ft^2.°F
	CONDENSING TEMPERATURE 40.6°C (105°F)					
1	18.0	32.5	4.40	15.0	1.50	264
2	16.2	29.1	4.05	13.8	1.54	271
3	12.5	22.6	3.27	11.1	1.60	283
4	10.8	19.5	2.87	9.79	1.63	287
5	7.9	14.3	2.29	7.82	1.77	312
6	6.1	11.0	1.80	6.17	1.81	318
7	4.5	8.1	1.40	4.78	1.90	334
8	2.5	4.5	0.88	3.02	2.18	385
9	16.2	29.1	4.03	13.7	1.53	270
10	12.5	22.6	3.24	11.0	1.59	280
11	9.5	17.1	2.57	8.79	1.66	294
12	6.2	11.3	1.84	6.30	1.81	318
13	4.0	7.3	1.28	4.39	1.94	341
14	17.6	31.8	4.36	14.8	1.52	268
15	14.2	25.5	3.62	12.3	1.57	277
16	10.8	19.5	2.90	9.91	1.65	290
17	7.7	13.9	2.20	7.50	1.75	308
18	5.3	9.6	1.62	5.56	1.88	331
19	3.4	6.2	1.15	3.92	2.04	360

TABLE 18

TEST RESULTS OF CONDENSATION OF 2% OIL AND R-22 MIXTURE ON A HORIZONTAL TUBE OF 15.9 mm X 812 mm LONG

TEST RUN NO.	VAPOR-SURFACE TEMPERATURE DROP		HEAT TRANSFER RATE		CONDENSING COEFFICIENT	
	°C	°F	W x 10^3	Btu/hr x 10^3	W/m^2K x 10^3	Btu/hr.ft^2.°F
AT CONDENSING TEMPERATURE 32.2°C (90°F)						
1	20.7	37.3	1.40	4.80	1.67	294
2	20.2	36.5	1.38	4.72	1.68	296
3	16.0	28.9	1.15	3.94	1.77	312
4	13.9	25.1	1.02	3.49	1.80	318
5	8.2	14.8	.684	2.33	2.04	360
6	4.7	8.5	.442	1.50	2.30	405
7	3.5	6.3	.356	1.21	2.50	441
8	6.5	11.7	.567	1.93	2.14	377
9	10.0	18.1	.794	2.71	1.94	342
AT CONDENSING TEMPERATURE 40.6°C (105°F)						
1	20.6	37.1	1.40	4.78	1.67	295
2	18.2	32.8	1.26	4.31	1.70	301
3	13.9	25.1	1.02	3.49	1.80	318
4	9.6	17.4	.771	2.63	1.96	346
5	6.5	11.7	.566	1.93	2.13	376
6	5.4	9.7	.495	1.69	2.25	397
7	3.1	5.7	.330	1.12	2.56	452

TABLE 19

TEST RESULTS OF CONDENSATION OF 4% OIL AND R-22 MIXTURE ON A HORIZONTAL TUBE OF 15.9 mm OD X 812 mm LONG

TEST RUN NO.	VAPOR-SURFACE TEMPERATURE DROP		HEAT TRANSFER RATE		CONDENSING COEFFICIENT	
	°C	°F	W x 10^3	Btu/hr x 10^3	W/m^2K x 10^3	Btu/hr.ft^2.°F
AT CONDENSING TEMPERATURE 32.2°C (90°F)						
1	20.7	37.3	1.39	4.75	1.65	291
2	18.0	32.4	1.25	4.26	1.71	301
3	15.9	28.6	1.11	3.79	1.72	303
4	12.6	22.8	.939	3.20	1.82	321
5	8.5	15.4	.682	2.32	1.96	346
6	5.7	10.3	.510	1.74	2.18	385
7	3.1	5.7	.322	1.10	2.49	440
AT CONDENSING TEMPERATURE 40.6°C (105°F)						
1	20.5	37.0	1.37	4.68	1.64	289
2	17.7	31.9	1.21	4.15	1.69	298
3	14.0	25.2	1.01	3.45	1.77	313
4	11.5	20.7	.867	2.96	1.85	326
5	9.3	16.8	.727	2.48	1.91	336
6	8.6	15.5	.687	2.34	1.96	345
7	7.3	13.1	.599	2.04	2.02	356
8	5.1	9.31	.464	1.58	2.21	390

TABLE 20

TEST RESULTS OF CONDENSATION OF 6% OIL AND R-22 MIXTURE ON A HORIZONTAL TUBE OF 15.9 mm OD X 812 mm LONG

TEST RUN NO.	VAPOR-SURFACE TEMPERATURE DROP		HEAT TRANSFER RATE		CONDENSING COEFFICIENT	
	°C	°F	W x 10^3	Btu/hr x 10^3	W/m^2K x 10^3	Btu/hr.ft^2.°F
AT CONDENSING TEMPERATURE 32.2°C (90°F)						
1	20.1	36.2	1.33	4.542	1.62	287
2	18.3	33.0	1.21	4.151	1.63	288
3	14.1	25.5	1.01	3.463	1.76	310
4	12.6	22.7	.905	3.088	1.76	311
5	9.4	17.0	.725	2.474	1.89	333
6	8.7	15.7	.686	2.341	1.93	341
7	7.7	13.9	.614	2.098	1.96	345
8	5.2	9.5	.460	1.572	2.14	377
9	3.3	5.9	.329	1.125	2.46	433
AT CONDENSING TEMPERATURE 40.6°C (105°F)						
1	21.3	38.3	1.38	4.74	1.60	283
2	18.0	32.5	1.21	4.14	1.65	292
3	14.4	26.0	1.01	3.46	1.73	304
4	13.2	23.9	.949	3.24	1.76	310
5	12.1	21.8	.879	3.00	1.78	314
6	9.2	16.7	.713	2.43	1.95	334
7	7.3	13.2	.597	2.03	2.00	353
8	4.3	7.9	.398	1.36	2.24	394
9	2.8	5.1	.291	.993	2.52	444

TABLE 21

TEST RESULTS OF CONDENSATION OF 8% OIL AND R-22 MIXTURE ON A HORIZONTAL TUBE OF 15.9 mm X 812 mm LONG

TEST RUN NO.	VAPOR-SURFACE TEMPERATURE DROP		HEAT TRANSFER RATE		CONDENSING COEFFICIENT	
	°C	°F	W x 10^3	Btu/hr x 10^3	W/m^2K x 10^3	Btu/hr.ft^2.°F
AT CONDENSING TEMPERATURE 32.2°C (90°F)						
1	18.9	34.1	1.24	4.24	1.61	285
2	17.5	31.6	1.16	3.96	1.63	287
3	15.7	28.3	1.05	3.61	1.65	292
4	11.6	21.0	.835	2.85	1.76	310
5	10.1	18.2	.752	2.56	1.83	322
6	19.6	35.4	1.27	4.34	1.59	281
7	6.5	11.8	.536	1.83	2.01	354
8	4.3	7.8	.396	1.35	2.23	392
AT CONDENSING TEMPERATURE 40.6°C (105°F)						
1	21.2	38.3	1.35	4.61	1.56	276
2	17.7	32.0	1.19	4.07	1.65	291
3	14.1	25.5	.983	3.35	1.70	301
4	11.3	20.4	.823	2.80	1.78	314
5	9.2	16.6	.689	2.35	1.84	324
6	6.9	12.4	.550	1.87	1.96	346
7	3.3	6.0	.323	1.10	2.38	419

TABLE 22

TEST RESULTS OF CONDENSATION OF 2% OIL AND R-22 MIXTURE ON FOUR HORIZONTAL PLAIN TUBES, 15.9 mm OD X 812 mm LONG, IN A VERTICAL BANK

TEST RUN NO.	VAPOR-SURFACE TEMPERATURE DROP		HEAT TRANSFER RATE		CONDENSING COEFFICIENT	
	°C	°F	W x 10^3	Btu/hr x 10^3	W/m^2K x 10^3	Btu/hr.ft^2.°F
	CONDENSING TEMPERATURE 32.2°C (90°F)					
1	8.0	14.4	2.23	7.62	1.71	302
2	9.1	16.4	2.46	8.42	1.67	294
3	7.2	13.0	2.07	7.06	1.76	311
4	5.0	9.1	1.51	5.17	1.84	325
5	4.0	7.3	1.27	4.33	1.91	337
6	3.4	6.2	1.10	3.78	1.95	344
CONDENSING TEMPERATURE: 40.6°C (105°F)						
1	17.1	30.8	4.20	14.3	1.51	265
2	12.1	21.8	3.13	10.6	1.58	279
3	10.1	18.3	2.70	9.21	1.63	288
4	9.4	17.0	2.51	8.59	1.64	288
5	4.5	8.1	1.38	4.72	1.88	331
6	1.8	3.2	.681	2.32	2.30	405
7	13.4	24.1	3.41	11.6	1.56	275
8	10.5	18.9	2.76	9.42	1.61	285
9	3.6	6.6	1.16	3.96	1.94	342

TABLE 23

TEST RESULTS OF CONDENSATION OF 4% OIL AND R-22 MIXTURE ON FOUR HORIZONTAL PLAIN TUBES, 15.9 mm OD X 812 mm LONG, IN A VERTICAL BANK

TEST RUN NO.	VAPOR-SURFACE TEMPERATURE DROP		HEAT TRANSFER RATE		CONDENSING COEFFICIENT	
	°C	°F	W x 10^3	Btu/hr x 10^3	W/m^2K x 10^3	Btu/hr.ft^2.°F
	CONDENSING TEMPERATURE 32.2°C (90°F)					
1	9.4	16.9	2.53	8.66	1.65	292
2	7.4	13.4	2.08	7.12	1.73	304
3	6.4	11.5	1.84	6.30	1.76	311
4	5.2	9.3	1.56	5.33	1.85	325
5	4.2	7.6	1.30	4.45	1.89	333
6	3.6	6.6	1.12	3.85	1.89	334
CONDENSING TEMPERATURE: 40.6°C (105°F)						
1	7.3	13.2	2.06	7.04	1.72	304
2	4.6	8.3	1.38	4.73	1.83	323
3	17.4	31.4	4.15	14.1	1.46	258
4	13.6	24.5	3.39	11.5	1.53	270
5	11.3	20.3	2.90	9.91	1.58	278
6	9.2	16.6	2.44	8.34	1.62	286
7	6.3	11.3	1.81	6.19	1.76	311
8	3.7	6.7	1.17	4.02	1.92	339

TABLE 24

TEST RESULTS OF CONDENSATION OF 6% OIL AND R-22 MIXTURE ON FOUR HORIZONTAL PLAIN TUBES, 15.9 mm X 812 mm LONG, IN A VERTICAL BANK

TEST RUN NO.	VAPOR-SURFACE TEMPERATURE DROP		HEAT TRANSFER RATE		CONDENSING COEFFICIENT	
	°C	°F	W x 10^3	Btu/hr x 10^3	W/m^2K x 10^3	$Btu/hr.ft^2.°F$
	CONDENSING TEMPERATURE 32.2°C (90°F)					
1	9.4	17.0	2.49	8.52	1.62	285
2	6.4	11.6	1.83	6.25	1.74	306
3	7.4	13.4	2.05	7.02	1.69	298
4	8.6	15.4	2.29	7.82	1.64	289
5	5.5	10.0	1.58	5.40	1.74	307
6	4.5	8.1	1.35	4.63	1.84	324
CONDENSING TEMPERATURE: 40.6°C (105°F)						
1	13.7	24.6	3.39	11.5	1.51	267
2	11.4	20.5	2.86	9.79	1.54	272
3	9.5	17.1	2.49	8.50	1.61	284
4	4.0	7.3	1.22	4.18	1.85	326
5	3.2	5.8	1.01	3.45	1.91	338
6	6.9	12.4	1.91	6.54	1.70	300

TABLE 25

TEST RESULTS OF CONDENSATION OF 8% OIL AND R-22 MIXTURE ON FOUR HORIZONTAL PLAIN TUBES, 15.9 mm OD X 812 mm LONG, IN A VERTICAL BANK

TEST RUN NO.	VAPOR-SURFACE TEMPERATURE DROP		HEAT TRANSFER RATE		CONDENSING COEFFICIENT	
	°C	°F	W x 10^3	Btu/hr x 10^3	W/m^2K x 10^3	Btu/hr.ft^2.°F
	CONDENSING TEMPERATURE 32.2°C (90°F)					
1	9.2	16.6	2.38	8.12	1.59	280
2	7.0	12.6	1.90	6.50	1.67	294
3	6.0	10.9	1.65	5.65	1.68	296
4	4.9	8.9	1.40	4.80	1.74	306
5	3.9	7.1	1.16	3.99	1.81	320
6	8.3	14.9	2.20	7.51	1.63	288
	CONDENSING TEMPERATURE: 40.6°C (105°F)					
1	11.0	19.8	2.74	9.37	1.53	270
2	7.0	12.6	1.95	6.68	1.69	298
3	4.8	8.9	1.45	4.96	1.78	314
4	3.5	6.4	1.09	3.73	1.88	332
5	9.5	17.1	2.47	8.44	1.59	230
6	6.1	11.0	1.69	5.77	1.70	299

Condensate film average temperature							
	21.1 °C (70°F)	23.8 °C (75 °F)	26.6 °C (80°F)	28 °C (82.5°F)	29.4 °C (85 °F)	30 °C (86 °F)	30.8 °C (87.5
Vapor-surface temp. drop	22.2 °C (40°F)	16.6 °C (30 °F)	11.1 °C (20°F)	8.3 °C (15°F)	5.5 °C (10 °F)	4.4 °C (8 °F)	2.7 °C (5 °F)
R-12							
Density kg/m^3	1325	1315	1305	1299	1294	1292	1289
Viscosity $x10^4$ kg/ms	2.23	2.18	2.14	2.11	2.09	2.09	2.07
Thermal cond. $x\ 10^2$ W/m °C	7.07	6.95	6.87	6.82	6.76	6.73	6.71
Specific heat kJ/kg °C	0.969	0.974	0.979	0.983	0.986	0.987	0.989
R-22							
Density kg/m^3	1209	1198	1198	1182	1176	1174	1170
Viscosity $x\ 10^4$ kg/ms	2.05	2.02	1.98	1.97	1.95	1.94	1.93
Thermal cond. $x\ 10^2$ W/m °C	8.96	8.83	8.68	8.62	8.55	8.53	8.48
Specific heat kJ/kg °C	1.23	1.24	1.25	1.26	1.27	1.27	1.27

Table no.26 : Thermal and physical properties of R-12 and R-22 pure condensate liquid at the liquid temperature range 21.1 °C to 30.8 °C (70 °F to 87.5 °F).

Condensate film average temperature							
	21.1 °C (70°F)	23.8 °C (75 °F)	26.6 °C (80°F)	28 °C (82.5°F)	29.4 °C (85 °F)	30 °C (86 °F)	30.8 °C (87.5
Vapor-surface temp. drop	22.2 °C (40°F)	16.6 °C (30 °F)	11.1 °C (20°F)	8.3 °C (15°F)	5.5 °C (10 °F)	4.4 °C (8 °F)	2.7 °C (5 °F)
R-12 condensate-oil mixture properties							
Density kg/m^3	1312	1302	1292	1287	1282	1280	1277
Viscosity $x10^4$ kg/ms	2.4	2.35	2.3	2.27	2.25	2.24	2.22
Thermal cond. $x\ 10^2$ W/m °C	7.09	6.99	6.89	6.84	6.79	6.77	6.73
Specific heat kJ/kg °C	0.986	0.99	0.99	1.00	1.00	1.00	1.00
R-22 condensate-oil mixture properties							
Density kg/m^3	1200	1190	1179	1174	1168	1166	1163
Viscosity $x\ 10^4$ kg/ms	2.07	2.06	2.02	2.02	2.00	1.99	1.98
Thermal cond. $x\ 10^2$ W/m °C	8.97	8.97	8.70	8.63	8.56	8.54	8.50
Specific heat kJ/kg °C	1.24	1.25	1.26	1.27	1.28	1.28	1.29

Table 27 : Thermal and physical properties of R-12 and R-22 condensate liquid mixed with 2% Alkylbenzene based refrigeration oil (150 SSU at 37.7 °C) at the liquid temperature range 21.1 °C to 30.8 °C (70 °F to 87.5 °F).

Condensate film average temperature							
	21.1 °C (70°F)	23.8 °C (75 °F)	26.6 °C (80°F)	28 °C (82.5°F)	29.4 °C (85 °F)	30 °C (86 °F)	30.8 °C (87.5°
Vapor-surface temp. drop	22.2 °C (40°F)	16.6 °C (30 °F)	11.1 °C (20°F)	8.3 °C (15°F)	5.5 °C (10 °F)	4.4 °C (8 °F)	2.7 °C (5 °F)
R-12 condensate-oil mixture properties							
Density kg/m^3	1300	1290	1281	1276	1271	1269	1266
Viscosity $x10^4$ kg/ms	2.57	2.51	2.46	2.43	2.41	2.39	2.38
Thermal cond. $x\ 10^2$ W/m °C	7.11	7.01	6.91	6.86	6.81	6.79	6.76
Specific heat kJ/kg °C	1.00	1.00	1.01	1.01	1.02	1.02	1.02
R-22 condensate-oil mixture properties							
Density kg/m^3	1192	1181	1171	1166	1161	1158	1155
Viscosity $x\ 10^4$ kg/ms	2.19	2.52	2.12	2.1	2.08	2.07	2.06
Thermal cond. $x\ 10^2$ W/m °C	8.98	8.85	8.71	8.64	8.58	8.55	8.51
Specific heat kJ/kg °C	1.26	1.27	1.28	1.28	1.29	1.29	1.30

Table 28 : Thermal and physical properties of R-12 and R-22 condensate liquid mixed with 4% Alkylbenzene based refrigeration oil (150 SSU at 37.7 °C) at the liquid temperature range 21.1 °C to 30.8 °C (70 °F to 87.5 °F).

Condensate film average temperature							
	21.1 °C (70°F)	23.8 °C (75 °F)	26.6 °C (80°F)	28 °C (82.5°F)	29.4 °C (85 °F)	30 °C (86 °F)	30.8 °C (87.5°
Vapor-surface temp. drop	22.2 °C (40°F)	16.6 °C (30 °F)	11.1 °C (20°F)	8.3 °C (15°F)	5.5 °C (10 °F)	4.4 °C (8 °F)	2.7 °C (5 °F)
R-12 condensate-oil mixture properties							
Density kg/m^3	1288	1279	1270	1265	1260	1258	1255
Viscosity $x10^4$ kg/ms	2.74	2.68	2.62	2.59	2.56	2.55	2.53
Thermal cond. $x\ 10^2$ W/m °C	7.13	7.04	6.94	6.89	6.84	6.82	6.78
Specific heat kJ/kg °C	1.01	1.02	1.03	1.03	1.03	1.03	1.04
R-22 condensate-oil mixture properties							
Density kg/m^3	1184	1174	1164	1159	1153	1151	1148
Viscosity $x\ 10^4$ kg/ms	2.29	2.24	2.20	2.18	2.17	2.16	2.15
Thermal cond. $x\ 10^2$ W/m °C	8.99	8.86	8.72	8.66	8.59	8.56	8.53
Specific heat kJ/kg °C	1.27	1.28	1.29	1.29	1.30	1.30	1.31

Table 29: Thermal and physical properties of R-12 and R-22 condensate liquid mixed with 6% Alkylbenzene based refrigeration oil (150 SSU at 37.7 °C) at the liquid temperature range 21.1 °C to 30.8 °C (70 °F to 87.5 °F).

Condensate film average temperature							
	21.1 °C (70°F)	23.8 °C (75 °F)	26.6 °C (80°F)	28 °C (82.5°F)	29.4 °C (85 °F)	30 °C (86 °F)	30.8 °C (87.5°
Vapor-surface temp. drop	22.2 °C (40°F)	16.6 °C (30 °F)	11.1 °C (20°F)	8.3 °C (15°F)	5.5 °C (10 °F)	4.4 °C (8 °F)	2.7 °C (5 °F)
R-12 condensate-oil mixture properties							
Density kg/m^3	1277	1268	1259	1254	1250	1248	1245
Viscosity x10^4 kg/ms	2.91	2.84	2.78	2.75	2.72	2.71	2.69
Thermal cond. x 10^2 W/m °C	7.16	6.96	6.96	6.91	6.86	6.84	6.81
Specific heat kJ/kg °C	1.03	1.04	1.04	1.05	1.05	1.06	1.05
R-22 condensate-oil mixture properties							
Density kg/m^3	1176	1167	1157	1152	1147	1145	1142
Viscosity x 10^4 kg/ms	2.38	2.34	2.29	2.28	2.26	2.25	2.24
Thermal cond. x 10^2 W/m °C	9.00	8.87	8.74	8.67	8.60	8.58	8.54
Specific heat kJ/kg °C	1.28	1.29	1.30	1.30	1.31	1.31	1.32

Table 30: Thermal and physical properties of R-12 and R-22 condensate liquid mixed with 8% Alkylbenzene based refrigeration oil (150 SSU at 37.7 °C) at the liquid temperature range 21.1 °C to 30.8 °C (70 °F to 87,5 °F).

Vapor-surface temperature drop	Pure refrigerant condensation heat transfer coefficient		2% oil-vapor mixture condensation heat transfer coefficient		4% oil-vapor mixture condensation heat transfer coefficient		6% oil-vapor mixture condensation heat transfer coefficient		8% oil-vapor mixture condensation heat transfer coefficient	
	W/m^2 °C	Btu / hr ft^2 °F	W/m^2 °C	Btu/ hr ft^2°F	W/m^2 °C	Btu/ hr ft^2°F	W/m^2 °C	Btu/ hr ft^2 °F	W/m^2 °C	Btu/ hr ft^2 °F
22.2 °C (40 °F)	1.17	206	1.14	201	1.11	197	1.09	192	1.07	188
16.6 °C (30 °F)	1.24	219	1.21	214	1.18	209	1.16	204	1.13	200
11.1 °C (20 °F)	1.36	239	1.32	233	1.29	228	1.26	223	1.24	219
8.3 °C (15 °F)	1.45	256	1.41	249	1.38	243	1.35	238	1.32	233
5.5 °C (10 °F)	1.59	281	1.55	274	1.52	268	1.48	262	1.45	256
4.4 °C (8 °F)	1.68	296	1.64	289	1.60	282	1.57	276	1.53	270
2.7 °C (5 °F)	1.88	332	1.84	323	1.79	316	1.75	309	1.72	303

Table 31: Theoretical film coefficients for condensing R-12 vapor, pure and mixed with oil percentages 2, 4, 6 and 8 by weight, on the external surface of a single horizontal tube 25.4mm (1 inch) O.D. at the condensing temperature 32.2 °C (90 °F).

Vapor-surface temperature drop	Pure refrigerant condensation heat transfer coefficient		2% oil-vapor mixture condensation heat transfer coefficient		4% oil-vapor mixture condensation heat transfer coefficient		6% oil-vapor mixture condensation heat transfer coefficient		8% oil-vapor mixture condensation heat transfer coefficient	
	W/m^2 °C	Btu / hr ft^2 °F	W/m^2 °C	Btu/ hr ft^2°F	W/m^2 °C	Btu/ hr ft^2°F	W/m^2 °C	Btu/ hr ft^2 °F	W/m^2 °C	Btu/ hr ft^2 °F
22.2 °C (40 °F)	1.32	232	1.28	227	1.25	221	1.23	216	1.20	212
16.6 °C (30 °F)	1.40	247	1.36	240	1.33	235	1.30	230	1.28	225
11.1 °C (20 °F)	1.53	269	1.49	263	1.46	257	1.42	251	1.40	246
8.3 °C (15 °F)	1.63	287	1.59	280	1.55	274	1.52	268	1.49	262
5.5 °C (10 °F)	1.79	316	1.75	308	1.71	301	1.67	295	1.64	288
4.4 °C (8 °F)	1.89	333	1.84	325	1.80	317	1.76	310	1.73	304
2.7 °C (5 °F)	2.12	373	2.06	364	2.02	355	1.97	348	1.93	341

Table 32: Theoretical film coefficients for condensing R-12 vapor, pure and mixed with oil percentages 2, 4, 6 and 8 by weight, on the external surface of a single horizontal 15.8mm (5/8 inch) O.D. tube at the condensing temperature 32.2 °C (90 °F).

Vapor-surface temperature drop	Pure refrigerant condensation heat transfer coefficient		2% oil-vapor mixture condensation heat transfer coefficient		4% oil-vapor mixture condensation heat transfer coefficient		6% oil-vapor mixture condensation heat transfer coefficient		8% oil-vapor mixture condensation heat transfer coefficient	
	W/m^2 °C	Btu / hr ft^2 °F	W/m^2 °C	Btu/ hr ft^2 °F	W/m^2 °C	Btu/ hr ft^2 °F	W/m^2 °C	Btu/ hr ft^2 °F	W/m^2 °C	Btu/ hr ft^2 °F
22.2 °C (40 °F)	1.65	290	1.62	286	1.60	281	1.57	276	1.54	272
16.6 °C (30 °F)	1.74	307	1.72	303	1.69	298	1.66	292	1.63	287
11.1 °C (20 °F)	1.90	334	1.87	330	1.84	324	1.81	319	1.78	314
8.3 °C (15 °F)	2.02	356	1.99	351	1.95	344	1.93	340	1.90	334
5.5 °C (10 °F)	2.22	391	2.19	386	2.15	379	2.12	373	2.08	367
4.4 °C (8 °F)	2.34	412	2.31	407	2.27	400	2.23	394	2.20	387
2.7 °C (5 °F)	2.62	461	2.58	455	2.54	448	2.50	440	2.46	433

Table 33: Theoretical film coefficients for condensing R-22 vapor, pure and mixed with oil percentages 2, 4, 6 and 8 by weight, on the external surface of a single horizontal 15.8mm (5/8 inch) O.D. tube at the condensing temperature 32.2 °C (90 °F).

Vapor-surface temperature drop	Pure refrigerant condensation heat transfer coefficient		2% oil-vapor mixture condensation heat transfer coefficient		4% oil-vapor mixture condensation heat transfer coefficient		6% oil-vapor mixture condensation heat transfer coefficient		8% oil-vapor mixture condensation heat transfer coefficient	
	$W/m^2\ °C \times 10^3$	Btu / hr ft^2 °F	$W/m^2\ °C \times 10^3$	Btu/ hr ft^2 °F	$W/m^2\ °C \times 10^3$	Btu/ hr ft^2 °F	$W/m^2\ °C \times 10^3$	Btu/ hr ft^2 °F	$W/m^2\ °C \times 10^3$	Btu/ hr ft^2 °F
22.2 °C (40 °F)	0.919	162	0.896	158	0.874	154	0.854	150	0.836	147
16.6 °C (30 °F)	0.979	172	0.954	168	0.932	164	0.911	160	0.892	157
11.1 °C (20 °F)	1.07	189	1.04	184	1.02	180	0.999	176	0.979	172
8.3 °C (15 °F)	1.14	202	1.12	197	1.09	192	1.07	188	1.04	184
5.5 °C (10 °F)	1.26	222	1.23	217	1.20	212	1.17	207	1.15	203
4.4 °C (8 °F)	1.33	235	1.30	229	1.27	224	1.24	219	1.22	214
2.7 °C (5 °F)	1.49	263	1.46	257	1.42	251	1.39	245	1.36	240

Table 34: Theoretical film coefficients for condensing R-12, pure and mixed with oil at percentages 2, 4, 6 and 8 by weight, on the external surface of a vertical bank of 4 horizontal 15.8mm O.D. tubes at the condensing temperature 32.2 °C (90 °F).

Vapor-surface temperature drop	Pure refrigerant condensation heat transfer coefficient		2% oil-vapor mixture condensation heat transfer coefficient		4% oil-vapor mixture condensation heat transfer coefficient		6% oil-vapor mixture condensation heat transfer coefficient		8% oil-vapor mixture condensation heat transfer coefficient	
	$W/m^2\ °C \times 10^3$	Btu / hr ft^2 °F	$W/m^2\ °C \times 10^3$	Btu/ hr ft^2 °F	$W/m^2\ °C \times 10^3$	Btu/ hr ft^2 °F	$W/m^2\ °C \times 10^3$	Btu/ hr ft^2 °F	$W/m^2\ °C \times 10^3$	Btu/ hr ft^2 °F
22.2 °C (40 °F)	1.15	202	1.13	199	1.11	196	1.09	192	1.07	189
16.6 °C (30 °F)	1.22	214	1.20	211	1.18	208	1.16	204	1.14	201
11.1 °C (20 °F)	1.33	234	1.31	231	1.29	227	1.27	224	1.25	220
8.3 °C (15 °F)	1.42	250	1.40	247	1.37	242	1.35	239	1.33	235
5.5 °C (10 °F)	1.56	275	1.54	272	1.52	267	1.49	263	1.46	258
4.4 °C (8 °F)	1.65	290	1.63	287	1.60	282	1.57	277	1.55	273
2.7 °C (5 °F)	1.85	325	1.82	321	1.79	316	1.76	311	1.73	305

Table 35: Theoretical film coefficients for condensing R-22 vapor, pure and mixed with oil at percentages 2, 4, 6 and 8 by weight, on the external surface of a vertical bank of 4 horizontal 15.8mm O.D. (5/8 inch) tubes at the condensing temperature 32.2 °C (90 °F).

Vapor-surface temperature drop	Pure refrigerant condensation heat transfer coefficient		2% oil-vapor mixture condensation heat transfer coefficient		4% oil-vapor mixture condensation heat transfer coefficient		6% oil-vapor mixture condensation heat transfer coefficient		8% oil-vapor mixture condensation heat transfer coefficient	
	$W/m^2 °C \times 10^3$	Btu / hr ft^2 °F	$W/m^2 °C \times 10^3$	Btu/ hr ft^2 °F	$W/m^2 °C \times 10^3$	Btu/ hr ft^2 °F	$W/m^2 °C \times 10^3$	Btu/ hr ft^2 °F	$W/m^2 °C \times 10^3$	Btu/ hr ft^2 °F
22.2 °C (40 °F)	1.03	181	1.00	177	0.98	173	0.959	169	0.938	165
16.6 °C (30 °F)	1.1	193	1.07	188	1.04	184	1.02	180	1.00	176
11.1 °C (20 °F)	1.20	212	1.17	207	1.14	202	1.12	197	1.09	193
8.3 °C (15 °F)	1.28	227	1.25	221	1.22	216	1.20	211	1.17	207
5.5 °C (10 °F)	1.42	249	1.38	243	1.35	238	1.32	233	1.29	228
4.4 °C (8 °F)	1.49	263	1.46	257	1.42	251	1.39	245	1.36	240
2.7 °C (5 °F)	1.67	295	1.63	288	1.59	281	1.56	275	1.53	270

Table 36: Based ($\bar{N}^{0.167}$) theoretical film coefficients for condensing R-12 vapor, pure and mixed with oil at percentages 2, 4, 6 and 8 by weight, on the external surface of a vertical bank of 4 horizontal 15.8mm O.D. (5/8 inch) tubes at the condensing temperature 32.2 °C (90 °F).

Vapor-surface temperature drop	Pure refrigerant condensation heat transfer coefficient		2% oil-vapor mixture condensation heat transfer coefficient		4% oil-vapor mixture condensation heat transfer coefficient		6% oil-vapor mixture condensation heat transfer coefficient		8% oil-vapor mixture condensation heat transfer coefficient	
	$W/m^2 °C \times 10^3$	Btu / hr ft^2 °F	$W/m^2 °C \times 10^3$	Btu/ hr ft^2 °F	$W/m^2 °C \times 10^3$	Btu/ hr ft^2 °F	$W/m^2 °C \times 10^3$	Btu/ hr ft^2 °F	$W/m^2 °C \times 10^3$	Btu/ hr ft^2 °F
22.2 °C (40 °F)	1.29	227	1.27	224	1.25	220	1.22	216	1.20	212
16.6 °C (30 °F)	1.36	241	1.35	237	1.32	233	1.30	229	1.28	225
11.1 °C (20 °F)	1.49	263	1.47	260	1.45	255	1.42	251	1.40	247
8.3 °C (15 °F)	1.59	281	1.57	277	1.54	272	1.52	268	1.49	263
5.5 °C (10 °F)	1.75	309	1.73	305	1.70	300	1.67	295	1.64	290
4.4 °C (8 °F)	1.85	326	1.83	322	1.79	316	1.77	311	1.74	306
2.7 °C (5 °F)	2.07	365	2.05	360	2.01	354	1.98	349	1.95	343

Table 37: Based ($N^{-0.167}$) theoretical film coefficients for condensing R-22 vapor, pure and mixed with oil at percentages 2, 4, 6 and 8 by weight, on the external surface of a vertical bank of 4 horizontal 15.8mm O.D. (5/8 inch) tubes at the condensing temperature 32.2 °C (90 °F).

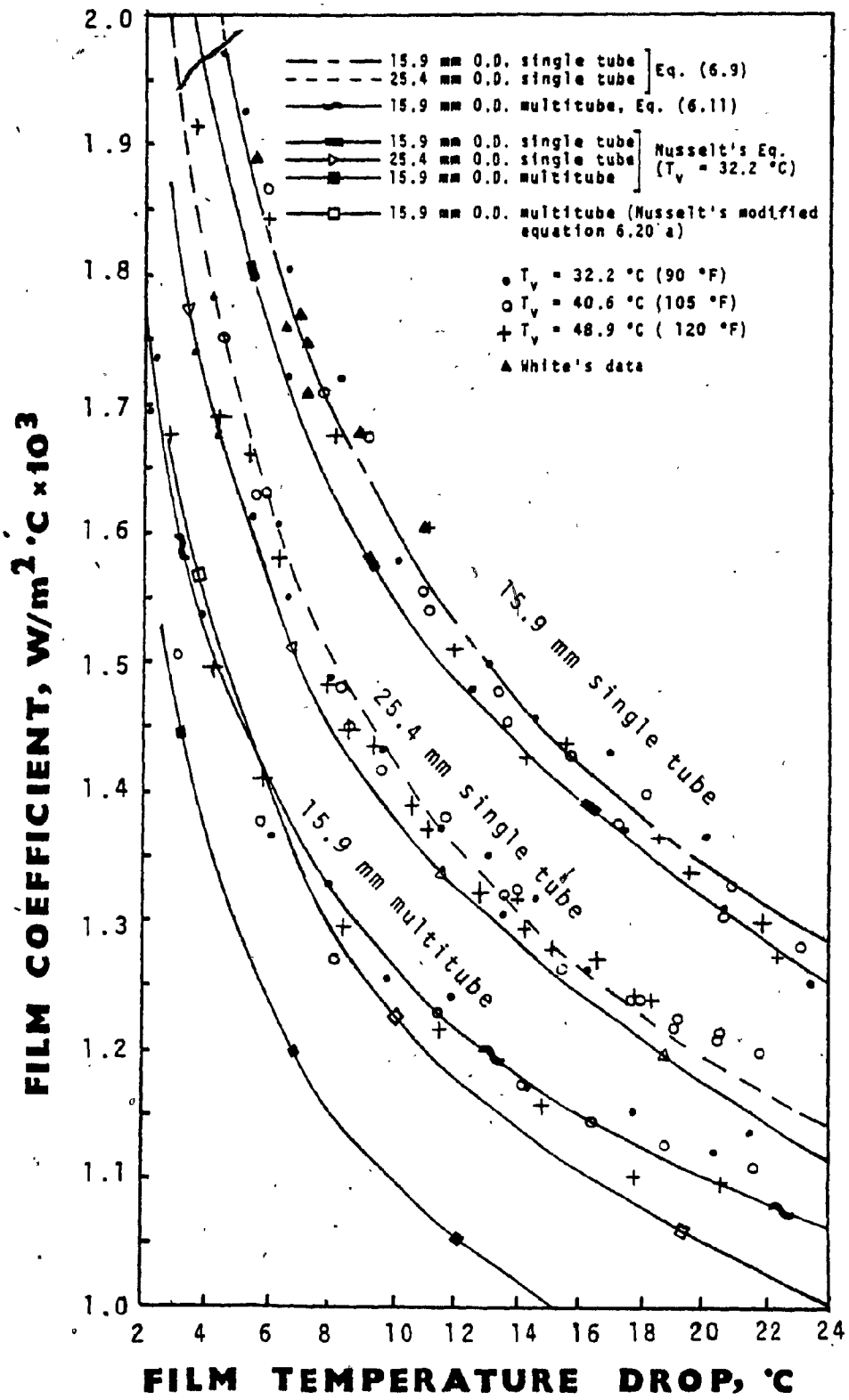

Figure 13: Film coefficient for condensing R-12 pure vapor on the external surface of a single 15.8mm, 25.4mm O.D. tubes and a vertical bank of 4 horizontal tubes, 15.8mm O.D. each, at the condensing temperatures 32.2-48.9 °C (90-120 °F).

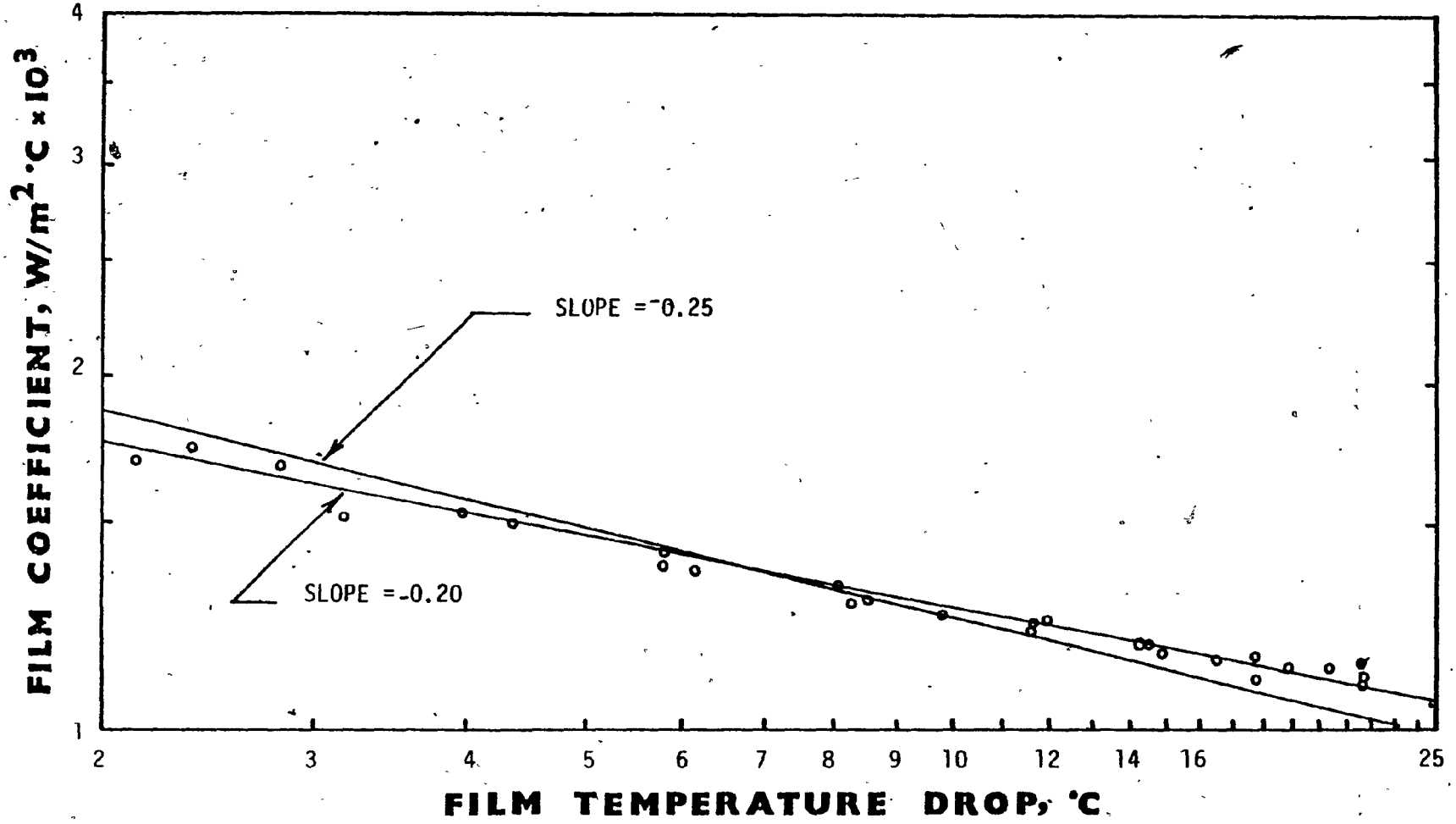

Figure 14: Film coefficient for condensing pure R-12 vapor on the external surface of a vertical bank of 4 horizontal 15.8mm (5/8 inch) O.D. tubes, at the condensing temperature range 32.2-48.9 °C (90-120 °F).

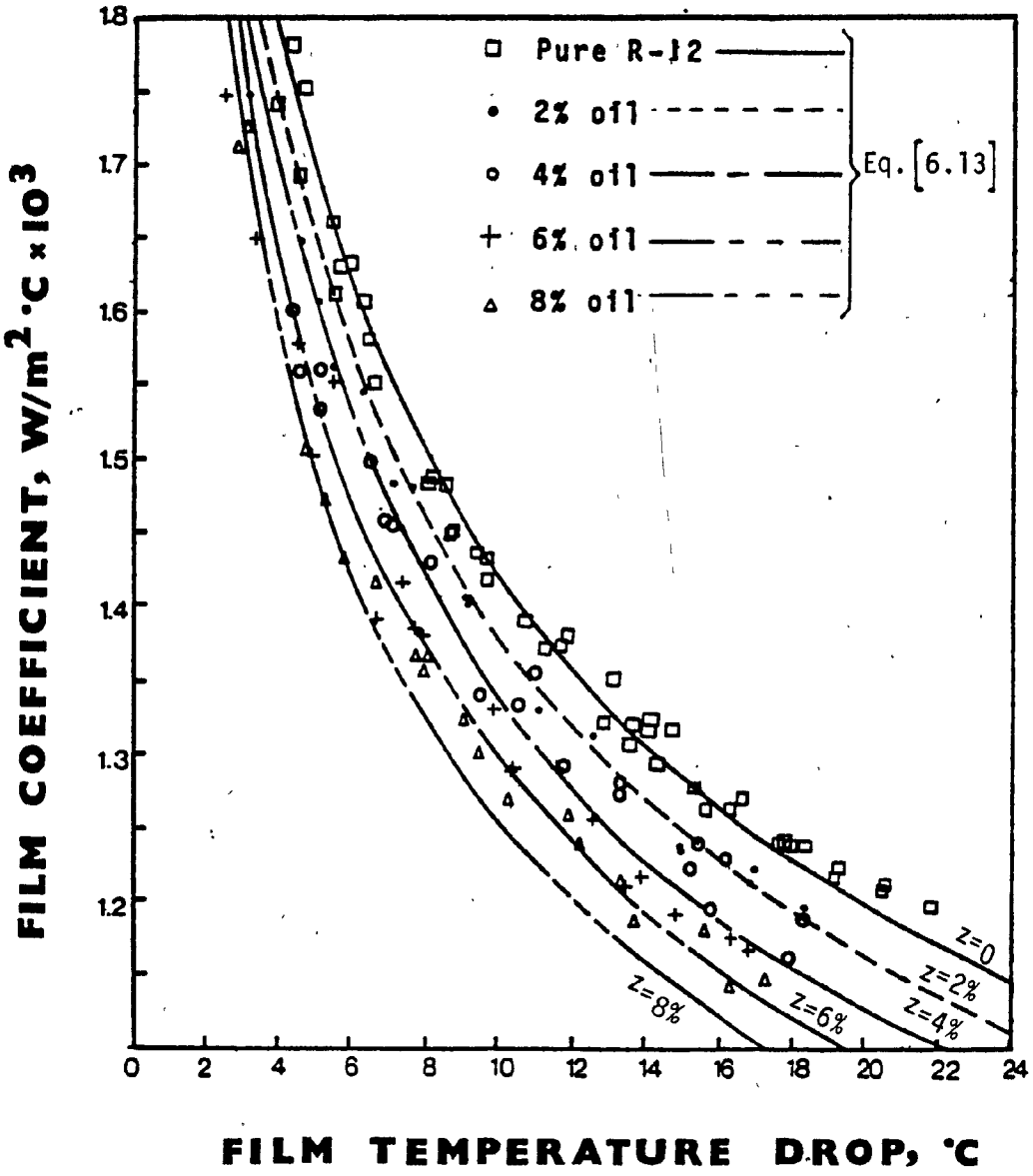

Figure 15: Film coefficient for condensing R-12 vapor, pure and with oil mixture on the external surface of a single horizontal 25.4mm (1 inch) O.D. tube, at the condensing temperature range 32.2-48.9 °C (90-120 °F).

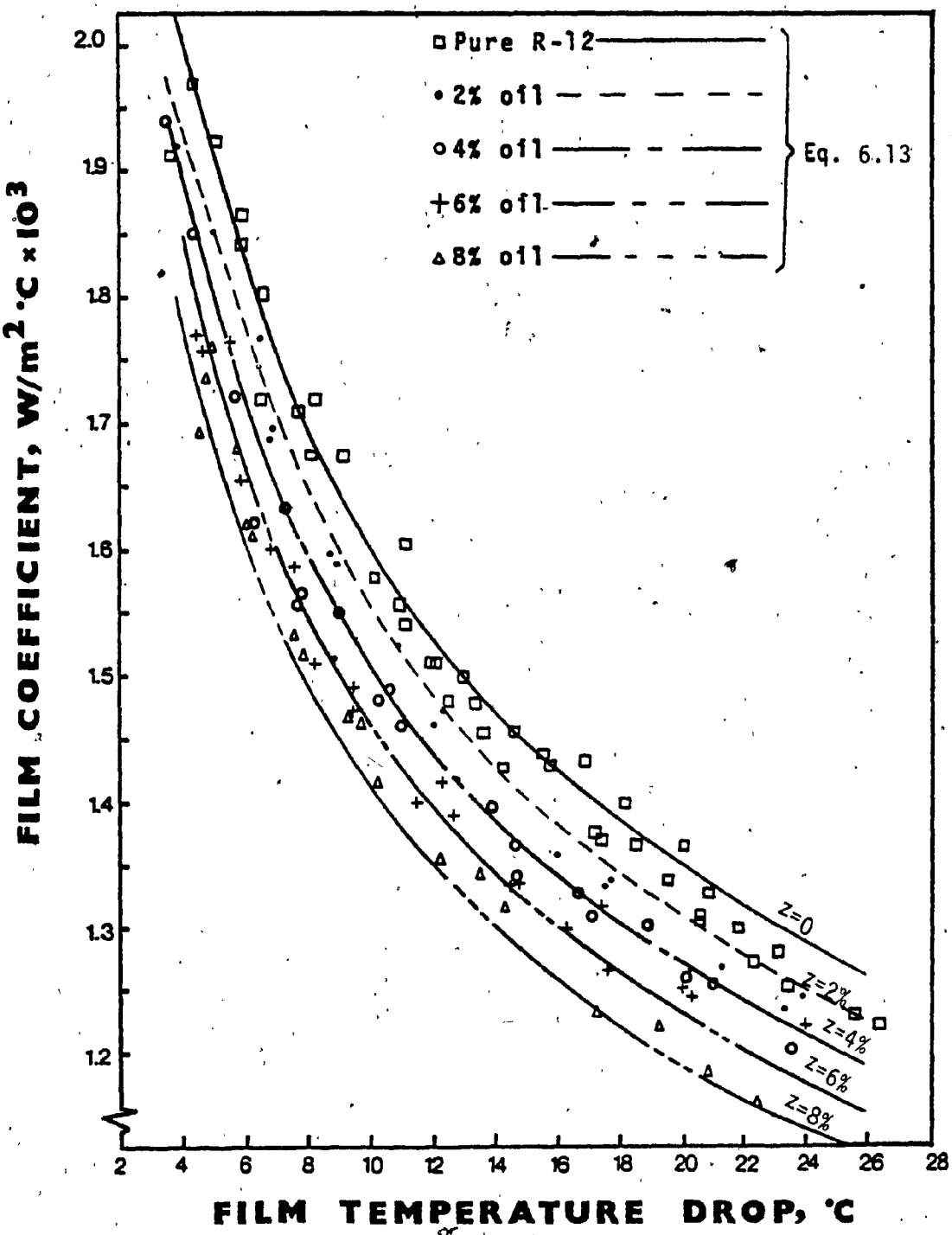

Figure 16: Film coefficient for condensing R-12 vapor, pure and with oil mixture on the external surface of a single horizontal 15.8mm (5/8inch) O.D. tube, at the condensing temperature range 32.2-48.9 °C (90-120 °F).

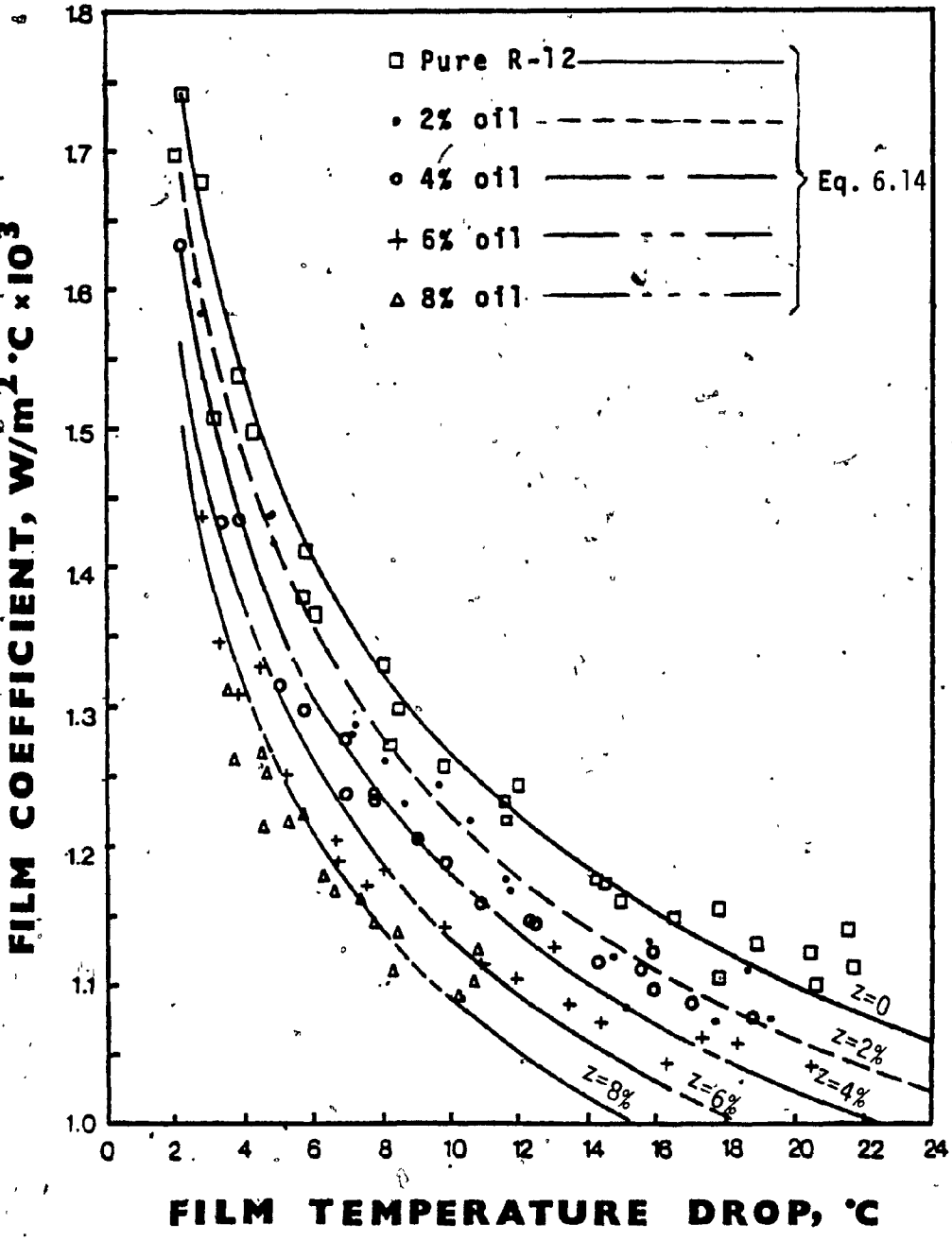

Figure 17: Film coefficient for condensing R-12 vapor, pure and with oil mixture on the external surface of a vertical bank of 4 horizontal 15.8mm O.D. (5/8 inch) tubes, at the condensing temperature range 32.2-48.9 °C (90-120 °F).

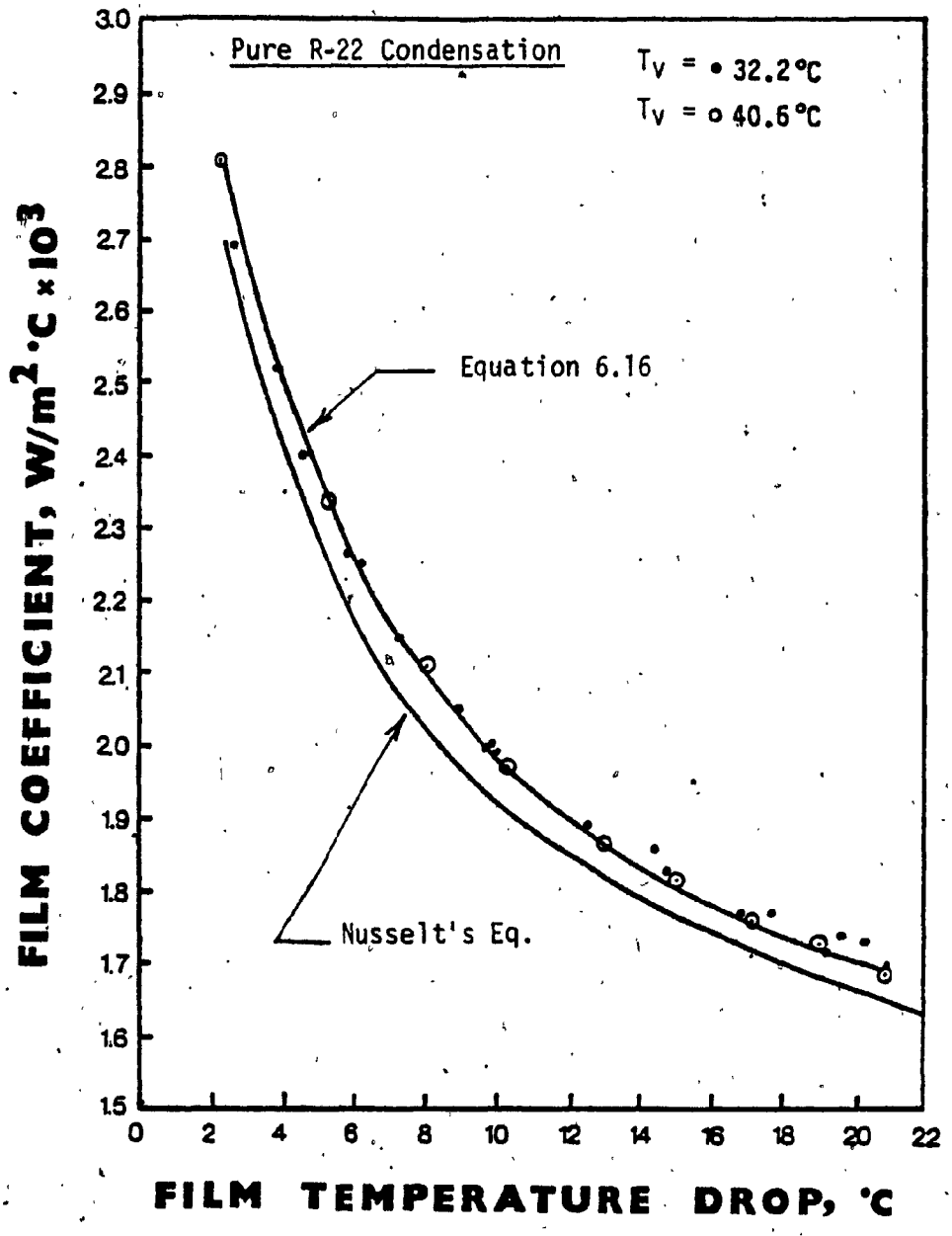

Figure 18: Film coefficient for condensing pure R-22 vapor on the external surface of a 15.8mm (5/8 inch) O.D. horizontal tube, at the condensing temperature 32.2-40.6 °C (90-105 °F).

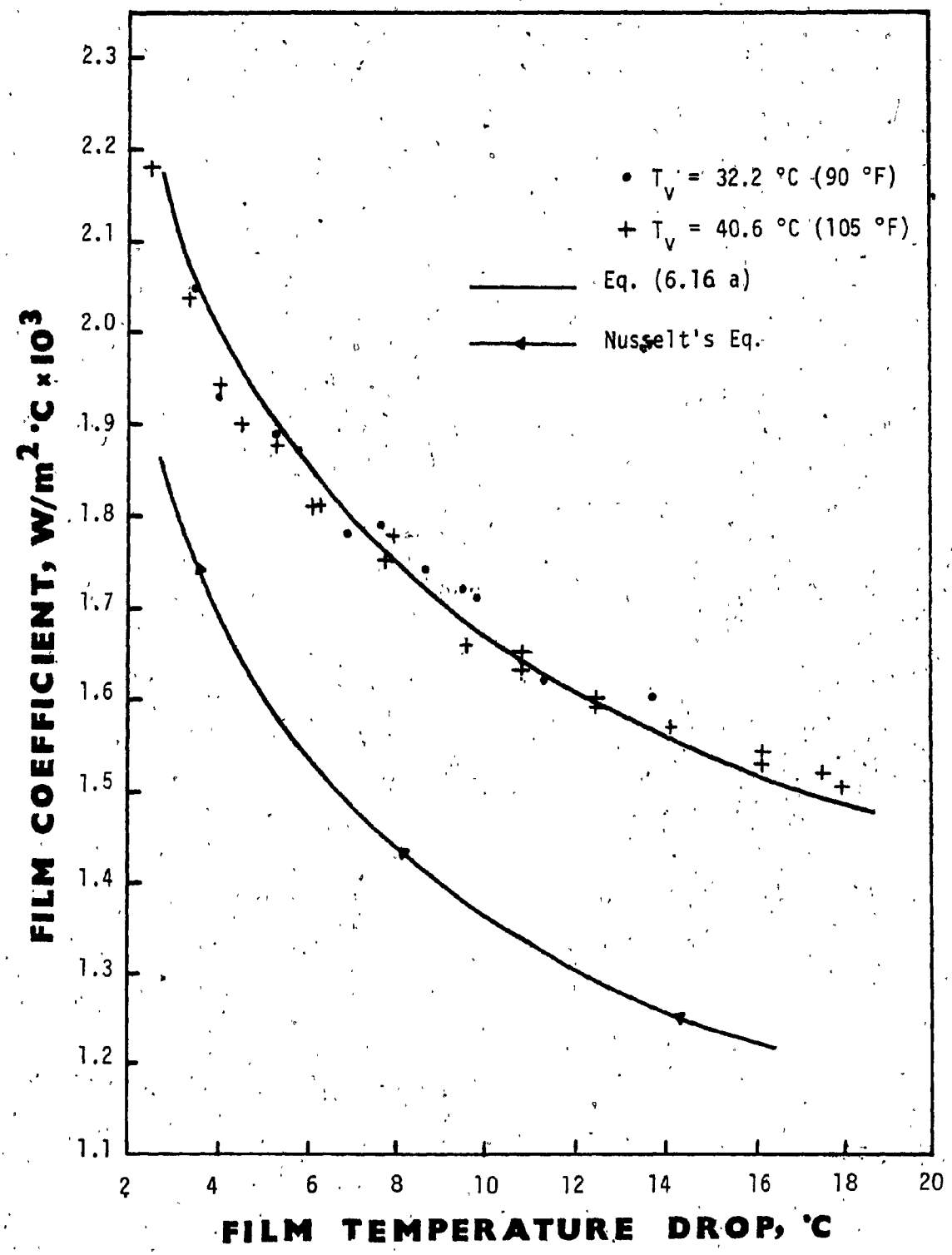

Figure 19: Film coefficient for condensing pure R-22 vapor on the external surface of a vertical bank of 4 horizontal 15.8mm (5/8 inch) O. D. tubes at the condensing temperature range 32.2-40.6 °C (90-105 °F).

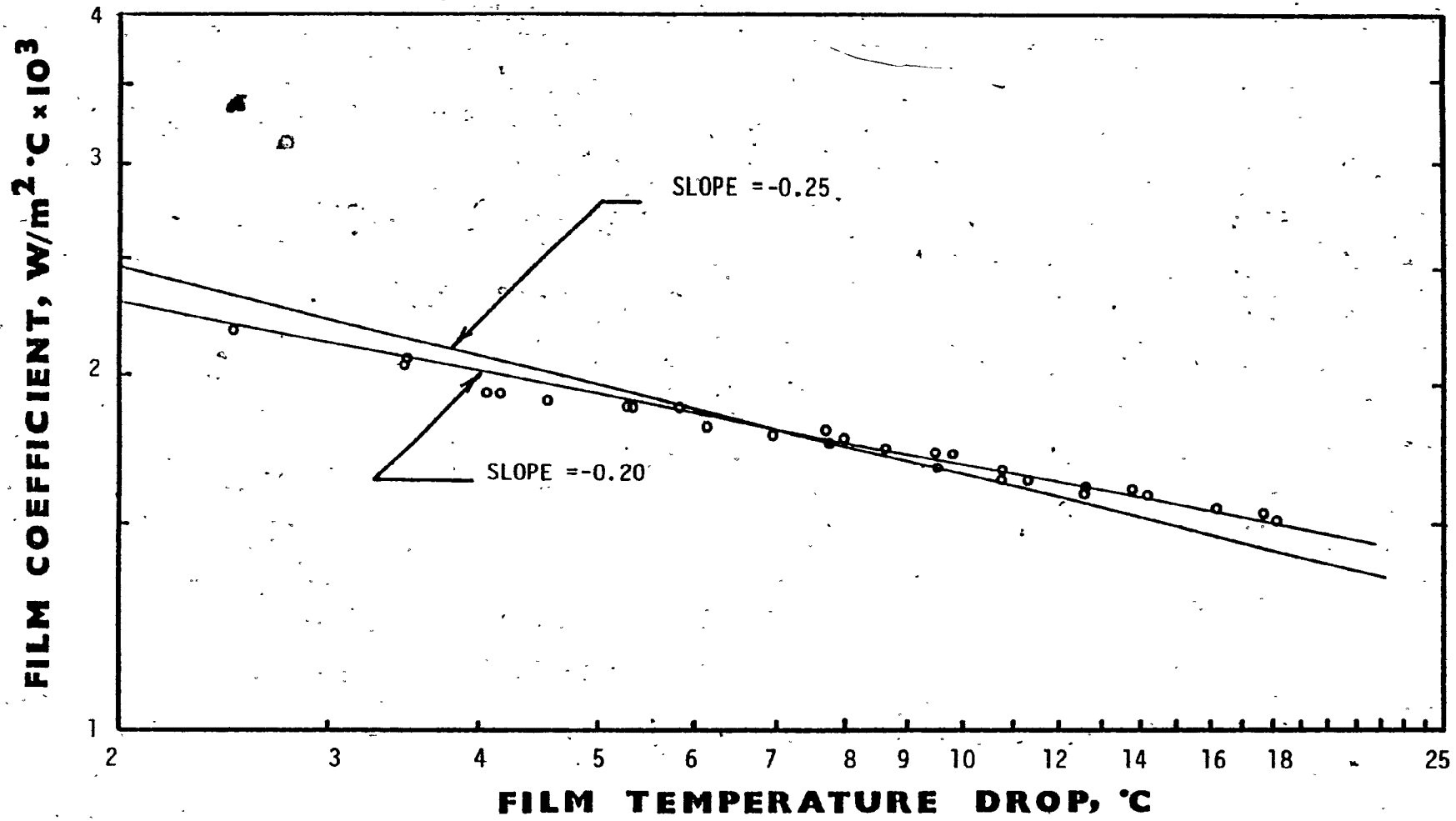

Figure 20: Film coefficient for condensing pure R-22 vapor on the external surface of a vertical bank of 4 horizontal 15.8mm (5/8 inch) O.D. tubes, at the condensing temperature range 32.2-40.6 °C (90-105 °F).

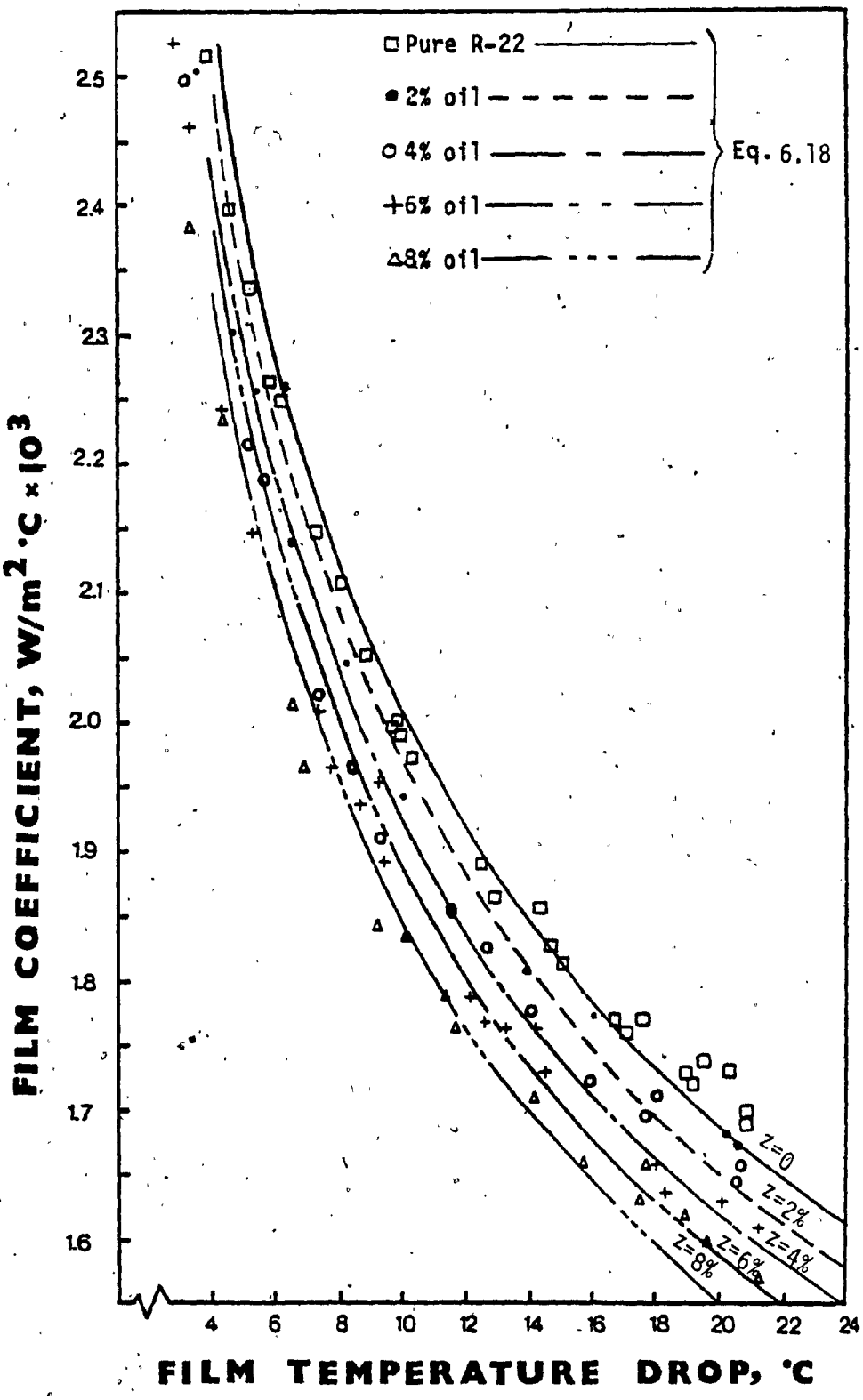

Figure 21:- Film coefficient for condensing R-22 vapor, pure and with oil mixture on the external surface of a single horizontal 15.8mm (5/8 inch) O.D. tube at the condensing temperature range 32.2-40.6 °C (90-105 °F).

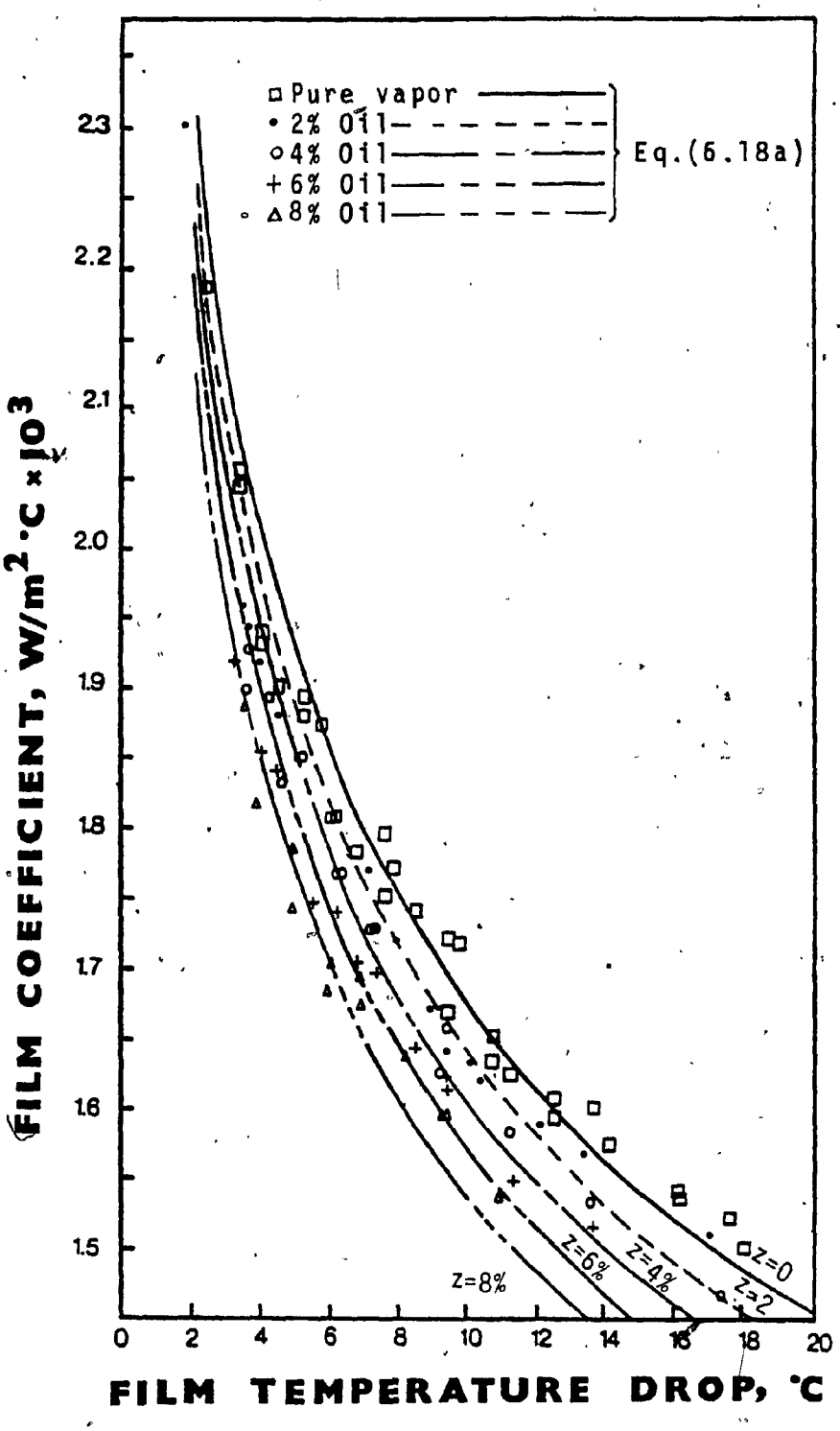

Figure 22: Film coefficient for condensing R-22 vapor, pure and with oil mixture on the external surface of a vertical bank of 4 horizontal 15.8mm (5/8 inch) O.D. tubes at the condensing temperature range 32.2-40.6 °C (90-105 °F).

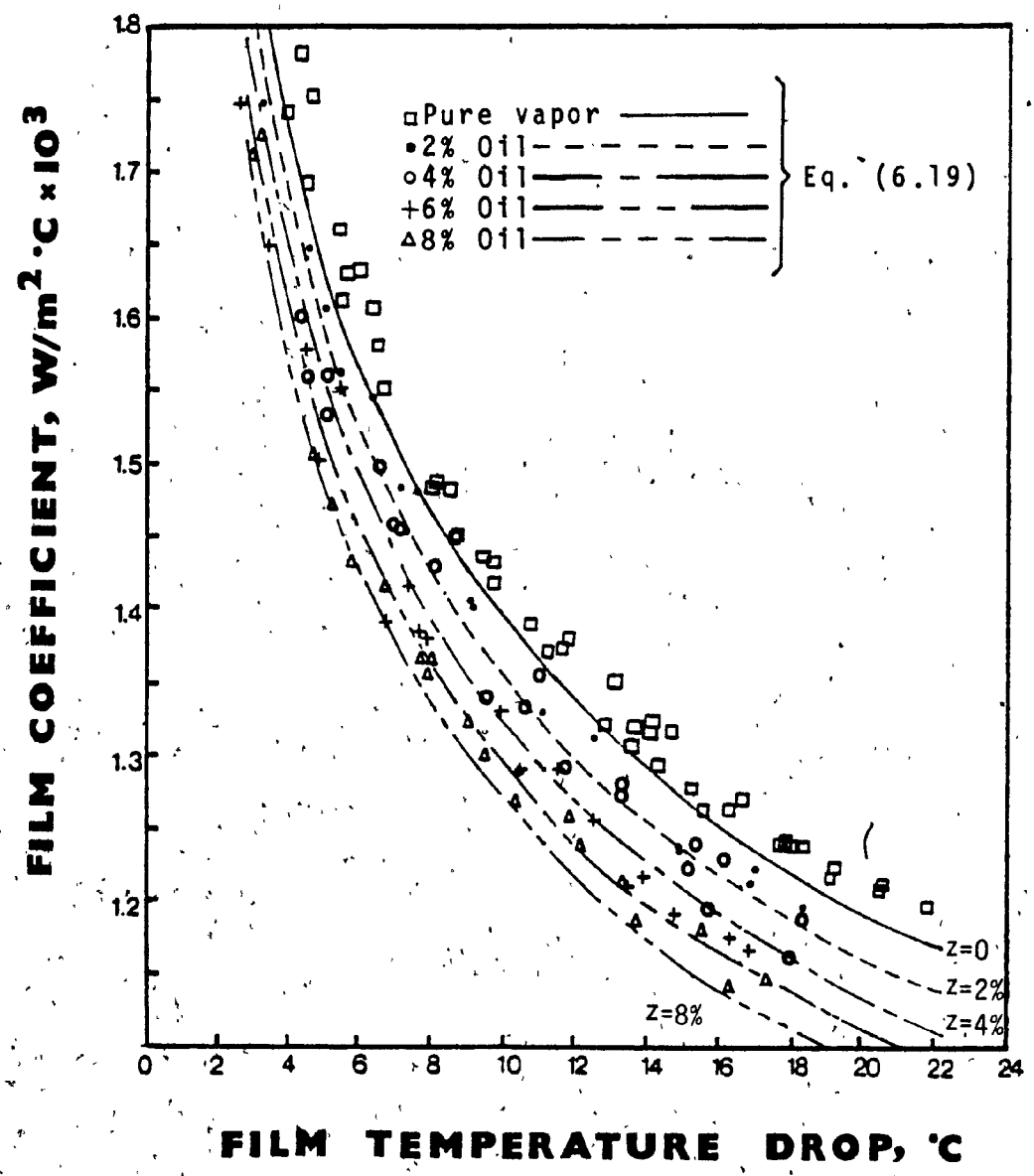

Figure 23: Analytical film coefficient for condensing R-12 vapor, pure and with oil mixture on the external surface of a single horizontal 25.4mm (1 inch) O.D. tube, based on 32.2 °C (90 °F) condensing temperature.

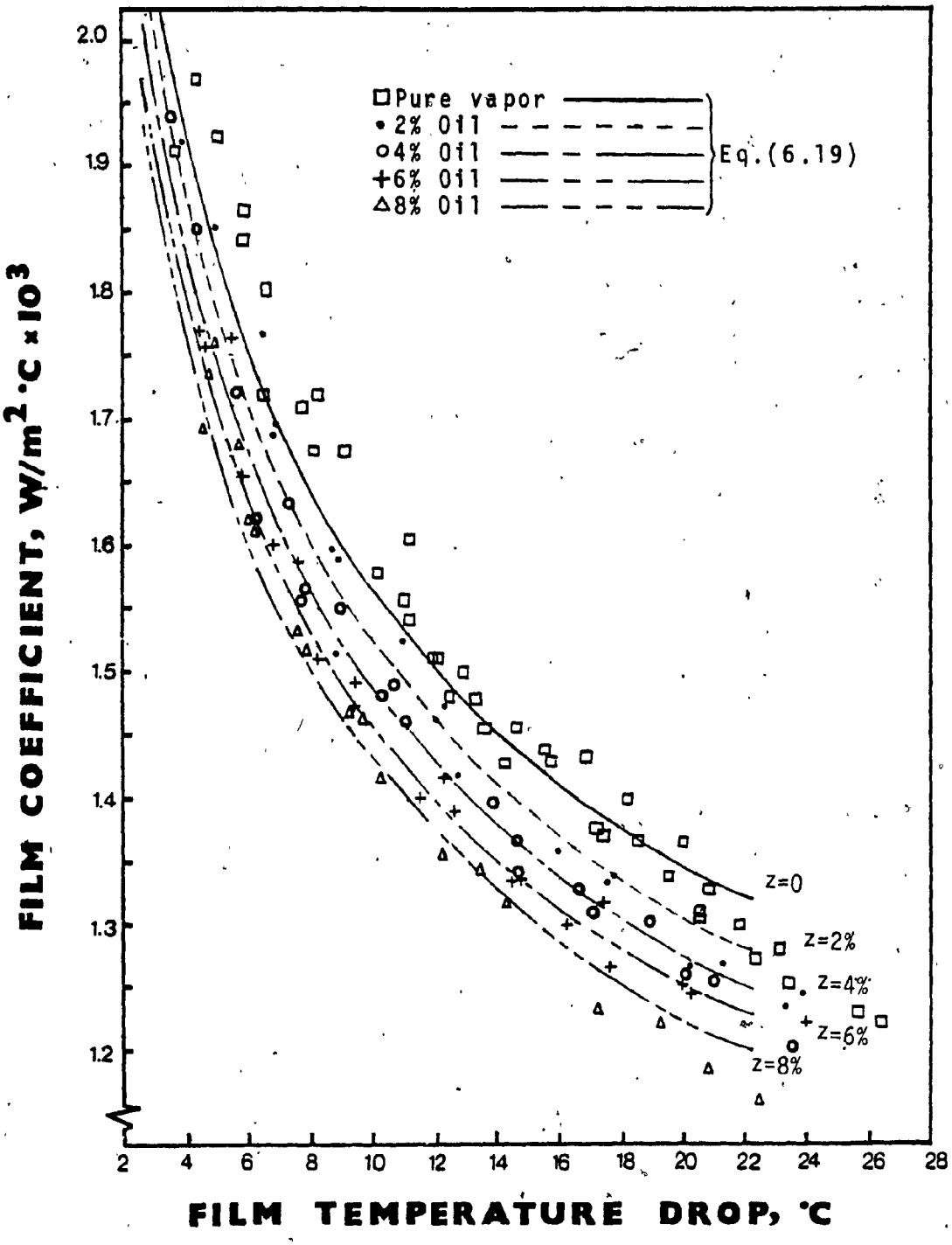

Figure 24: Analytical film coefficient for condensing R-12 vapor, pure and with oil mixture on the external surface of a single horizontal 15.8mm (5/8 inch) O.D. tube, based on 32.2 °C (90 °F) condensing temperature.

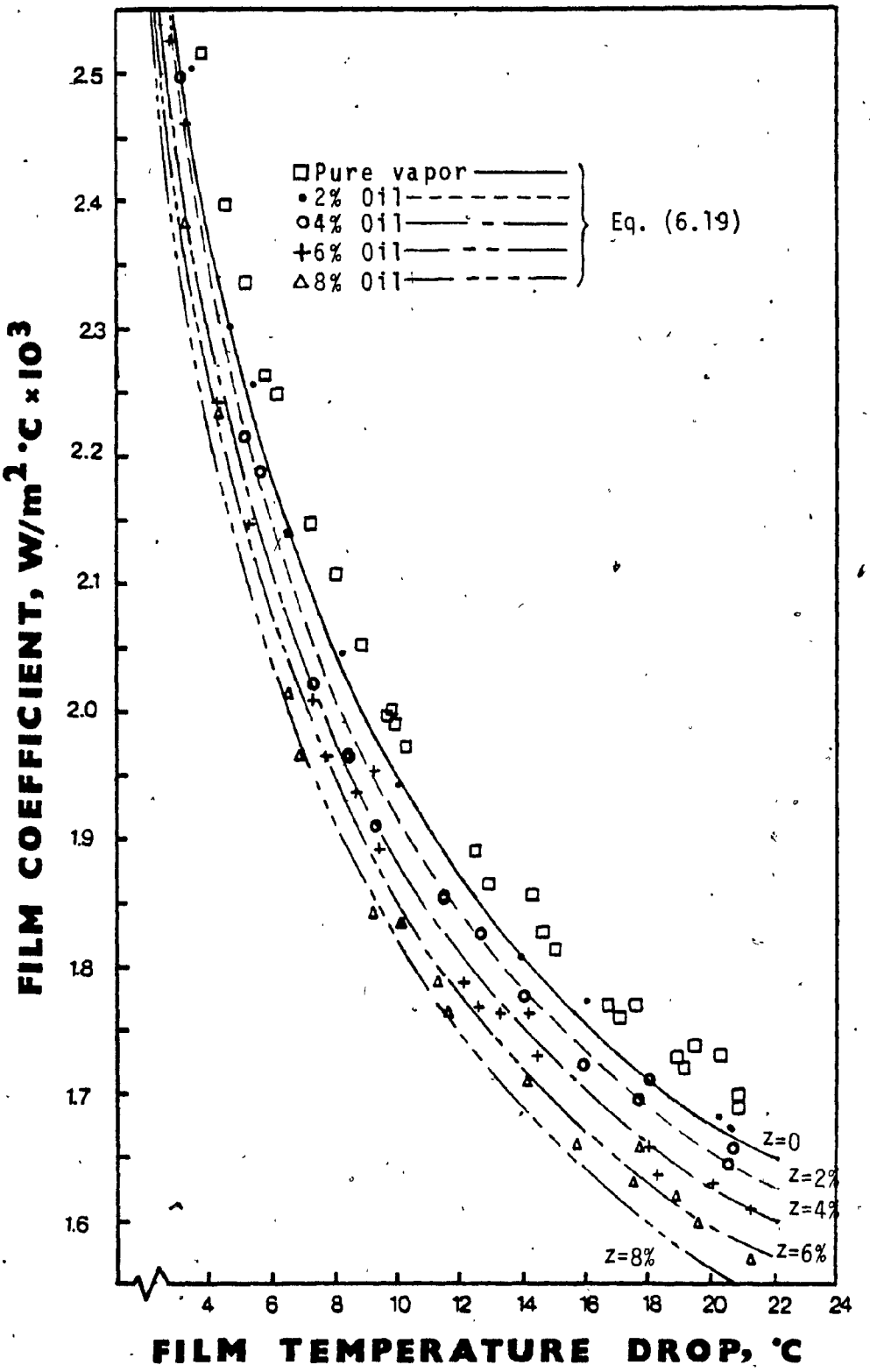

Figure 25: Analytical film coefficient for condensing R-22 vapor, pure and with oil mixture on the external surface of a single horizontal 15.8mm (5/8 inch) O.D. tube, based on 32.2 °C (90 °F) condensing temperature.

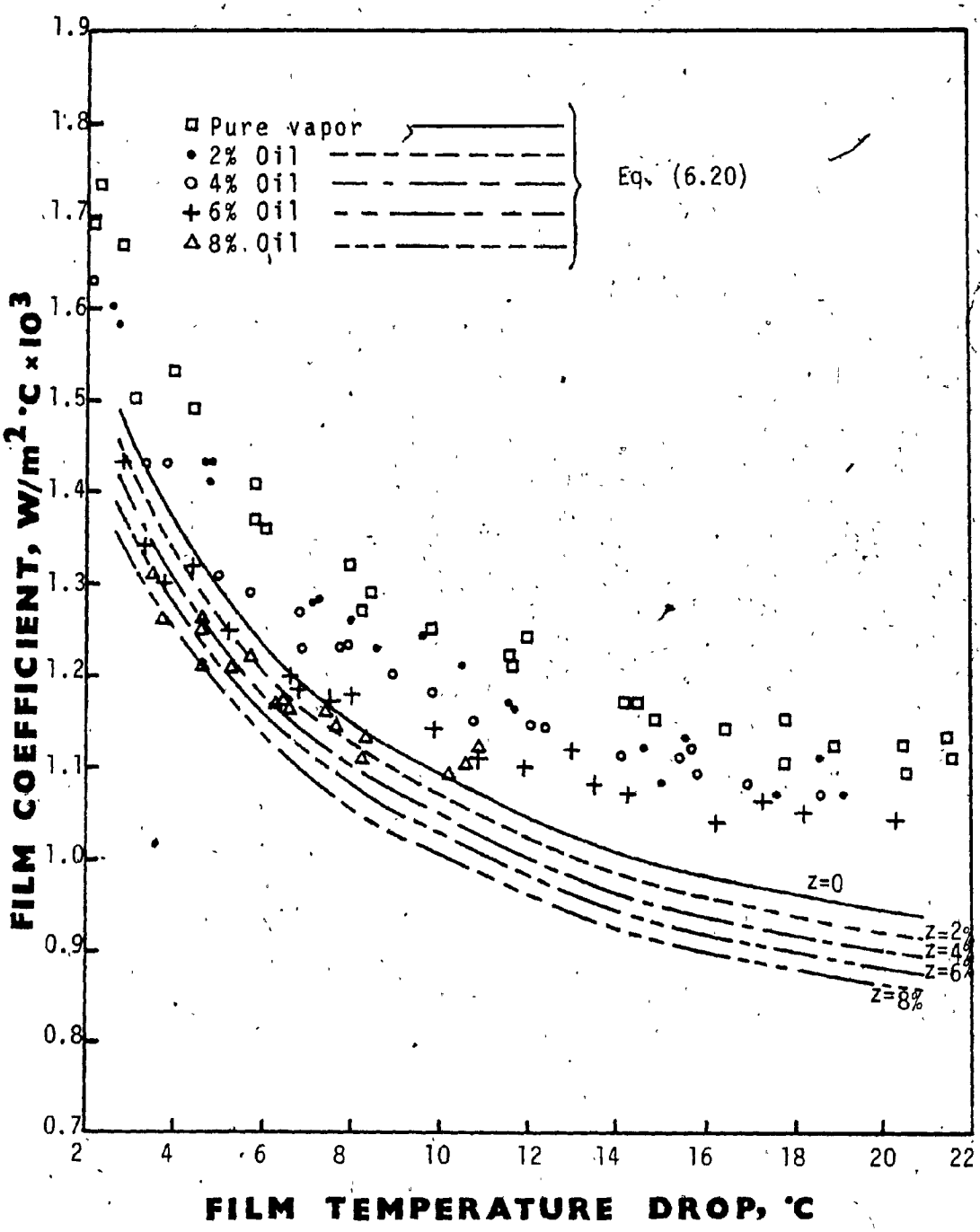

Figure 26: Analytical film coefficient for condensing R-12 vapor, pure and with oil mixture on the external surface of a vertical bank of 4 horizontal 15.8mm (5/8 inch) O.D. tubes, based on 32.2 °C (90 °F) condensing temperature.

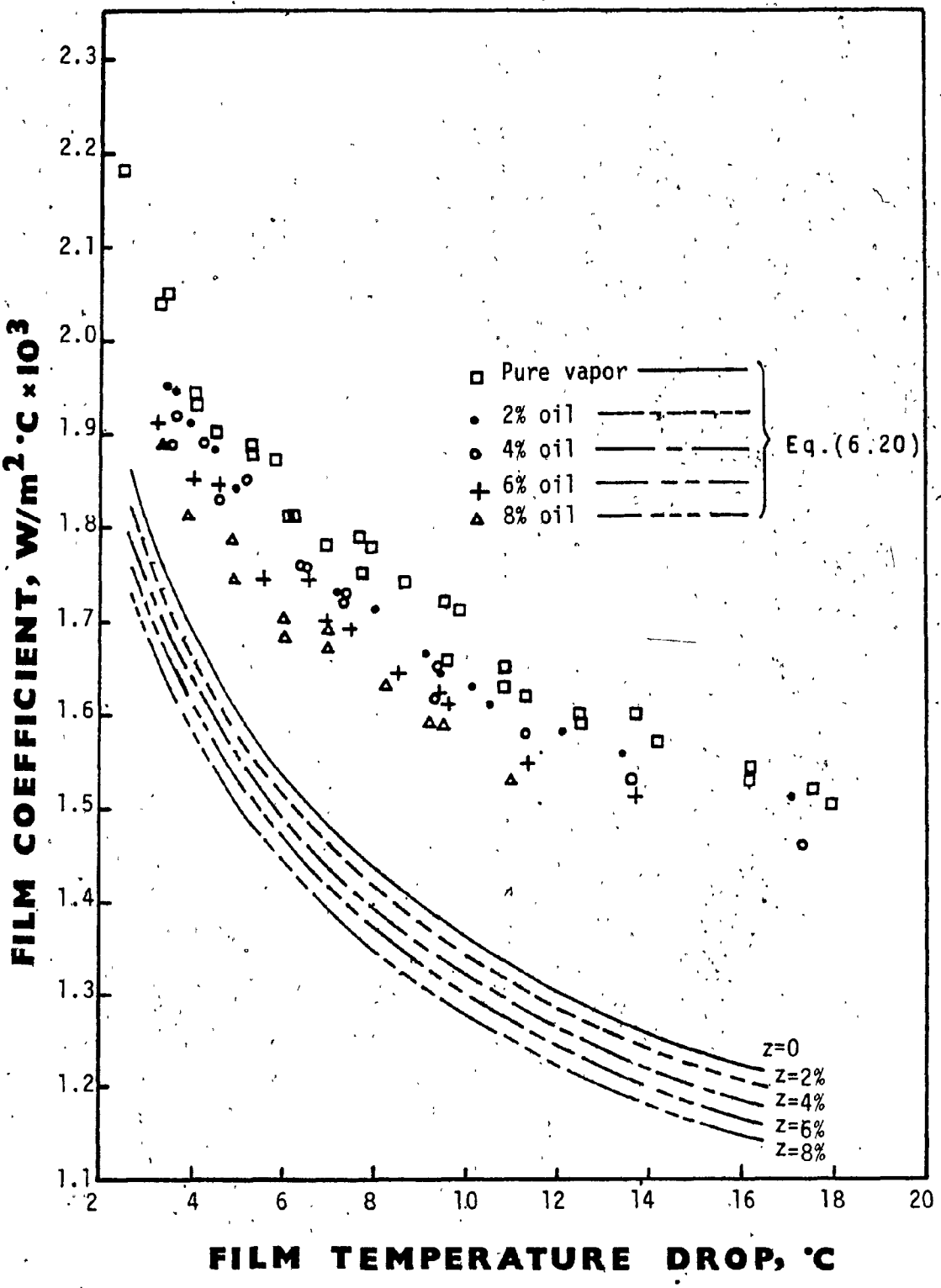

Figure 27: Analytical film coefficient for condensing R-22 vapor, pure and with oil mixture on the external surface of a vertical bank of 4 horizontal 15.8mm (5/8 inch) O.D. tubes, based on 32:2 °C (90 °F) condensing temperature.

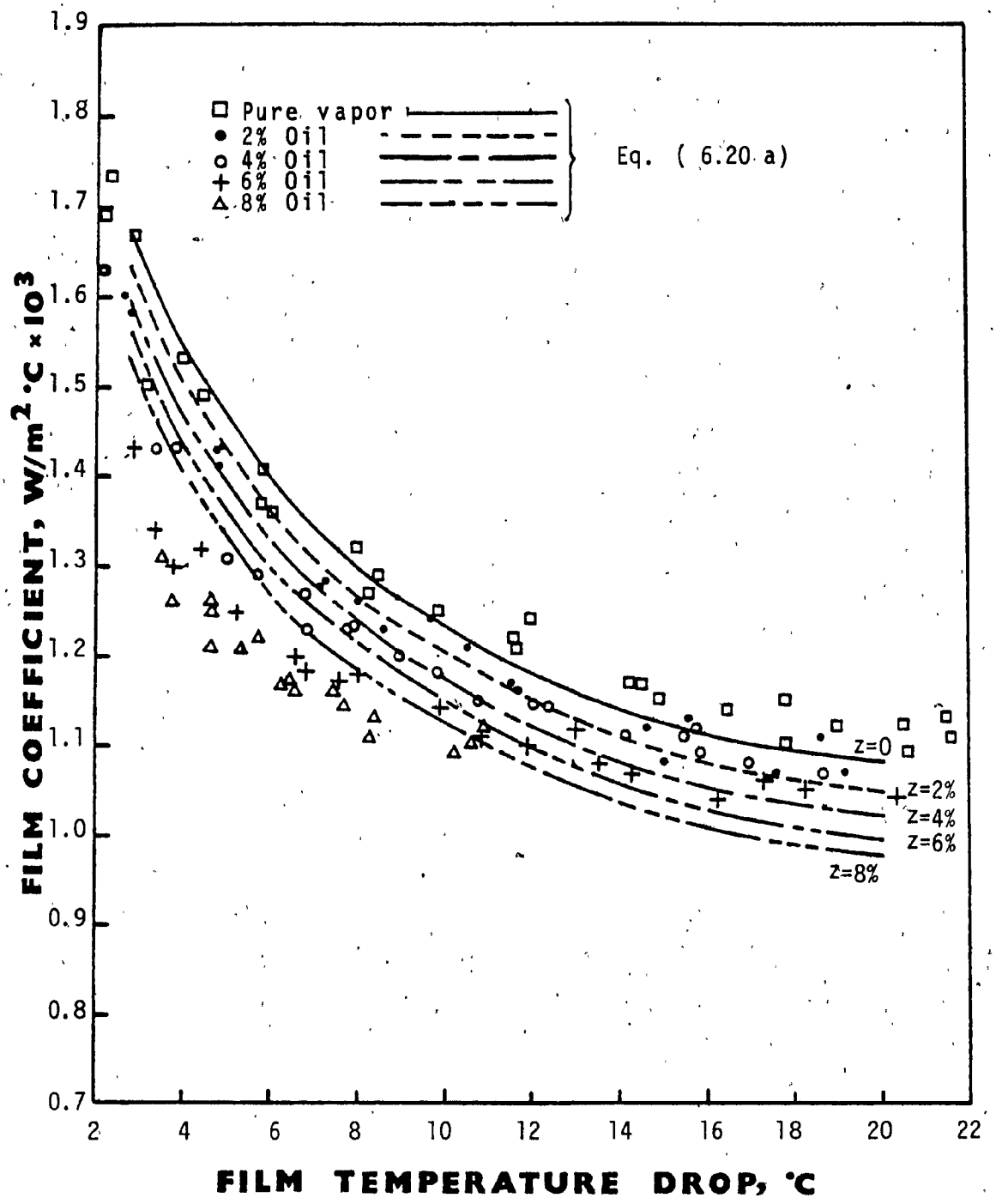

Figure 28: Based ($N^{-0.167}$) analytical film coefficient for condensing R-12 vapor, pure and with oil mixture on the external surface of a vertical bank of 4 horizontal 15.8mm (5/8 inch) O.D. tubes, at the condensing temperature range 32.2-48.9 °C (90-120 °F).

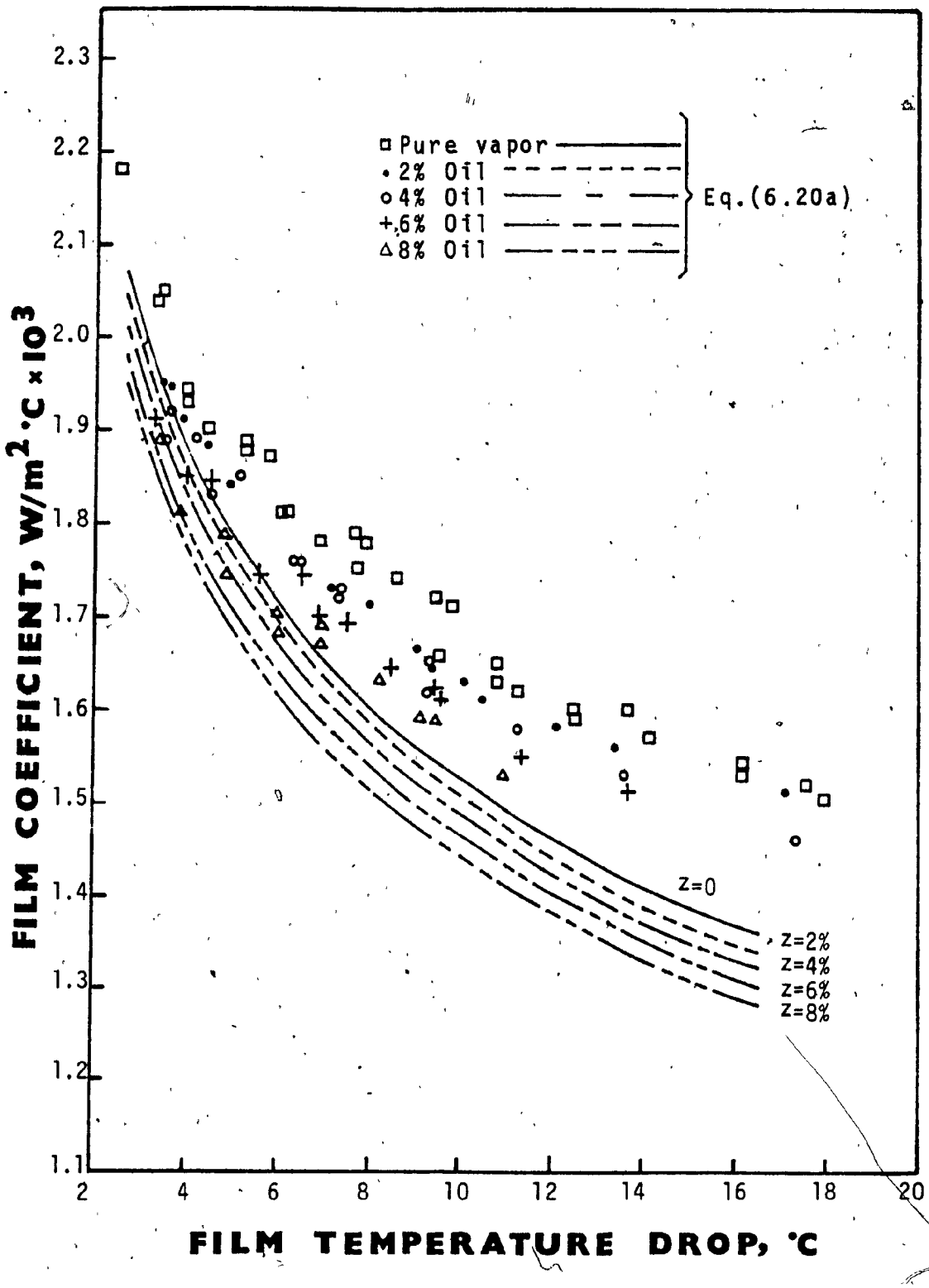

Figure 29: Based ($N^{-0.167}$) analytical film coefficient for condensing R-22 vapor pure and mixed with oil on the external surface of a vertical bank of 4 horizontal 15.8mm (5/8 inch) O.D. tubes, based on 32.2 °C (90 °F) condensing temperature.

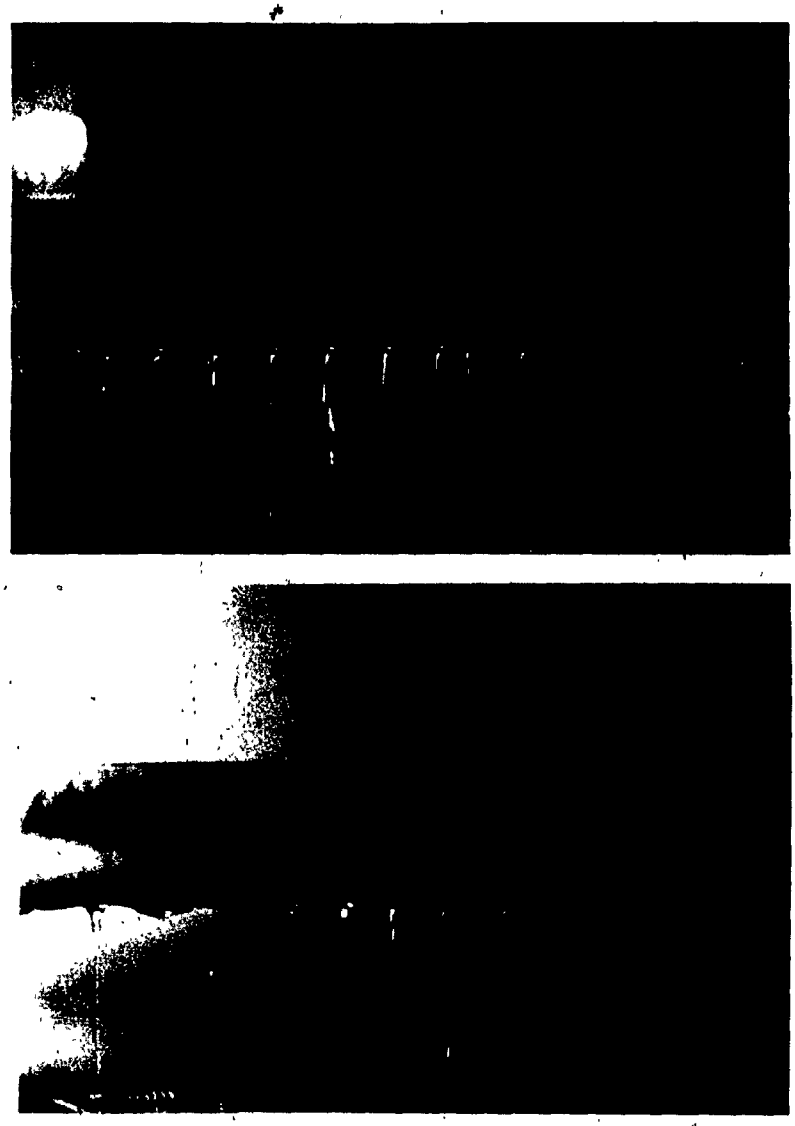

Plates 1 & 2 : Condensation of R-12 vapor on the external surface of 25.4 mm (1 inch) O.D. horizontal tube at (ΔT) 18 and 14 °C respectively, at the condensing temperature 32.2 °C (90°F).

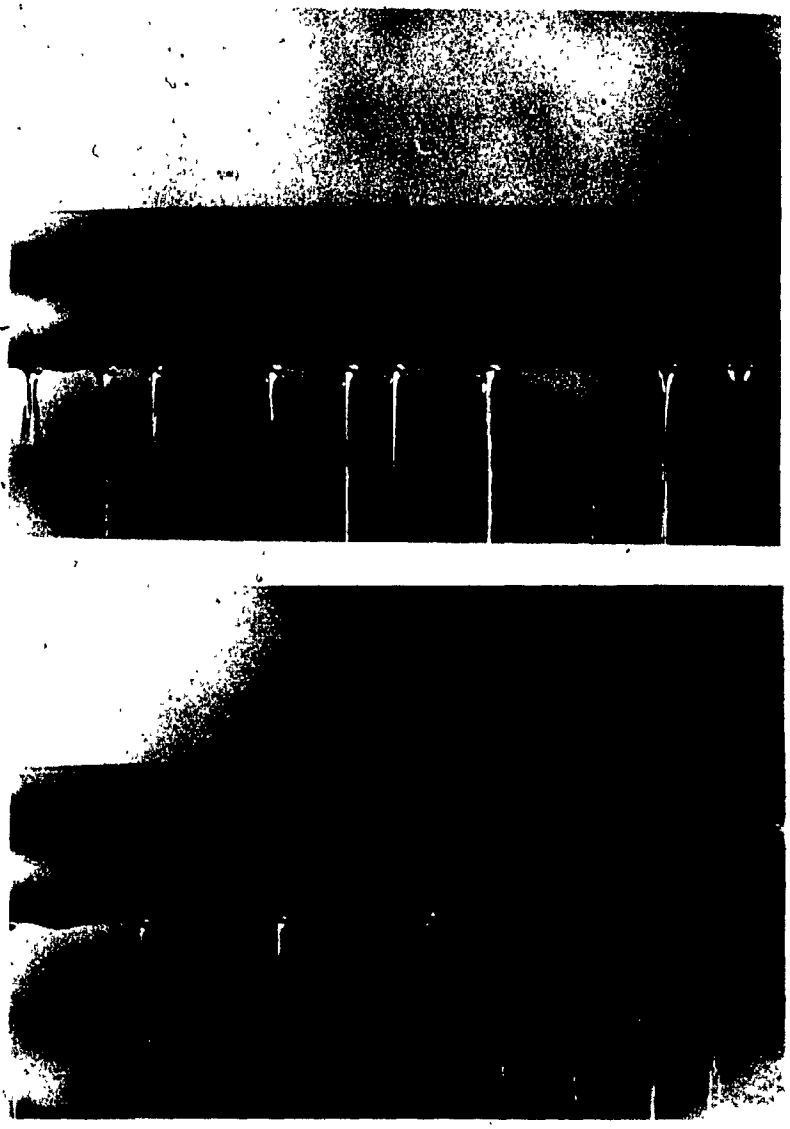

Plates 3 & 4 : Condensation of R-12 vapor on the external surface of a 25.4 mm (1 inch) O.D. horizontal tube at (ΔT) 11 and 7 °C respectively, at the condensing temperature 32.2 °C (90°F).

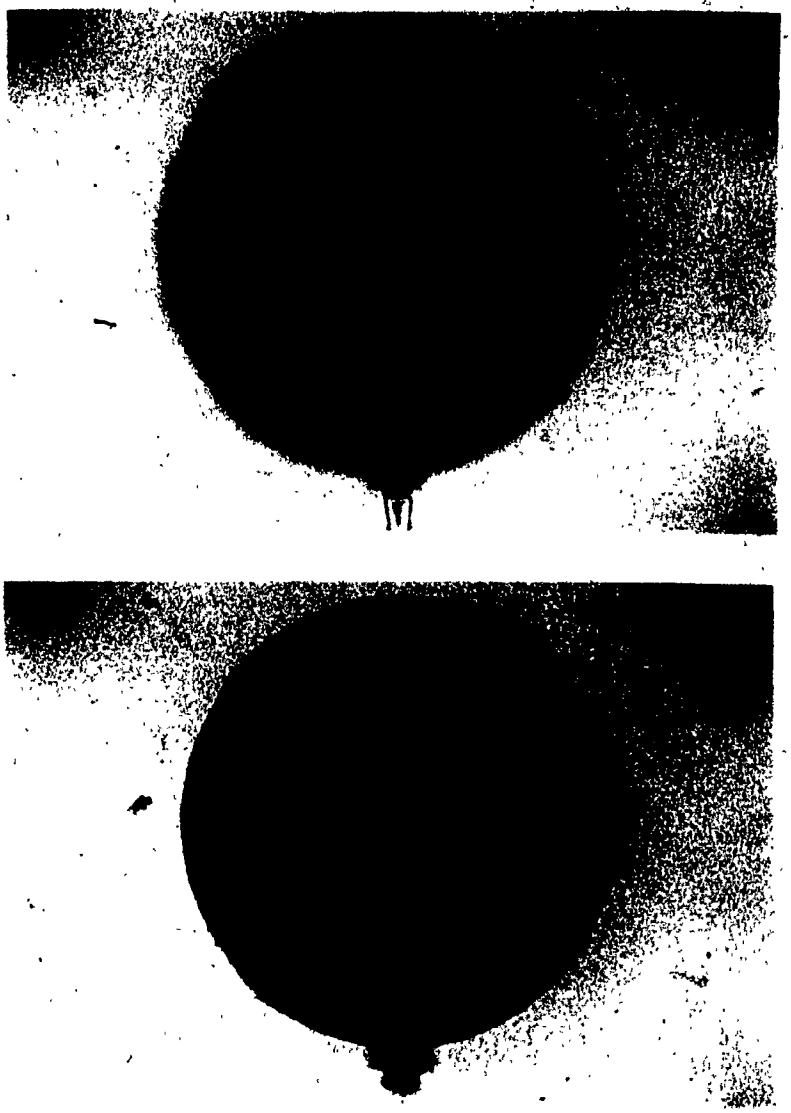

Plates 5 & 6 : Condensation of R-12 vapor on the external surface of a single 15.8 mm (5/8 inch) O.D. horizontal tube with condensing rates, 1.2×10^{-2} kg/ms and 0.97×10^{-2} kg/ms respectively, at the condensing temperature 32.2°C (90°F).

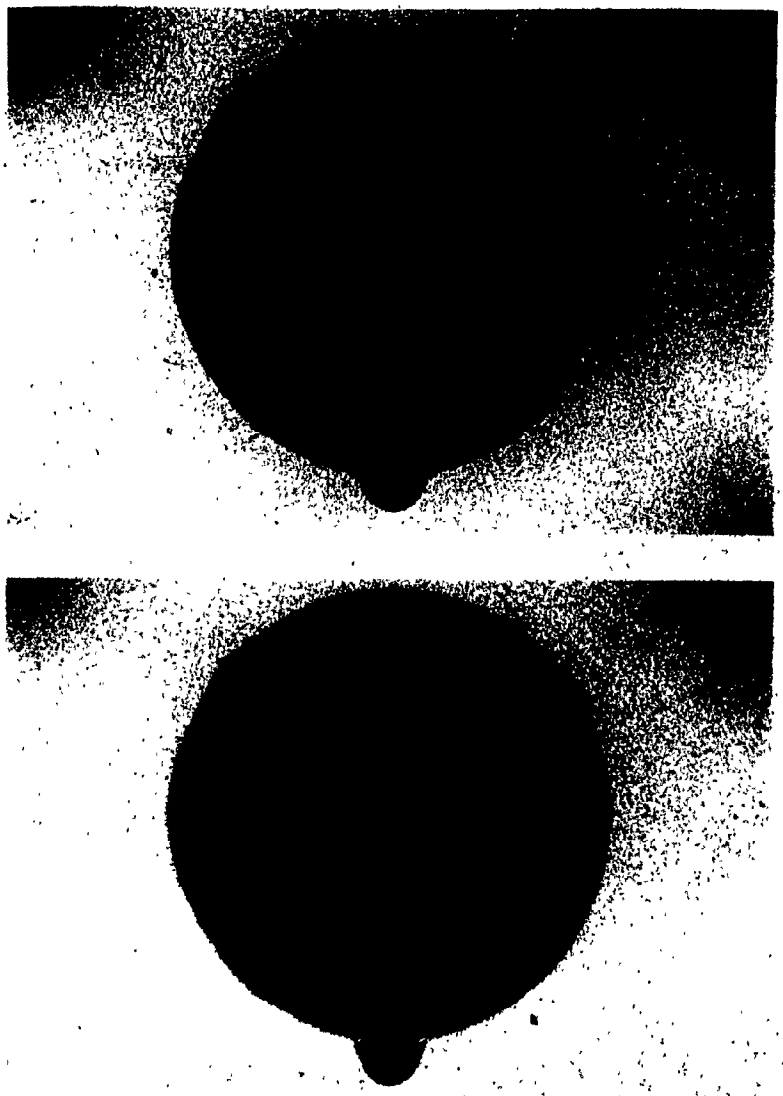

Plates 7 & 8 : Condensation of R-12 vapor on the external surface of a single 15.8 mm (5/8 inch) O.D. horizontal tube with condensing rates, $.82 \times 10^{-2}$ kg/ms and 0.65×10^{-2} kg/ms respectively, at the condensing temperature 32.2°C (90°F).

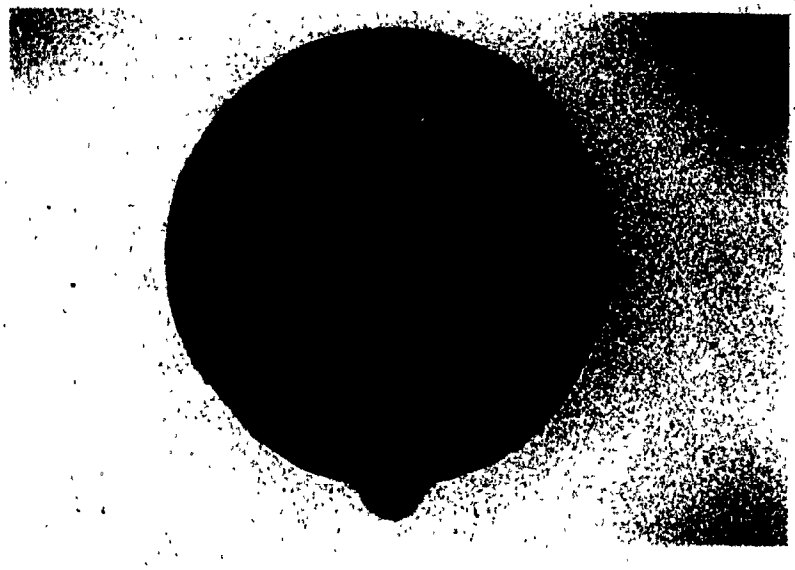

Plate 9: Condensation of R-12 vapor on the external surface of a single 15.8 mm (5/8 inch) O.D. horizontal tube with condensing rate 0.52×10^{-2} kg/ms, at the condensing temperature 32.2°C (90°F).

CHAPTER 7

STATISTICAL AND ERROR ANALYSIS

7.1- Statistical analysis

A statistical analysis was performed for the data obtained in this study. The relations between these data and the correlation equations were analysed using a software package "Stat Pac", and the results obtained are listed in the following table:

Table No.	Correlation Coefficient	Range of Residuals $W/m^2{}^\circ C$	Standard Deviation $W/m^2{}^\circ C$	Standard error of estimate $W/m^2{}^\circ C$	Max. Posative and Neg. deviation from regression line
1	0.995	114	199	32.3	2.92% , 2.99%
2	0.987	189	210	33.2	3.37% , 7.01%
3	0.988	138	197	29.8	3.59% , 4.95%
4	0.997	36.6	163	12.1	1.24% , 1.24%
5	0.992	76.7	159	19.6	2.93% , 3.25%
6	0.996	53.9	171	15.9	1.50% , 2.17%
7	0.995	71.6	174	17.2	2.65% , 1.79%
8	0.995	88.1	216	20.2	2.72% , 2.0%
9	0.996		207	19.2	

continued on the next page;

Table No.	Correlation Coefficient	Range of Residuals $W/m^2{}^\circ C$	Standard Deviation $W/m^2{}^\circ C$	Standard error of estimate $W/m^2{}^\circ C$	Max. Posative and Neg. deviation from regression line
10	0.992	97.9	186	23.3	3.98% , 1.82%
11	0.994	104	201	22.4	2.38% , 3.67%
12	0.993	64.1	170	19.3	3.50% , 1.96%
13	0.988	90.0	145	22.2	3.36% , 2.83%
14	0.985		115	20.0	
15	0.961	57.7	64.3	17.8	2.70% , 2.24%
16	0.999	60.9	300	14.4	1.16% , 1.17%
17	0.990	73.4	174	21.2	2.00% , 1.85%
18	0.999	40.2	294	13.6	0.82% , 0.83%
19	0.997	57.9	241	19.4	1.01% , 1.69%
20	0.997	70.0	283	20.5	1.70% , 1.43%
21	0.996	66.7	239	20.0	1.98% , 1.72%
22	0.994	85.7	214	23.3	2.37% , 1.64%
23	0.990	67.5	144	19.5	1.61% , 1.98%
24	0.994	39.2	130	13.5	1.17% , 1.21%
25	0.985	48.1	105	18.2	1.39% , 1.40%

7.2- Experimental errors:

The experimental errors were estimated at selected high ΔT = 18.1°C (32.5°F) and low ΔT = 2.5°C (4.5°F), with respectively measured heat transfer rates 4270 W and 860 W. The error sources are:

1- The measurements of the condensing surface temperature:

The local surface temperature of the condensing tube was found to vary in a range of $\pm$ 0.001-0.004 mv (0.025-0.1°C) at high ΔT due to the relatively high condensation rate, and $\pm$ 0.001-0.002 mv (0.025-0.05°C) at low ΔT with small condensation rate. Thus, the condensing surface temperature can be as high as T_{sh} or as low as T_{sL}. If the saturation temperature is 40.6°C (105°F), then the respective T_{sh} , T_{sL} and the percentage variation are as follows:

a)- at ΔT = 18.1°C (32.5°F)

$$\Delta T = T_v - T_s$$

$$T_{sh} = 22.5 + 0.1 = 22.6°C$$

$$T_{sL} = 22.5 - 0.1 = 22.4°C$$

and under this condition, the percentage variation of the condensing surface temperature is:

$$\pm\ 0.1/22.5 * 100\% = \pm\ 0.44\%$$

b)- at ΔT = 2.5°C (4.5°F)

$$T_{sh} = 38.1 + 0.05 = 38.15°C$$

$$T_{sL} = 38.1 - 0.05 = 38.05°C$$

and the corresponding percentage variation of the condensing surface temperature is:

$$0.05/38.1 \quad *100\% = 0.13\%$$

2- The determination of the saturation temperature:

The pressure transducer measurements were always checked against a laboratory test pressure gauge calibrated to 1 psi. The saturation pressure variation can be ± 0.5 psi (3.4 kPa) which is equivalent to ± 0.16° F (0.1°C) change in the condensing temperature. T_v , thus can rise to T_{vh} = T_v + 0.1°C or drop to T_{vL} = T_v - 0.1°C.

$$T_{vh} = 40.6 + 0.1 = 40.7°C$$

$$T_{vL} = 40.6 - 0.1 = 40.5°C$$

the percentage variation of the vapor saturation temperature is:

$$\pm 0.1/40.6 \quad *100\% = \pm 0.22\%$$

3- The reading of condensate level:

The condensate mass flow rate entering the receiver was obtained by measuring the time required for the condensate to rise 18 inches (457 mm). The condensate level reading can be 1/16 inch (1.6 mm) off at both beginning and end of the accumulation period, thus the heat transfer rate can rise to

$$Q_h = Q + (2/16*18)\ Q$$

or drop to

$$Q_L = Q - (2/16*18)\ Q$$

and the possible percentage variation of the condensate level is:

$$\pm 2/(16*18) * 100 = \pm 0.7\%$$

for both low and high ΔT.

Under the conditions described above, the maximum and minimum values of the condensing coefficient can be:

$$h_{max.} = Q_h / A_s\ (T_{vL} - T_{sh})$$

$$h_{min.} = Q_L / A_s\ (T_{vh} - T_{sL})$$

a)- $\Delta T = 18.1°C$ (32.5°F)

$$Q_h = 4270 + 0.7/100 * 4270 = 4300\ W$$

$$Q_L = 4270 + 0.7/100 * 4270 = 4240\ W$$

$$h_{max.} = 4300/\ 0.16(40.5 - 22.6) = 1500\ W/m^2°C$$

$$h_{min.} = 4240/\ 0.16(40.7 - 22.4) = 1448\ W/m^2°C$$

The calculated condensing coefficient $h = 1474 W/m^2°C$, therefore, the possible variation of the condensing coefficient is:

$$+1.8\ \%,\ \text{or}\ -2.3\ \%$$

b)- $\Delta T = 2.5°C$ (4.5°F)

$$Q_h = 860 + 0.7/100 * 860 = 866\ W$$

$$Q_L = 860 - 0.7/100 * 860 = 854\ W$$

$$h_{max.} = 866/\ 0.16(40.5 - 38.1) = 2255\ W/m^2°C$$

$$h_{min.} = 854/\ 0.16(40.7 - 38) = 1977\ W/m^2°C$$

The calculated condensing coefficient $h = 2150\ W/m^2°C$,

therefore, the possible variation of the condensing coefficient, at the worst conditions, will be:

+5 %, or - 8 %

CHAPTER 8

CONCLUSIONS AND RECOMMENDATIONS

8.1- Conclusions

(1)- Presence of oil in R-12 and R-22 vapors in any proportion affects the condensation process by reducing the condensing film coefficients for both single and multiple tubes. The higher the oil to refrigerant mass flow ratio, the lower the condensing film coefficient.

(2)- For both single and multiple plain tubes, the condensing coefficient of R-22 is less affected by the presence of oil than that of R-12. The average decrease in the condensing coefficient for each 2 per cent increase of oil is about 2 per cent for R-22 and about 3 per cent for R-12.

(3)- For R-12 and R-22, no significant difference in the condensing film coefficient was observed for the condensing temperatures used in this study, for both single and multiple plain tubes. Nusselt's theory, for a single tube, based on 32.2°C (90°F) would predict a figure of about 3 per cent lower than the experimental results of both refrigerants in the range of the condensing temperatures

employed. Further deviation would be expected in the Nusselt's theory for the higher condensing temperatures.

(4)- The pattern of the condensing curves obtained with the oil-vapor mixtures, for both R-12 and R-22, has the same tendency as those of pure vapors.

(5)- The results for a vertical row of 4 horizontal tubes obtained from R-12 tests are higher than those predicted by Nusselt's theory by an average of 13 per cent, and by 18 per cent for R-22.

(6)- For a vertical row of 4 tubes, the following relationship between the condensing coefficient and the vapor-surface temperature drop was obtained

$$h \propto (\Delta T)^{-0.2}$$

(7)- The theoretical results confirm that the effect of subcooling is appreciable only at high rates of condensation. Closer results to the experimental coefficients are obtained by the theoretical equation of single tube condensation, when solved for large ΔT than for lower ΔT.

(8)- For the multitube condensation, the increase of ΔT results in a higher condensing coefficient than that predicted by Nusselt's modified equation. The deviation for instance, is about 9 per cent at $\Delta T = 22°C$.

(9)- Examination of plates (5-9) shows that the maximum thickness of R-12 condensate layer along the bottom of the single 15.8 mm O.D. tube, under the test conditions, is approximately 1.1 mm and the subtended angle is about 10 degrees. The thickness of the layer and the subtended angle were not affected by the variation of the rate of condensation.

8.2- Claims of contribution to knowledge:

(1)- The study has added new information concerning the oil-vapor mixture condensation to the existing, limited knowledge. Data bank of R-12 and R-22 vapors-oil mixture condensation, at 2, 4, 6 and 8 per cent oil to refrigerant mass ratios, are furnished.

(2)- Analytical and empirical equations which take into account the effects of oil on vapor condensation of commonly used refrigerants, have been provided.

(4)- For a vertical bank of 4 tubes, the study revealed a new relation between the condensing coefficient and the vapor surface temperature drop ΔT. This relation can provide more accurate condensing coefficient than that obtained by Nusselt's theory.

(5)- For oil-vapor mixture condensation, a new experimental technique has been developed by which the study can be carried out at constant oil-refrigerant mass ratios.

8.3- Future work recommended:

(1)- Further studies on the effects of partially miscible and non-miscible oil-vapor mixtures on condensation are needed, since many refrigeration systems in use today are with such oil-refrigerant combinations.

(2)- The condensing coefficient for a single tube condensation is known to vary with $(\Delta T)^{-0.25}$. In this study, for a bundle of 4 tubes, the exponent of ΔT was found to be (-0.2), and in Ref.(23), where a ten tube bundle was investigated, the condensing coefficient was reported to vary with $(\Delta T)^{-0.148}$.

Following this trend, the exponent of ΔT would increase with the increase of the number of tubes in a bundle within

the range stated above. Therefore, further studies are required to verify this expectation for condensation of pure vapors on different tube bundles.

(3)- Further work is required to study the effect of oil on the film coefficient for condensing R-12 and R-22 vapors on the external surface of a single and a vertical bank of finned tubes.

8.4- Recommendations:

Since the condenser has a major impact on the energy consumption of a refrigeration system, the followig recommendations should be considered:

(1)- The effects of oil on the condensation of a totally miscible refrigerants, especially those whose viscosity is largely affected by the oil, such as R-12, should be taken into consideration. The presence of oil will reduce the condensation rate resulting in a higher condensing pressure and, hence, higher power requirements for the driving source.

(2)- In already built refrigeration systems, utilizing plain tube condensers and operating with R-12 or R-22, oil should be prevented from reaching the condenser.

(3)- In Ref.(37), it is mentioned that for multi-tube condensation, the heat transfer coefficient for a bank of N tubes can be predicted by Nusselt's equation for plain multi-tubes increased by 10 per cent. In this study, and for both refrigerants tested, it was found that this figure is conservative. The results obtained shows that Nusselt's theory, based on 32.2 °C (90 °F) saturation temperature, increased by an average of 15 per cent is more realistic and may be used for the condensing temperature range 32.2-48.9°C (90-120°F) for R-12 and 32.2-40.6°C (90-105°F) for R-22.

(4)- For single plain tube condensation, Nusselt's theory, increased by 3 per cent and based on 32.2 °C (90°F) saturation temperature is recommended for predicting the condensing heat transfer coefficient in the condensing temperature range 32.2-48.9 °C (90-120 °F) for R-12 and 32.2-40.6°C (90-105°F) for R-22.

REFERENCES

1- Glicksman, L.R.; Mikic, B.B. and Snow, D.F.;"Augmentation of Film Condensation on the Outside Surface of Horizontal Tubes" A.I.Ch.E. Journal, Vol. 19, No. 3, May 1973 pp-636.

2- Ramsey, M.A.; "Avoiding Oil Problems in Refrigerating Systems" ASHRAE Journal, Vol. 6, part 2, 1964, pp-69.

3- ASHRAE "Handbook and Product Directory" 1980 Systems, pp 32.8.

4- Nusselt,W.; "Die Oberflachen Kondensation des Wasserdamfes" Zeitschrift des Vereines Deutscher Ingenieure, Vol. 60, 1916, pp (541-569).

5- Kern, D.Q. "Process Heat Transfer" McGraw-Hill Company, 1950, pp-263.

6- Kirkbride, C.G.; "Heat Transmission by Condensing Pure and Mixed Substances on Horizontal Tubes" Industrial Engineering Chemistry Vol. 25, 1933, pp (1324-1330).

7- Baker, E.M. and Mueller, A.C.; "Condensation of Vapors on a Horizontal Tube" Trans. American Institute of Chemical Engineering, Vol.33, 1937, pp (531-558).

8- Baker, E.M. and Tsao, U.; "Condensation of Vapors on Horizontal Tube" Industrial and Engineering Chemistry, Vol.32, 1940, pp (1115-1121).

9- Young, F.L., and Wohlenberg, W.J.; "Condensation of Saturated Freon-12 Vapor on a Bank of Horizontal Tubes" Trans. ASME, Vol.64 issue 8, 1942, pp (787-794).

10-White, R.E.; "Condensation of Refrigerant Vapor-Apparatus and Film Coefficient for Freon 12" Trans. ASME, August 1948, pp (689-693).

11-Colburn, A.P.; "Problems in Design and Research on Condensers of Vapors and Vapor Mixtures" Inst. Mech. Eng. and ASME, Proc. General Discussion on Heat Transfer, 1951, pp (1-11).

12-Short, B.E. and Brown, H.E.; "Condensation of Vapors on Vertical Banks of Horizontal Tubes" Inst. Mech. Eng. and ASME, Proc. General Discussion on Heat Transfer, 1951, pp (27-31).

13-Peck, R.E. and Reddie, W.A.; "Heat Transfer Coefficients for Vapors Condensing on Horizontal Tubes" Industrial and Engineering Chemistry, Vol.43, 1951, pp (2926-2931).

14-Rohsenow, W.M.; "Heat Transfer and Temperature Distribution in Laminar Film Condensation" Trans. ASME, Vol. 78, No. 1-3, 1956, pp (1645-1648).

15-Kern, D.Q.; "Mathematical Development of Tube Loading in Horizontal Condensers" A.I.Ch.E. Journal, Vol.4, No.2, 1958, pp (157-169).

16-Sparrow, E.M. and Gregg, J.L.; "Laminar Condensation Heat Transfer on a Horizontal Cylinder" ASME Journal of Heat Transfer, November 1959, pp (291-296).

17-Chen, M.M.; "An Analytical Study of Laminar Film Condensation: Part 2-Single and Multiple Horizontal Tubes" ASME Journal of Heat Transfer, Feb. 1961, pp (55-60).

18-Shekriladze, I.G. and Gomelauri, V.I.; "Theoretical Study of Laminar Film Condensation of Flowing Vapors" Int. Journal Heat Mass Transfer, Vol. 9, 1966, pp (581-591).

19-Henderson, C.L. and Marchello, J.M.;"Role of Surface Tension and Tube Diameters in Film Condensation on Horizontal Tubes" A.I.Ch.E. Journal, Vol. 13, No. 3, 1967, pp (613-614).

20-Denny, V.E. and Mills, A.F.; "Laminar Film Condensation of a Flowing Vapor on a Horizontal Cylinder at Normal Gravity" Journal of Heat Transfer, Nov. 1969, pp (495-501).

21-Fujii, T., Uehara, H. ,Hirata, K. and Oda, K.; "Heat Transfer and Flow Resistance in Condensation of Low Pressure Steam Flowing Through Tube Banks" Int. Journal Heat Mass Transfer, Vol. 15, 1972, pp (247-260).

22-Fujii, T., Uehara, H. and Kurata, C.; "Laminar Filmwise Condensation of Flowing Vapor on a Horizontal Cylinder" Int. Journal Heat Mass Transfer, Vol. 15, 1972, pp (235-246).

23-Ivanov, O.P.; Butyrskaya, S.T. and Mamchenko, V.O.; "Heat Transfer Attending the Condensation of R-12 Vapor Moving at Bundles of Smooth and Finned Tubes" Heat Transfer-Soviet Research, Vol. 4, No. 6, Nov.-Dec. 1972, pp (143-149).

24-Gaddis, E.S.; "Solution of the Two Phase Boundary Layer Equations for Laminar Film Condensation of Vapor Flowing Perpendicular to a Horizontal Tube" Int. Journal Heat Mass Transfer, Vol. 22, 1979, pp (371-382).

25-Kutateladze, S.S.; Gogonin, N.I.; Dorokhov, A.R. and Sosunov, V.I.; "Film Condensation of Flowing Vapor on a Bundle of Plain Horizontal Tubes" Thermal Engineering 26 (5), 1979, pp (270-273).

26-Kutateladze, S.S., Gogonin, N.I., Dorokhov, A.R. and Sosunov, V.I.; "Heat Transfer in Vapor Condensation on a Horizontal Tube Bundle" Heat Transfer-Soviet Research, Vol. 13, No. 3, May-June 1981, pp (32-50).

27-Abdulmanov, K.H.A. and Mirmov, N.I.; "Experimental Study of Heat Transfer from Oil-Contaminated Ammonia Vapor Condensing on Horizontal Tubes" Heat Transfer-Soviet Research, Vol. 3, No. 6, Nov.-Dec. 1971, pp (176-180).

28-Mirmov, N.I. and Yemel'Yanov, Yu.V.; "Coefficient of Heat Transfer for Ammonia Condensers" Heat Transfer-Soviet Research, Vol. 8, No. 1, Jan.-Feb. 1976.

29-ASHRAE "Handbook and Product Directory" 1980 Systems, pp (32.1-32.11).

30-Williams, P.E. and Sauer, H.J.; "Condensation of Refrigerant-Oil Mixtures on Horizontal Tubes" ASHRAE Transactions 1981, Vol. 87, Part 1, pp (52-69).

31-ASHRAE "Handbook of Fundamentals" 1977, pp 32.2

32-Technical Information Center, Energy Research and Development Administration; "Handbook of Aerosols" Chapter 2, 1976, pp (9-39).

33-Green, H.L.; "Particulate Clouds: Dust, Smokes and Mists" D.Van Nostrand Company, Inc., Princeton, New Jersey, 1964, pp-37.

34-Hrubeck, H.F.; Journal of Applied Physics 29, 1958, pp-572

35-ASHRAE "Handbook and Product Directory" 1980 Systems, pp-32.9.

36-Jackman, D.L. and Jensen, M.K.; "Nucleate Pool Boiling of Refrigerant-Oil Mixtures" Trans. ASME, J. Heat Transfer, Feb. 1984, pp-184.

37-ASHRAE "Handbook of Fundamentals" 1977, pp-2.24

APPENDIX I

```
      PROGRAM OMAR (INPUT,OUTPUT)
C     ***************************************************
C     *                                                 *
C     *                                                 *
C     *     THE FOLLOWING PROGRAMME WAS DESIGNED        *
C     *                                                 *
C     *     TO SOLVE THE FOLLOWING INTEGRATION          *
C     *                                                 *
C     *     NUMERICALLY.                                *
C     *                                                 *
C     *                  θ  1                           *
C     *                 ⌠  ---                          *
C     *                 ⌡  3                            *
C     *                0 SIN θ  dθ                      *
C     *           ------------------------              *
C     *                                                 *
C     *                 [  4     θ  1      ]0.25        *
C     *                 [ ---    ⌠  ---    ]            *
C     *                 [  3     ⌡  3      ]            *
C     *                 [ 4      0 SIN θ dθ]            *
C     *                                                 *
C     ***************************************************
C
C     INPUT PARAMETER
C     ---------------
C
C     θ = HIGH LIMIT OF THE INTEGRATION, DEGREES
C
      COMMON ALFAD,N,EPSI,IN
      DIMENSION H(180)
      DO 10 I=1,180
10    H(I)=0.0
      ALFAD=.017453
      READ*,N
      DO 20 IN=1,N
      CALL E1230
20    H(IN)=EPSI
      HA=0.0
```

```
      NN=N-1
      DO 30 I=1,NN
30    HA=HA+H(I)*2

      HA=HA+H(I+1)
      HA=HA*ALFAD/2.0
      PRINT*,HA
      STOP
      END
      SUBROUTINE E1230
      COMMON ALFAD,N,EPSI,IN
      DIMENSION Y(180)
      DO 30 II=1,180
30    Y(II)=0.0
      DH=ALFAD
      FA=1./3.
      DO 10 I=1,IN
10    Y(I)=(SIN(I*ALFAD))**FA
      Z=0
      M=IN-1
      DO 20 I=1,M
20    Z=Z+2*Y(I)
      Z=Z+Y(IN)
      ALFA=ALFAD*IN
      Z=Z*ALFAD/(2.0*(SIN(ALFA)**(4./3.)))
      Z=Z*4./3.
      EPSI=(Z)**.25

      EPSI=1./EPSI

      RETURN

      END


 EOI ENCOUNTERED.
/
```

APPENDIX II

```
      PROGRAM AHMED(INPUT,OUTPUT)


C     ******************************************************
C     *                                                    *
C     *   THIS PROGRAMME WAS DESIGNED TO CALCULATE THE     *
C     *   EXPERIMENTAL CONDENSING COEFFICIENT AT DIF-      *
C     *   FERENT OIL-VAPOR MASS RATIOS. TWO DIRECT         *
C     *   METHODS AND ONE INDIRECT WERE USED.   THE        *
C     *   PROGRAMME ALSO TRANSFORM THE  MILLIVOLTS         *
C     *   READINGS OF THE THERMOCOUPLES TO DEGREES         *
C     *   FEHRENHEIT                                       *
C     *                                                    *
C     ******************************************************


C  INPUT PARAMETERS:
C  -----------------

C  NTEST1 = NUMBER OF STARTING TEST, USUALLY = 1
C  NTEST2 = NUMBER OF TEST IN THE GROUP
C  NTUBES = NUMBER OF TUBES IN A VERTICAL ROW,
C           EITHER 1 FOR SINGLE TUBE OR 4 FOR
C           THE MULTITUBE CASE.
C  AMRRT  = RATE OF LIQUID REFRIGERANT RISE IN THE
C           REFRIGERANT RECIEVER, IN/MIN
C  HFG    = LATENT HEAT OF CONDENSATION, BTU/LB

C  W1,W2*
C       * = COOLING WATER FLOW RATE IN TUBE 1 TO
C  W3,W4*   TUBE 4 OF THE MULTITUBE CONDENSER
C           RESPECTIVELY, LB/HR

C  WS   = COOLING WATER FLOW RATE IN THE SINGLE
C         TUBE CONDENSER, LB/HR

C  T1,T2....T24 = MULTITUBE  SURFACE LOCAL
C                 TEMPERATURES, MILLIVOLTS

C  T1S,T2S...T6S= SINGLE TUBE LOCAL SURFACE
C                 TEMPERATURES, MILLIVOLTS

C  T7S   = SINGLE TUBE INLET WATER TEMPERATURE,
C          MILLIVOLT
```

```
C  T8S,T9S AND T10S= SINGLE TUBE OUTLET WATER
C                   TEMPERATURES, MILLIVOLTS

C  TSAT  = VAPOR CONDENSING TEMPERATURE, MILLIVOLTS

C  T25,T26*
C        * = MULTITUBE INLET WATER TEMPERATURES,
C  T27,T28*   FOR TUBE 1 TO 4 RESPECTIVELY, MILLIVOLTS

C  T29,T30*
C        * = MULTITUBE OUTLET WATER TEMPERATURES,
C  T31,T32*   FOR TUBE 1 TO 4 RESPECTIVELY, MILLIVOLTS

C  DENLRS    = PURE REFRIGERANT DENSITY AT THE
C              SATURATION TEMPERATURE, LB/CU.FT

C  Z         = OIL-REFRIGERANT MASS RATIO

C  OILDS     = PURE OIL DENSITY AT THE SATURATION


C  OUTPUT PARAMETERS
C  -----------------

C  DELTAT = FILM TEMPERATURE DROP
C  TAV    = FILM AVERAGE TEMPERATURE
C  XLMTD  = LOG MEAN TEMPERATURE DIFFERENCE, F
C  Q1     = WATER SIDE HEAT TRANSFER RATE,
C           BTU/HR

C  Q2     = REFRIGERANT SIDE HEAT TRANSFER
C           RATE, BTU/HR

C  QAVE   = WATER SIDE AND REFRIGERANT SIDE
C           AVERAGE HEAT TRANSFER RATE

C  TSAVE  = TUBE SURFACE AVERAGE TEMPERATURE, F

C  H1     = HEAT TRANSFER COEFFICIENT BASED ON
C           QAVE, BTU/HR SQ.FT F

C  HQ1    = HEAT TRANSFER COEFFICIENT BASED ON
C           Q1, BTU/HR.SQFT.F

C  HQ2    = CONDENSING COEFFICIENT BASED ON
C           Q2, BTU/HR.SQFT.F
```

```
C  U      = OVERALL HEAT TRANSFER COEFFICIENT
C           BTU/HR.SQFT.F

C  VW     = WATER VELOCITY IN TUBE, FT/SEC.

C  RE     = REYNOLD NUMBER INSIDE THE TUBE

C  PR     = PRANDTL NUMBER


C  HW2O = WATER SIDE HEAT TRANSFER COEFFICIENT
C         BTU/HR.SQFT.F

C  HT2  = VAPOR SIDE CONDENSING COEFFICIENT
C         BTU/HR.SQFT.F


      COMMON DI,DO

      READ*,NTEST1,NTEST2

      DO 80 ITEST=NTEST1,NTEST2

      PRINT 90, ITEST

      READ*,NTUBES

      READ*, AMRRT,HFG
      IF(NTUBES.EQ.1) GO TO 505

      W1=2480.88

      W2=2483.4

      W3=2344.44

      W4=2438.88

      GO TO 506
505   READ*,WS

      GO TO 514
```

```
506   AMW=(W1+W2+W3+W4)/4
      GO TO 510
514   AMW=WS

510   CPW=1.0

      CPO=.25

      CPR=.2350
      IF(NTUBES.EQ.1) GO TO 520

      A=1.74532
       GO TO 523
520   A=0.43633
      GO TO 525


523   READ*,T1,T2,T3,T4,T5,T6,T7,T8,T9,T10,
     + T11,T12,T13,T14,T15,T16,T17,T18,T19,T20,T21,T22,T23,T24
       GO TO 527
525    READ*,T1S,T2S,T3S,T4S,T5S,T6S,
     + T7S,T8S,T9S,T10S,TSAT
       GO TO 538
527   READ*,T25,T26,T27,T28

       READ*,T29,T30,T31,T32,TSAT

538   PRINT10,AMW,CPW,AMRRT,HFG,A,CPR,CPO
      IF(NTUBES.EQ.1) GO TO 541

      PRINT20,T1,T2,T3,T4,T5,T6,T7,T8,T9,T10,
     +T11,T12,T13,T14,T15,T16,T17,T18,T19,T20,T21,T22,T23,T24
```

```
      PRINT15,T25,T26,T27,T28,T29,T30,T31,T32,TSAT

      GO TO 552

541   PRINT750,T1S,T2S,T3S,T4S,T5S,T6S,T7S,T8S,T9S,T10S,TSAT

552   READ*,DENLRS,Z,OILDS

      V=AMRRT*0.0891868*60./12.

      PRINT100,DENLRS,V

      PRINT200,OILDS

200   FORMAT(//,5X,13HOIL DENSITY =,F10.6,///)

      CALL TRANS(T1)$CALL TRANS(T2)$CALL TRANS(T3)$CALL TRANS(T4)
      CALL TRANS(T5)$CALL TRANS(T6)$CALL TRANS(T7)$CALL TRANS(T8)
      CALL TRANS(T9)$CALL TRANS(T10)$CALL TRANS(T11)$CALL TRANS(TSAT)
      CALL TRANS(T12)$CALL TRANS(T13)$CALL TRANS(T14)
      CALL TRANS(T15)$CALL TRANS(T16)$CALL TRANS(T17)
      CALL TRANS(T18)$CALL TRANS(T19)$CALL TRANS(T20)
      CALL TRANS(T21)$CALL TRANS(T22)
      CALL TRANS(T24)$CALL TRANS(T25)$CALL TRANS(T23)
      CALL TRANS(T26)$CALL TRANS(T27)$CALL TRANS(T28)
      CALL TRANS(T29)$CALL TRANS(T30)$CALL TRANS(T31)$CALL TRANS(T32)
      CALL TRANS(T1S)$CALL TRANS(T2S)$CALL TRANS(T3S)
      CALL TRANS(T4S)$CALL TRANS(T5S)$CALL TRANS(T6S)
      CALL TRANS(T7S)$CALL TRANS(T8S)$CALL TRANS(T9S)
      CALL TRANS(T10S)

      IF(NTUBES.EQ.1) GO TO 567

      PRINT20,T1,T2,T3,T4,T5,T6,T7,T8,T9,T10,T11,T12,
     + T13,T14,T15,T16,T17,T18,T19,T20,T21,T22,T23,T24

      PRINT15,T25,T26,T27,T28,T29,T30,T31,T32,TSAT

      GO TO 578

567   PRINT750,T1S,T2S,T3S,T4S,T5S,T6S,T7S,T8S,T9S,T10S,TSAT

578   WR=1/(1+Z/100)

      WO=1-WR
```

```
      IF(NTUBES.EQ.1) GO TO 586
      QW1=W1*CPW*(T29-T25)
      QW2=W2*CPW*(T30-T26)
      QW3=W3*CPW*(T31-T27)
      QW4=W4*CPW*(T32-T28)
      Q1=(QW1+QW2+QW3+QW4)
      GO TO 591
586   TSO=(T8S+T9S+T10S)/3
      Q1=AMW*CPW*(TSO-T7S)
      IF(Z.EQ.0) GO TO 592
591   AMR=(V/(1+Z/100))*(OILDS/(1+WR*((OILDS/DENLRS)-1)))
      GO TO 594
592   AMR=V*DENLRS

594   OMRT=AMR*Z/100
      Q2=AMR*HFG

      QAVE=(Q1+Q2)/2.
      IF(Q1.LT.Q2) GO TO 50
      PER=((Q1-Q2)/Q1)*100.
      GO TO 60

50    PER=((Q2-Q1)/Q2)*100.
60    IF(NTUBES.EQ.1) GO TO 595

      TSAVE=(T1+T2+T3+T4+T5+T6+T7+T8+T9+T10
     ++T11+T12+T13+T14+T15+T16+T17+T18+T19+T20+T21+T22+T23+T24)/24
      GO TO 598
```

```
595     TSAVE=(T1S+T2S+T3S+T4S+T5S+T6S)/6

598    TVAVE=TSAT

       TAV=(TVAVE+TSAVE)/2

        DELTAT=TVAVE-TSAVE

        PRINT300,DELTAT,AMR,Z,TAV,OMRT

300     FORMAT(///,5X,
      +36HVAPOUR TO SURFACE TEMPERATURE DROP =,F10.6,//,
      +5X,28HREFRIGERANT MASS FLOW RATE =,F10.4,//,
      +5X,32HOIL TO REFRIGERANT MASS RATIOS =,F10.4,//,
      +5X,38HVAPOR TO SURFACE AVERAGE TEMPERATURE =,F10.4,//,
      +5X,20HOIL MASS FLOW RATE =,F10.6,////)


        H1=QAVE/(A*DELTAT)

        HQ1=Q1/(A*DELTAT)

        HQ2=Q2/(A*DELTAT)

        IF(NTUBES.EQ.1) GO TO 603

        XLMTD1=((TVAVE-T25)-(TVAVE-T29))/ALOG((TVAVE-T25)/(TVAVE-
      +T29))

       XLMTD2=((TVAVE-T26)-(TVAVE-T30))/ALOG((TVAVE-T26)/(TVAVE-T30))

       XLMTD3=((TVAVE-T27)-(TVAVE-T31))/ALOG((TVAVE-T27)/(TVAVE-T31))

        XLMTD4=((TVAVE-T28)-(TVAVE-T32))/ALOG((TVAVE-T28)/(TVAVE-T32))


        XLMTD=(XLMTD1+XLMTD2+XLMTD3+XLMTD4)/4

        GO TO 609

603     XLMTD=((TVAVE-T7S)-(TVAVE-TSO))/ALOG((TVAVE-T7S)/(TVAVE-TSO))
```

```
609   DO=.05208


      U=QAVE/(A*XLMTD)
       DI=.04125

       DENW=62.4

       VISW=3.63

       XKW=.33

       IF(NTUBES.EQ.1) GO TO 613

      PRINT500,XLMTD1,XLMTD2,XLMTD3,XLMTD4,XLMTD

       GO TO 663
613    PRINT651,XLMTD


500   FORMAT(5X,8HXLMTD1 =,F10.4,5X,8HXLMTD2 =,F10.4,5X,
     +8HXLMTD3 =,F10.4,//,5X,8HXLMTD4 =,F10.4,10X,7HXLMTD =,F10.4,///)
651    FORMAT(5X,7HXLMTD =,F10.4,///)


663   PRINT30,DI,DENW,VISW,XKW,DENLR,DO


       TCA=(DI**2)*ATAN(1.)


       VW=AMW/(3600*DENW*TCA)

       RE=(DENW*VW*3600*DI)/VISW

       PR=VISW*CPW/XKW

       CF=2./(((2.236*ALOG(RE))-4.639)**2)

       XNU=(RE*PR*(CF/2.))/(1.07+12.7*((PR**.6667)-1.)*(SQRT(CF/
     +2.)))

       HW1=XNU*XKW/DI
```

```
      HW1O=HW1*DI/DO

      RW1=1./HW1O

      TH=.00541

      XKT=224.0

      PRINT40,TH,XKT

      RVT1=(1./U)-RW1-(TH/XKT)

      HT1=1./RVT1
      IF(NTUBES.EQ.1) GO TO 670



      TB1=(T25+T26+T27+T28)/4

      TB2=(T29+T30+T31+T32)/4

      TB=(TB1+TB2)/2.
      GO TO 675
670   TB1=T7S
      TB2=TSO

      TB=(T7S+TSO)/2

675   HW2=150.*(1.+0.011*TB)*(VW**0.8)/((DI*12)**0.2)

      HW2O=HW2*DI/DO

      RW2=1./HW2O

      RVT2=(1./U)-RW2-(TH/XKT)
```

```
      HT2=1./RVT2

      PRINT70,Q1,Q2,QAVE,TSAVE,TVAVE,H1,HQ1,HQ2,U,VW,RE,
     +PR,HW2O,HT2,PER

80    CONTINUE

      STOP

10    FORMAT(5X,17HWATER FLOW RATE =,F10.4,//,5X,
     +24HSPECIFIC HEAT OF WATER =,F10.4,//,
     +5X,23HREFRIGERANT RISE RATE =,F10.4,//,
     +5X,29HLATENT HEAT OF VAPORIZATION =,F10.4,//,
     +5X,19HTUBE SURFACE AREA =,F10.4,//,
     +5X,34HLIQUID REFRIFERANT SPECIFIC HEAT =,F10.4,//,
     +5X,19HOIL SPECIFIC HEAT =,F10.4,//)

750   FORMAT(//,5X,5HT1S =,F10.4,5X,5HT2S =,F10.4,5X,5HT3S =,F10.4,//,
     + 5X,5HT4S =,F10.4,5X,5HT5S =,F10.4,5X,5HT6S =,F10.4,//,
     + 5X,5HT7S= ,F10.4,5X,5HT8S =,F10.4,5X,5HT9S =,F10.4,//,
     + 5X,6HT10S =,F10.4,7HTSAT =,F10.4,//)
15    FORMAT(//,5X,
     +5X,5HT25 =,F10.4,5X,5HT26 =,F10.4,5X,5HT27 =,F10.4,5X,
     +5HT28 =,F10.4,//,5X,5HT29 =,F10.4,5X,5HT30 =,F10.4,5X,5HT31 =,
     +F10.4,5X,5HT32 =,F10.4,
     + //,5X,6HTSAT =,F10.4)

20    FORMAT(5X,5HT1  =,F10.4,5X,5HT2  =,F10.4,
     +5X,5HT3  =,F10.4,5X,5HT4  =,F10.4,//,5X,5HT5  =,F10.4,5X,
     +5HT6 =,F10.4,5X,5HT7 =,F10.4,5X,5HT8 =,F10.4,//,5X,5HT9 =,
     +F10.4,5X,5HT10 =,F10.4,//,5X,5HT11 =,F10.4,5X,5HT12 =,F10.4,
     +5X,5HT13 =,F10.4,5X,5HT14 =,F10.4,//,5X,5HT15 =,F10.4,//,5X,
     +5HT16 =,F10.4,5X,5HT17 =,F10.4,5X,5HT18 =,F10.4,//,
     + 5X,5HT19 =,F10.4,5X,5HT20 =,F10.4,5X,5HT21 =,F10.4,//,
     + 5X,5HT22 =,F10.4,5X,5HT23 =,F10.4,5X,5HT24 =,F10.4,////)

30    FORMAT(5X,22HINSIDE TUBE DIAMETER =,F10.5,//,
     +5X,18HDENSITY OF WATER =,F10.5,//,
     +5X,20HVISCOSITY OF WATER =,F10.5,//,
     +5X,31HTHERMAL CONDUCTIVITY OF WATER =,F10.5,//,
     + 5X,28HLIQUID REFRIGERANT DENSITY =,F10.4,//,
     + 5X,25HACCELERATION OF GRAVITY =,F13.2,//,
     + 5X,23HOUTSIDE TUBE DIAMETER =,F10.5)
```

```
40     FORMAT(5X,19HTHICKNESS OF TUBE =,F10.6,//,
      +5X,30HTHERMAL CONDUCTIVITY OF TUBE =,F10.6)

70     FORMAT(5X,22HWATER HEAT FLOW RATE =,F10.3,//,
      +5X,33HREFRIGERANT SIDE HEAT FLOW RATE =,F10.3,//,
      +5X,19HAVERAGE Q1 AND Q2 =,F10.3,//,
      +5X,34HTUBE AVERAGE SURFACE TEMPERATURE =,F10.3,//,
      +5X,28HVAPOUR AVERAGE TEMPERATURE =,F10.4,
      +//,5X,36HVAPOUR SIDE CONDENSING COEFFICIENT =,F10.4,//,
      +5X,45HQ1 BASED VAPOUR SIDE CONDENSING COEFFICIENT =,F10.4,//,
      +5X,45HQ2 BASED VAPOUR SIDE CONDENSING COEFFICIENT =,F10.4,//,
      +5X,35HOVERALL HEAT TRANSFER COEFFICIENT =,F10.4,//,
      +5X,16HWATER VELOCITY =,F10.4,//,
      +5X,16HREYNOLD NUMBER =,F10.4,//,5X,16HPRANDTL NUMBER =,F10.4,
      +5X,//,38HWATER SIDE HEAT TRANSFER COEFFICIENT =,F12.4,//,5X,
      +36HVAPOUR SIDE CONDENSING COEFFICIENT =,F10.4,//,5X,
      +15HPERCENT ERROR =,F10.4)


90     FORMAT(/////,5X,10HTEST NO. =,I10,/,5X,10(1H-),///)
100    FORMAT(//,
      +5X,41HDENSITY OF SUBCOOLED LIQUID REFRIGERANT =,
      +F10.6,//,5X,26HMIXTURE VOLUME FLOW RATE =,F10.6,//)
       END
C       SUBROUTINE TRANS(T) FOR TRANSFORMATION OF MILLIVOLT
C      TO DEGREE FEHRENHEIT

       SUBROUTINE TRANS(T)
       DIMENSION A(18,12)
```

```
A(1,1)=0.$A(1,2)=0.$A(1,3)=1.$A(1,4)=2.$A(1,5)=3.
A(1,6)=4.$A(1,7)=5.$A(1,8)=6.$A(1,9)=7.$A(1,10)=8.
A(1,11)=9.$A(2,1)=30.$A(2,2)=-.043$A(2,3)=-.022$A(2,4)=0.00
A(2,5)=.022
A(2,6)=.043$A(2,7)=.065$A(2,8)=.086$A(2,9)=.108$A(2,10)=.130
A(2,11)=.151$A(3,1)=40.$A(3,2)=.173$A(3,3)=.195$A(3,4)=.216
A(3,5)=.238$A(3,6)=.260$A(3,7)=.282$A(3,8)=.303$A(3,9)=.325
A(3,10)=.347$A(3,11)=.369$A(4,1)=50$A(4,2)=.391$A(4,3)=.413
A(4,4)=.435$A(4,5)=.457$A(4,6)=.479$A(4,7)=.501$A(4,8)=.523
A(4,9)=.545$A(4,10)=.567$A(4,11)=.589$A(5,1)=60$A(5,2)=.611
A(5,3)=.634$A(5,4)=.656$A(5,5)=.678$A(5,6)=.700$A(5,7)=.722
A(5,8)=.745$A(5,9)=.767$A(5,10)=.789$A(5,11)=.812$A(6,1)=70
A(6,2)=.834$A(6,3)=.857$A(6,4)=.879$A(6,5)=.902$A(6,6)=.924
A(6,7)=.947$A(6,8)=.969$A(6,9)=.992$A(6,10)=1.014$A(6,11)=1.037
A(7,1)=80.$A(7,2)=1.060$A(7,3)=1.082$A(7,4)=1.103$A(7,5)=1.128
A(7,6)=1.151$A(7,7)=1.173$A(7,8)=1.196$A(7,9)=1.219$A(7,10)=1.242
A(7,11)=1.265$A(8,1)=90.$A(8,2)=1.288$A(8,3)=1.311
A(8,4)=1.334$A(8,5)=1.357$A(8,6)=1.380$A(8,7)=1.403
A(8,8)=1.426$A(8,9)=1.449$A(8,10)=1.472$A(8,11)=1.495
A(1,12)=10. $ A(2,12)=.173 $ A(3,12)=.391 $ A(4,12)=.611
A(5,12)=.834 $ A(6,12)=1.060 $ A(7,12)=1.288 $ A(8,12)=1.518
A(9,1)=100. $ A(9,2)=1.518 $ A(9,3)=1.542 $ A(9,4)=1.565
A(9,5)=1.588 $ A(9,6)=1.611 $ A(9,7)=1.635 $ A(9,8)=1.658
A(9,9)=1.681 $ A(9,10)=1.705 $ A(9,11)=1.728 $ A(9,12)=1.752
A(10,1)=110. $ A(10,2)=1.752 $ A(10,3)=1.775 $ A(10,4)=1.799
A(10,5)=1.822 $ A(10,6)=1.846 $ A(10,7)=1.869 $ A(10,8)=1.893
A(10,9)=1.917 $ A(10,10)=1.940 $ A(10,11)=1.964 $ A(10,12)=1.988
A(11,1)=120. $ A(11,2)=1.988 $ A(11,3)=2.011 $ A(11,4)=2.035
A(11,5)=2.059 $ A(11,6)=2.083 $ A(11,7)=2.107 $ A(11,8)=2.131
A(11,9)=2.154 $ A(11,10)=2.178 $ A(11,11)=2.202 $ A(11,12)=2.226
A(12,1)=130. $ A(12,2)=2.226 $ A(12,3)=2.250 $ A(12,4)=2.274
A(12,5)=2.298 $ A(12,6)=2.322 $ A(12,7)=2.347 $ A(12,8)=2.371
A(12,9)=2.395 $ A(12,10)=2.419 $ A(12,11)=2.443 $ A(12,12)=2.467
A(13,1)=140. $ A(13,2)=2.467 $ A(13,3)=2.492 $ A(13,4)=2.516
A(13,5)=2.540 $ A(13,6)=2.565 $ A(13,7)=2.589 $ A(13,8)=2.613
A(13,9)=2.638 $ A(13,10)=2.662 $ A(13,11)=2.687 $ A(13,12)=2.711
A(14,1)=150. $ A(14,2)=2.711 $ A(14,3)=2.736
A(14,4)=2.760 $ A(14,5)=2.785 $ A(14,6)=2.809 $ A(14,7)=2.834
A(14,8)=2.859 $ A(14,9)=2.883 $ A(14,10)=2.908 $ A(14,11)=2.933
A(14,12)=2.958$A(15,1)=160.$A(15,2)=2.958$A(15,3)=2.982
A(15,4)=3.007$A(15,5)=3.032$A(15,6)=3.657$A(15,7)=3.082
A(15,9)=3.131$A(15,10)=3.156$A(15,11)=3.181$A(15,12)=3.206
A(16,2)=3.206$A(16,3)=3.231$A(16,4)=3.256$A(16,5)=3.281
A(16,7)=3.332$A(16,8)=3.357$A(16,9)=3.382$A(16,10)=3.407
A(16,12)=3.458$A(17,1)=180.$A(17,2)=3.458$A(17,3)=3.483
A(17,5)=3.533$A(17,6)=3.559$A(17,7)=3.584$A(17,8)=3.609
A(17,10)=3.66$A(17,11)=3.686$A(17,12)=3.711$A(18,1)=190.
A(18,3)=3.737$A(18,4)=3.762$A(18,5)=3.788$A(18,6)=3.813
A(18,8)=3.864$A(18,9)=3.89$A(18,10)=3.916$A(18,11)=3.941 7
A(15,8)=3.107$A(16,1)=170.$A(16,6)=3.307
A(16,11)=3.432$A(17,4)=3.508$A(17,9)=3.635
A(18,2)=3.711$A(18,7)=3.839$A(18,12)=3.96
```

```
      I=2 $ J=2
10    IF(T.GE. A(I,J)) GO TO 20
      IC=I-1
      IF(T.GT.A(I,J)) PRINT 70
      GO TO 30
20    I=I+1
      GO TO 10
30    IF(T.GE. A(IC,J)) GO TO 50
      JC=J-1
      IF(T.GT.A(I,J)) PRINT 70
      GO TO 60
50    J=J+1
      GO TO 30
60    T= A(IC,1)+A(1,JC)+(T-A(IC,JC))/(A(IC,JC+1)-A(IC,JC))
      RETURN
70    FORMAT(5X,30HYOUR READINGS OUT OF THE TABLE)
      END
-EOI-
:
```

APPENDIX III

```
      PROGRAM RANA (INPUT,OUTPUT)

C     ************************************************************
C     *                                                          *
C     *     THIS PROGRAMME WAS DESIGNED TO SOLVE THE ANALYT-     *
C     *   ICAL EQUATIONS NO. (5.39) AND (5.63) DERIVED IN        *
C     *   THIS STUDY. NUSSELT'S EQUATIONS FOR SINGLE AND MUL-    *
C     *   TITUBE CONDENSATION ARE ALSO INCLUDED IN THIS          *
C     *   PROGRAMME AS WELL AS NUSSELT'S MODIFIED EQUATION       *
C     *   NO. (6.21). THE REFRIGERANT-OIL SOLUTION THERMAL       *
C     *   CONDUCTIVITY IS EVALUATED INTERNALLY BY THE            *
C     *   PROGRAMME.                                             *
C     *                                                          *
C     ************************************************************


C     INPUT PARAMETERS
C     ----------------
C     Z = OIL TO REFRIGERANT MASS RATIO, KG. OIL/ KG. REFRIGERANT

C     DELTAT = FILM TEMPERATURE DROP, °C

C     D = CONDENSING TUBE OUT SIDE DIAMETER, METER

C     HFG = LATENT HEAT OF CONDENSATION, J/KG

C     DENSM = OIL-REFRIGERANT SOLUTION DENSITY, CALCULATED BY
C             EQUATION (5.64) AT THE FILM AVERAGE TEMPERATURE,
C             KG/ CU.M

C     ACCG  =  ACCELERATION OF GRAVITY, M/ SQ.S

C     UMIX  =  VISCOSITY OF OIL-REFRIGERANT SOLUTION, FOUND
C              FROM FIGURES (9 AND 10) AT THE FILM AVERAGE
C              TEMPERATURE, KG/ M.S


C     CP    =  PURE REFRIGERANT CONDENSATE SPECIFIC HEAT
C              J/KG.° C (TABLE 26).

C     CPM   =  OIL-CONDENSATE MIXTURE SPECIFIC HEAT
C              J/KG. °C (TABLE 26).

C     XKO   =  PURE OIL THERMAL CONDUCTIVITY, FOUND FROM FIGURE
C              (11) AT THE FILM AVERAGE TEMPERATURE,
C              W/M.°C
```

```
C  XKR   =  PURE REFRIGERANT THERMAL CONDUCTIVITY, AT THE
C             FILM AVERAGE TEMPERATURE. IT IS LISTED IN TABLE
C             (26). W/M.°C

C  DENR  =  PURE REFRIGERANT DENSITY, AT THE FILM AVERAGE
C             TEMPERATURE LISTED IN TABLE (26). KG/CU.M

C  UR    =  PURE REFRIGERANT VISCOSITY, AT THE FILM AVERAGE
C             TEMPERATURE LISTED IN TABLE (26). KG/CU.M


C  OUTPUT PARAMETERS@D
C  ------------------

C  HN1   =  NUSSELT'S EQUATION CONDENSING COEFFICIENT ON A SINGLE
C             HORIZONTAL TUBE. W./ SQ.M°C

C  HN4   =  CONDENSING COEFFICIENT OBTAINED BY NUSSELT'S
C             EQUATION FOR MULTI-TUBE BUNDLE,W/SQ.M°C

C  HP1   =  SINGLE TUBE CONDENSING COEFFICIENT FOR PURE
C             VAPOR CONDENSATION, OBTAINED FROM EQUATION
C             5.39, W/SQ.M°C.

C  HMX1  =  SINGLE TUBE CONDENSING COEFFICIENT FOR OIL
C             VAPOR MIXTURE CONDENSATION OBTAINED FROM
C             EQUATION 5.39, W/SQ.M.°C.

C  HMX4  =  FOUR TUBE MEAN CONDENSING COEFFICIENT FOR
C             OIL-VAPOR MIXTURE CONDENSATION OBTAINED
C             FROM EQUATION (5.63).

C  HNMOD =  MULTITUBE MODIFIED CONDENSING COEFFICIENT
C             FOR CONDENSING PURE VAPOR, OBTAINED FROM
C             EQUATION (6.21), W/SQ.M.°C.

C  HMX4MOD =  MULTI-TUBE MODIFIED CONDENSING COEFFICIENT
C             FOR CONDENSING OIL-VAPOR MIXTURE OBTAINED
C             FROM EQUATION (6.20 A), W/SQ.M.°C.

      DO 80 I=1,7

      READ *,Z,DELTAT,D

      PRINT 90,Z,DELTAT,D

90    FORMAT(///,5X,18HOIL PERCENTAGE Z =,F10.4,5X,8HDELTAT =,
     + F10.5,5X,15HTUBE DIAMETER =,F10.5,/,5X,81(1H*),/)

      READ *,HFG,DENSM,ACCG,UMIX,CP,CPM,XKO,XKR,
     + DENR,UR
```

```
      WO=Z/(Z+100)

      WR=1-WO

      XKM=XKR*WR+XKO*WO-0.72*(XKO-XKR)*WO*WR

      PRINT 100,XKM,HFG,DENSM,ACCG,UMIX,CP,CPM,XKO,XKR,
     + DENR,UR


100   FORMAT(/,5X,5HXKM =,F10.6,5X,5HHFG =,F10.4,5X,
     + 7HDENSM =,F10.4,//,5X,6HACCG =,F12.1,5X,6HUMIX =,
     + F10.6,5X,4HCP =,F18.2,//,5X,5HCPM =,F12.10,
     + 5X,5HXKO =,F16.14,5X,5HXKR =,F16.14,//,
     + 5X,6HDENR =,F10.4,
     + 5X,4HUR =,F10.8,///)


      A=(DENR**2)*HFG*(XKR**3)*ACCG

      B=(D/12)*DELTAT*UR

      C=(DENR**2)*ACCG*HFG

     Q=3*DELTAT*(DENR**2)*CP*ACCG/8


      E=UMIX*DELTAT*D/12


      F=(HFG*ACCG*(DENSM**2))/(1+Z/100)



      G=3*DELTAT*(DENSM**2)*CPM*ACCG/8
      S=0.25
      HN1=0.725*(A/B)**0.25
      HN4=HN1*(S**0.25)
      HP1=(0.725*(XKR**0.75)/(B**0.25))*(C+Q)**0.25
      HMX1=(0.725*(XKM**0.75)/(E**0.25))*(F+G)**0.25
      H=(0.725*((F*(XKM**3))**0.25))/(E*(1+Z/100))**0.25
      HMX4=H*(S**0.25)
      HNMOD=HN1*(S**0.167)
      HMX4MOD=H*(S**0.167)
       PRINT 120,HN1,HN4,HP1,HMX1,HMX4,HNMOD,HMX4MOD

      BB=0.625
      B=B/BB
      E=E/BB

      HP1=(0.725*(XKR**0.75)/(B**0.25))*(C+Q)**0.25
      HMX1=(0.725*(XKM**0.75)/(E**0.25))*(F+G)**0.25
       PRINT 150,HP1,HMX1
```

```
120     FORMAT(///,15X,5HHN1 =,F20.4,//,15X,5HHN4 =,F20.4,
     + //,15X,5HHP1 =,F20.4,//,15X,6HHMX1 =,F10.4,//,
     +15X,6HHMX4 =,F20.4,//,
     +15X,7HHNMOD =,F20.4,//,
     +15X,9HHMX4MOD =,F20.4,//)

150     FORMAT(///,15X,5HHP1 =,F20.4,//,
     +15X,6HHMX1 =,F20.4)
80      CONTINUE

        STOP

        END

 EOI ENCOUNTERED.
/
```